



Universidade de Aveiro Departamento de Química
2015

**Ana Isabel
Oliveira Almeida**

**Síntese de novas estruturas tricíclicas
por fotociclização-[2+2]**

**Synthesis of novel tricyclic scaffolds
by [2+2]-photocycloaddition**



Universidade de Aveiro Departamento de Química
2015

**Ana Isabel
Oliveira Almeida**

**Síntese de novas estruturas
tricíclicas por fotociclicização-[2+2]**

**Synthesis of novel tricyclic scaffolds
by [2+2]-photocycloaddition**

Dissertação apresentada à Universidade de Aveiro para cumprimento dos requisitos necessários à obtenção do grau de Mestre em Química – Ramo Química Orgânica e Produtos Naturais, realizada sob a orientação científica do Doutor Artur Manuel Soares da Silva, Professor Catedrático do Departamento de Química da Universidade de Aveiro e do Doutor Thomas Woltering, F. Hoffmann La Roche, Basileia, Suíça.



O júri

Professor Doutor Artur Manuel Soares da Silva,

Professor Catedrático do Departamento de Química da Universidade de Aveiro

Professor Doutor Hans Peter Wessel

Professor Catedrático Convidado do Departamento de Química da Universidade de Aveiro

Doutor Thomas Woltering,

F. Hoffmann La-Roche AG, Basileia, Suíça.

Acknowledgments

This research was supported by the Medicinal Chemistry internship program of F. Hoffmann-La Roche AG.

I would like to kindly thank: Professor Doutor Artur Silva and Professor Doutor Hans Peter Wessel for their trust, advice and guidance; Doctor Thomas Woltering for being an inspiration and supporting me throughout this journey; Roger Wermuth and Sandro Prato for making me feel like part of the family and sharing both the good and bad times of working in the lab; Fiona Woodhall and Alistair Mason for their English lessons and friendship.

Finally, the invaluable assistance of Eric Kusznir in determining the UV-spectrum, Wolfgang Guba in molecular modeling and Helmut Jacobsen's guidance on the biological aspects of BACE are gratefully appreciated.

Palavras - chave: Fotoquímica, [2+2]-fotocicloadição, enonas, ciclobutano, heterociclos, vectores tricíclicos, módulos compactos

Resumo: O uso de processos fotoquímicos em química orgânica de síntese tem aumentado significativamente nos últimos anos. Contudo o uso de reações fotoquímicas ainda é bastante limitado. A fotocicloadição [2+2] é uma das reações mais conhecidas e utilizadas em síntese orgânica.

O anel ciclobutano tem um elevado interesse sintético pois para além de estar presente em vários produtos naturais também pode ser utilizado como precursor na construção de anéis maiores. A fotocicloadição [2+2] de enonas é uma das ferramentas possíveis para a síntese de anéis ciclobutano com possibilidade de funcionalização posterior, com potencial interesse na formação de precursores interessantes em química medicinal.

O acesso a novos e complexos vectores tricíclicos foi alcançado através de reações de fotocicloadição [2+2]. A optimização das condições de reação foi conseguida através da versatilidade das reações de fotocicloadição [2+2].

Os novos vectores tricíclicos complexos foram funcionalizados com o objectivo de obter estruturas compactas com potencial actividade biológica.

Key words: Photochemistry, [2+2]-photocycloaddition, enones, cyclobutane, heterocycles, tricyclic scaffolds, compact modules

Abstract: The use of photochemistry in synthetic organic chemistry has been increasing in the last few years. However the use of photochemical processes is still quite limited. [2+2]-Photocycloaddition is one of the most known and used tool in organic synthesis.

The cyclobutane moiety is very useful in organic chemistry since it is present in several natural products but can also be used as precursor of larger rings. The [2+2]-photocycloaddition of enones is a way to synthesize cyclobutanes with the possibility of further functionalization with potential interest in building blocks for medicinal chemistry.

Access to novel and complex tricyclic scaffolds was achieved using [2+2]-photocycloaddition reactions. Optimization of reaction conditions was accomplished displaying the versatility of [2+2]-PCA.

The new complex scaffolds were further functionalized in order to obtain innovative compact modules with potential biological activity.

Abbreviations:

λ - wavelength

E - extinction coefficient

δ - chemical shift

ϕ - quantum yield

³**D** - birradical form

Ac - acetyl

AD - Alzheimer's disease

AIBN - azobisisobutyronitrile

BACE - β -site APP cleaving enzyme

Bn - benzyl

Boc - *tert*-butyloxycarbonyl

Bz - benzoyl

Cbz - carboxybenzyl

DCM - dichloromethane

DIBAH - diisobutylaluminium hydride

DIPEA - *N*-ethyldiisopropylamine

DMAP – 4-dimethylaminopyridine

DME - dimethoxyethane

DMF - *N,N*-dimethylformamide

DMSO - dimethyl sulfoxide

EDC - 1-ethyl-3-(3-dimethylaminopropyl)carbodiimide

Et₂O - diethyl ether

EtOAc - ethyl acetate

EtOH - ethanol

Equiv - equivalents

hERG - human Ether-à-go-go-Related Gene

HRMS - high resolution mass spectrometry

IC₅₀ - half maximum inhibitory concentration

ISC - intersystem crossing

IR - Infra-red spectroscopy

LC/MS - liquid chromatography-mass spectrometry

LDA - lithium diisopropylamide

LED - light emitting diode
LiHMDS - lithium bis(trimethylsilyl)amide
LiO^tBu - lithium *tert*-butoxide
Me - methyl
MeCN - acetonitrile
NBS - *N*-bromosuccinimide
NEt₃ - triethylamine
NMR - nuclear magnetic resonance
PCA - photocycloaddition
Phe - phenyl
PheMe - toluene
Py - pyridine
T₁ - lowest triplet state
TBAF - tetra-*n*-butylammonium fluoride
***t*BuCO** - pivaloyl
TBDMS - *tert*-butyl dimethyl silyl
TBDPS - *tert*-butyl diphenyl silyl
TBS - *tert*-butyl silyl
THF - tetrahydrofuran
TLC - thin layer chromatography
Trp - tryptophan
UV - ultraviolet spectroscopy

Table of Contents

1- Introduction	1
1.1.1-Historical remarks	2
1.1.2 -General photochemical considerations	3
1.1.3- Irradiation apparatus:lamps, photoreactors	5
1.1.4-Concentration and Scale	7
1.1.5-Photosensitizers	8
1.1.6-Photochemistry as a “green chemistry” approach	8
<u>1.2-[2+2]-Photocycloaddition of Enones</u>	9
<u>1.3-Compact Modules in Medicinal Chemistry</u>	13
<u>1.4-Alzheimer’s disease and BACE1</u>	14
1.4.1-The Amyloid cascade hypothesis	14
1.4.2-BACE1 as a target in Alzheimer’s disease therapy	16
<u>1.5-References</u>	18
2- [2+2]-Photocycloaddition of 1,3-dioxin-4-ones vs 1,3-oxathiin-6-ones	21
<u>2.1-1,3-dioxin-4-ones</u>	21
<u>2.2-Oxathiin-6-ones</u>	26
<u>2.3-Conclusions</u>	31
<u>2.4-Experimental section</u>	32
<u>2.5-References</u>	39
3- [2+2]-Photocycloaddition in the synthesis of novel conformationally restricted <i>bis</i>-pyrrolidines	41
<u>3.1-α,β-unsaturated lactones</u>	41
<u>3.2-Novel Spiro Compact Module</u>	46
<u>3.3-Synthesis of versatile 3-(hydroxymethyl)-2<i>H</i>-furan-5-ones-derivatives bearing a leaving group in 4-position</u>	50
<u>3.4-Conclusion</u>	55
<u>3.5-Experimental section</u>	56
<u>3.6-References</u>	67
4- Further Functionalization of [2+2]-PCA products	69
<u>4.1-Compact Modules</u>	69
<u>4.2-BACE1 inhibitors</u>	71
4.2.1-Molecura modeling and <i>de novo</i> design	73
4.2.2-Synthesis of potential BACE1 inhibitors	76
4.2.3-MR121 BACE assay and results	83
<u>4.3-Conclusion</u>	85
<u>4.4-Experimental section</u>	87
<u>4.5-References</u>	100
Supporting information	101

1-Introduction

Light, more precisely sun light, has been part of the daily life of the human beings since the beginning of times. The importance of sun light to life is undeniable, plays important roles such as providing the right environmental temperature on planet Earth, providing food, and playing a role in medicine since ancient times. The discovery of fire and electric light are examples of the intense studies around light and the attempt of humans to control light. Therefore it is not surprising that over the years many have dedicated their efforts to the understanding of physical and chemical properties and uses of light. Photochemistry is the branch of chemistry dealing with the chemical effects of light (far UV to IR).¹

In nature we can find several photochemical processes; photosynthesis is the best known. Photosynthesis is the ability of plants to transform water and carbon dioxide into carbohydrates and oxygen in the presence of light. Photochemistry is also exploited in our daily life in cosmetic industry (sunscreens), in sustainable technologies (solar energy storage) and among other uses are informatics and security devices.² Although nature and technological development have proven that photochemistry is a versatile tool in chemistry and material sciences, the use of photochemical steps in the synthesis of organic compounds is still quite limited.

One of the explanations for the low use of photochemistry in organic synthesis is the fact that there are a number of photophysical aspects to be considered and optimized in order to plan and predict the result of a light-induced synthetic step. Photochemistry also requires some appropriate equipment that can discourage the interested user.

When excitation by light occurs the chemistry of the excited singlet and triplet state are added to the chemistry of the ground state, what leaves to conclude that photochemistry might triple the reactivity options of a molecule. Often molecules in different excitation states behave as completely different molecules. The great potential of photochemistry lies on the fact that excitation by light achieves what ground state chemistry cannot.

Until the beginning of the 21st century photochemical synthetic steps were mainly focused on overcoming stereoselectivity problems in organic synthesis. In the beginning of the century the development of highly chemo-, regio-, diastereo- and

enantioselective reactions using light excitation, has made chemists realize that photochemistry is a fascinating synthetic tool.

Photochemical reactions can be performed at low temperatures, in the solid or liquid state or under gas-phase conditions, with spin-selective direct excitation or sensitization, and even multi-photon processes start to enter the synthetic scenery.³ Production of photoproducts at industrial scale is possible although there is the notion that photochemical reactions are unsuitable for scale-up. Vitamin D3 is commercially available and is produced at industrial scale using a synthetic photochemical step.^{4,5}

Photochemical reactions result from the absorbance of light by the starting material. Some conditions are required for a successful course of the photoreaction:

- The wavelength of the light source has to fall within the absorption band of the reagent.
- Nothing interferes with the photons before they reach the target molecule.
- Nothing will interfere with the electronic excited states and quench them before they react.⁶

1.1.1-Historical remarks

The first attempts to relate the color of organic compounds to their molecular structure date back to the mid 19th century, when synthetic dyes became one of the most important products of the chemical industry.

Another mark of the modern photochemistry happened in 1866, when the Russian chemist Carl Julius von Fritzsche discovered that a concentrated anthracene solution exposed to UV radiation would fall from the solution as a precipitate. This precipitation happens because the anthracene molecules form dimers by the action of UV-light, which are no longer soluble.⁷

In 1876 Witt introduced the terms *chromophore* (a molecular group that carries the potential of generating color) and *auxochrome* (polar substituents that increase the depth of color).³

Ciamician and Silber~~Erro! Marcador não definido.~~ studied photoreactions of carbonyl compounds and observed photoreductions, photopinacolization, intramolecular photoaddition, α - and β -cleavage. These studies would later reveal fundamental principles such as the concepts of excited singlet and triplet states.

Platt's free electron model, Hückel's molecular orbital theory and Pariser, Parr and Peple's configuration interaction model provided satisfactory models for the interpretation of electronic spectra of conjugated molecules.⁸

After 1950, T. Förster, M. Kasha, G. Porter, E. Havinga, G. Hammond, H. Zimmerman, J. Michl, N. Turro and L. Salem were among the scientists who developed the basic concepts for structure reactivity correlations in photochemistry.³

Paternó and Büchi observed the first cycloadditions of carbonyl compounds onto alkenes, the well-known Paternó-Büchi reaction.~~Erro! Marcador não definido.~~

The development of commercially available lasers and electronic equipment allowed for real-time detection of primary transient intermediates by flash photolysis. Photochemistry thus emerged as the principal science for the study of organic chemistry reaction mechanisms in general, because it can be used to generate the intermediates that are postulated to intervene in chemical reactions of the ground state.

This brief selection of the history of photochemistry shows that this branch of chemistry developed mainly in the latest half of the 20th century. However a lot remains to be discovered and studied. Photochemistry has not yet made its path into the daily life of the synthetic organic chemistry labs.

1.1.2-General photochemical considerations

Electronic states of a molecule and the transitions states between them can be illustrated by the Jablonski diagram (**Figure 1**). The states are arranged by energy vertically and horizontally according to the spin multiplicity.

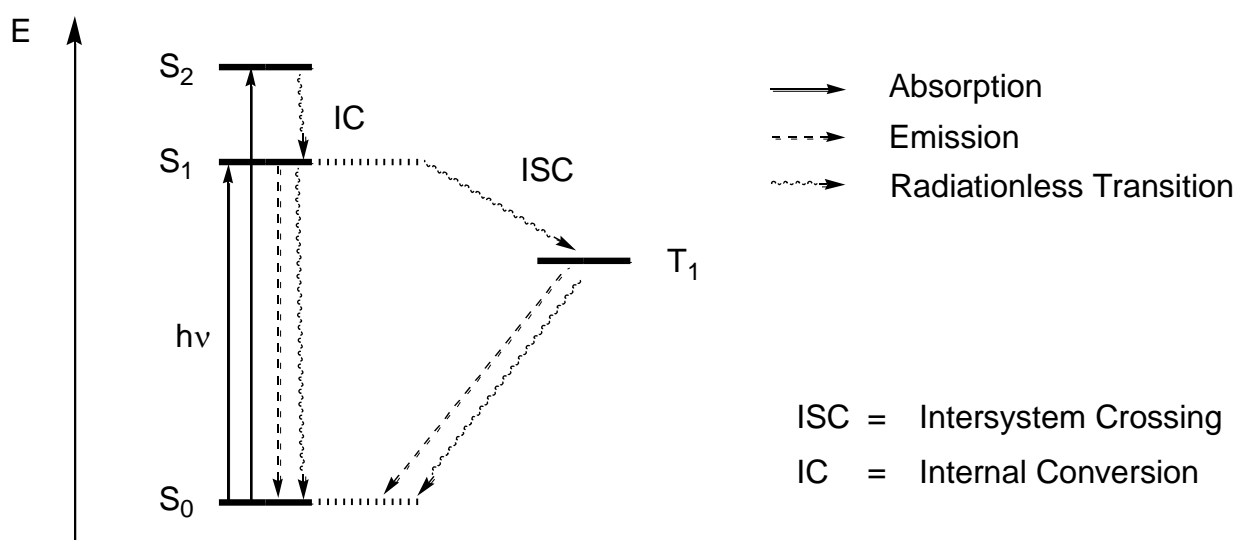


Figure 1: Jablonski diagram.⁶

In a photochemical process the molecule is irradiated at a certain wavelength which causes its excitation from the ground state (S_0) to the singlet state(s) (S_1 or higher state S_2) followed by the intersystem crossing to the triplet state (T_1) from which the reaction occurs. In order to obtain full conversion and avoid decomposition the ideal wavelength of irradiation is the one that provides the minimum of energy required for the excitation into S_1 .

To determine the wavelength at which we should irradiate a molecule the UV spectrum should be measured. From the UV spectrum it is possible to determine the wavelength at which the maximum of absorption takes place. If the molecule is irradiated at the wavelength of maximum absorption the amount of energy taken up by the molecule is so high that it shows a strong tendency of photodecomposition rather than following a directed photochemical pathway. The ideal wavelength of irradiation would be at longer wavelengths from the maximum of absorption which still results in excitation but with lesser input of energy. If we consider the exemplified UV spectrum displayed in **Figure 2**, the ideal wavelength of irradiation is a value along the “shoulder” of the absorption curve (along the green box).

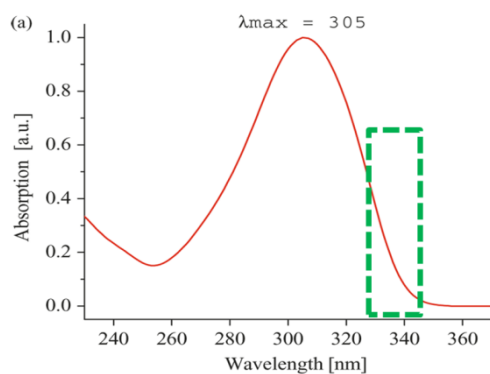


Figure 2: UV spectrum of an organic compound. The green dashed box represents the ideal wavelength of irradiation to perform a photoreaction.

From the UV-spectrum it is possible to determine the extinction coefficient (ϵ). This coefficient determines how many moles of molecules absorb energy at the particular wavelength and has its higher level in maximum wavelength of absorption.

The quantum yield ϕ indicates the fraction of excited states that reacts, provided that no competitive quenching occurs. It relates the number of molecules that undergo a transformation depending on the number of photons absorbed by a molecule.

$$\phi = \frac{\text{molecules that reacted}}{\text{photons absorbed}}$$

Regarding to [2+2]-photocycloaddition reactions the maximum of the quantum yield can be one.

1.1.3-Irradiation apparatus: lamps, photoreactors

In the present there are several companies which supply lamps as well as complete photochemical reactors (light source, power supply and reaction flasks with accessories). The complete photoreactor may be a big investment and might not be the most convenient solution for a research unit. The most commonly used flasks are made of quartz because being transparent to light at a wide spectrum of wavelengths (**Figure 3**).

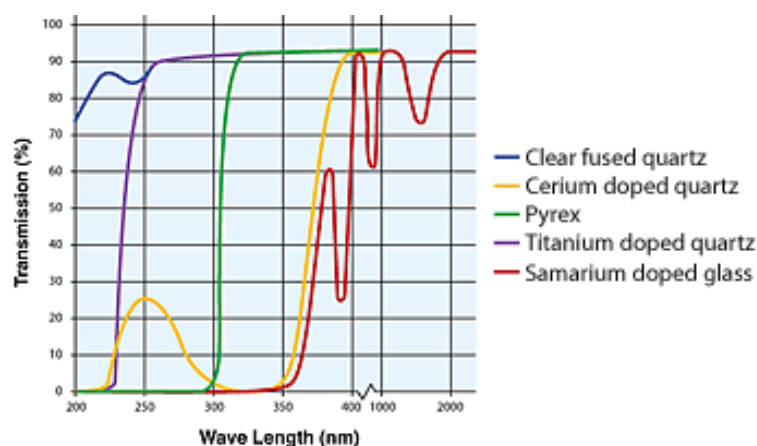


Figure 3: Transparency of different materials according to wavelength of irradiation.⁹

The most widely used light sources are mercury vapor arcs. The efficacy of conversion into light is low, and the lamp output is dispersed over a range of wavelengths and towards all directions, in consequence only a small amount of the emitted light is absorbed by the molecules. These lamps are most useful for external irradiation. The low-pressure mercury arcs are used for purposes other than preparative photochemistry and therefore are by far the cheapest light source. The lamp emission can be modified by means of a coating made from a phosphor that absorbs the almost monochromatic mercury radiation and emits a range of longer wavelengths.

The low pressure mercury arcs UV lamps have a spectral distribution of irradiance density. This means that the radiation emitted by the lamps is not accurate one value, but an interval of wavelengths of irradiation. Although the UV lamps of 254 nm have quite a sharp interval of wavelength of irradiation, higher wavelengths lamps have a tendency to have a more broad spectral distribution (**Figure 4**).

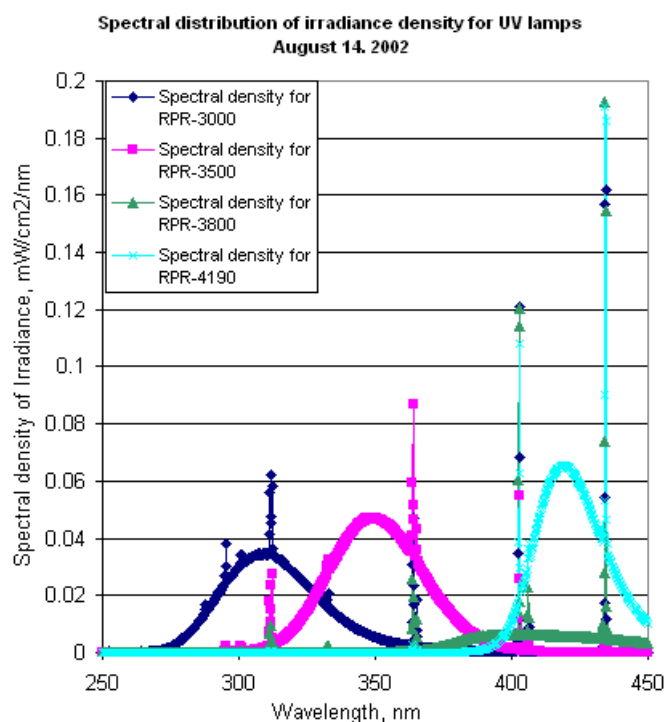


Figure 5: Spectral distribution of irradiance density for UV lamps provided by Rayonet®.¹⁰

There are other kinds of light sources that are definitely not as widely used as the low pressure mercury arcs, such as LEDs and Xenon arcs. LEDs are reasonably effective light sources and are available in a large range of monochromatic emitting types. These kinds of systems have developed rapidly in last few years. Having a long life and being quite cheap are two of the reasons why they will probably replace the mercury arcs as light sources for photoreactions.

1.1.4-Concentration and Scale

An external irradiation is often used in small scale photoreactions what is not an optimal solution for maximizing the exploitation of the emitted radiation. Relatively large scale photochemical reactions must take into consideration this fact and achieve optimal light irradiation and mass transfer. A clean reaction is rarely obtained with a concentration above 0.01-0.1 M.⁶

If the reaction product absorbs at the same wavelength as the starting material (what commonly occurs) it may hinder the completion of the photoreaction when it is photostable (the so called “inner-filter” effect) or it may lead to a mixture of primary and secondary photoproducts, if the primary product itself is photoreactive. A way of minimizing secondary photoreactions is to use lamps with a narrow wavelength range

emission, as this may match better the starting material absorption than the primary product.

The effect of impurities on photochemical reactions is relatively small. In order to compete for a chemical reaction with the light-driven reaction it must be quite fast, because the excited states have a very short life-time.

1.1.5-Photosensitizers

The direct excitation of the starting material may not be possible, or may not produce the desirable effects on the course of the photoprocess. In these particular cases, there is the possibility of using a photosensitizer or a photocatalyst. The irradiation of these particular molecules activates them and they will activate the starting material by some mechanism (energy transfer, redox step, hydrogen abstraction).

Triplet sensitization is one of the methods used to generate the triplet state of molecules that either do not undergo spontaneous ISC following direct excitation or undergo unwanted reactions when excited to the singlet state. The triplet energy of the donor should exceed that of the acceptor for efficient energy transfer. Benzophenone and xanthenes are often used as triplet sensitizers, because they absorb at relatively long wavelengths, undergo efficient ISC and have a small singlet-triplet energy gap. Acetone as a solvent is also one the methods of triplet sensitization, ensuring that it is responsible by absorbing most of the light.⁶

1.1.6-Photochemistry as a “green chemistry” approach

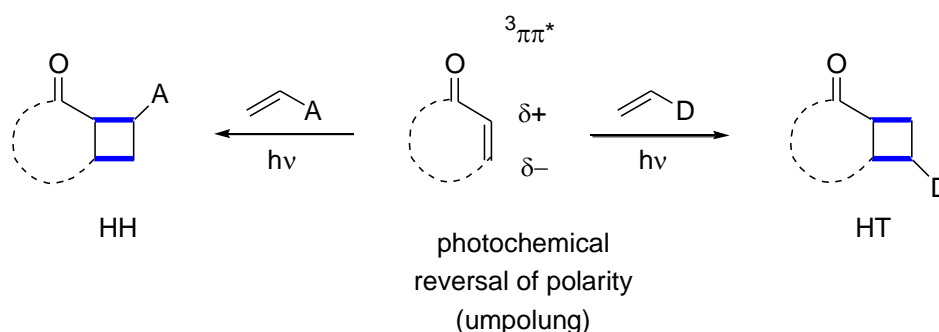
Photochemical reactions have been described as “green” chemical processes, because the driving force in the reaction is simple light irradiation, which is considered to be clean energy.

The role of photochemical processes in sustainable energy sources is recognized by the majority of the scientific community. The possibility of replacing the fossil fuels by sustainable technology such as solar energy storage with the help of photovoltaic cells is one of the most promising technologies. A great effort has been made to increase the quality and performance of photovoltaic systems in the last decades.

1.2-[2+2] Photocycloadditions of enones

Photochemistry reactions, in particular the [2+2]-photocycloaddition of α,β -unsaturated carbonyl compounds, known as the de Mayo cycloaddition, has been widely explored. The de Mayo cycloaddition is highly stereo- and regioselective.¹¹ The cycloadducts of cyclic enones are most often *cis*-fused.¹²

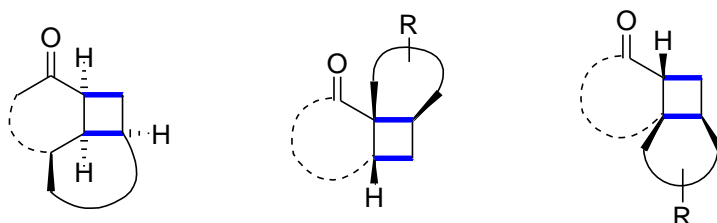
Regioselectivity of the de Mayo cycloaddition can be anticipated by analyzing electronic properties of the double bonds (**Scheme 1**).



Scheme 1

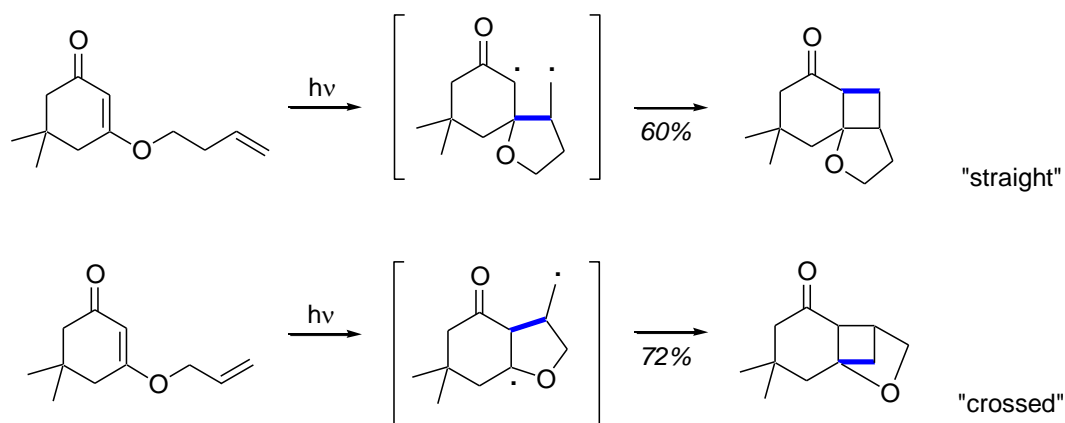
Olefins substituted with the so called acceptors substituents (A) originate as a major product the head-to-head products. On the contrast olefins substituted with the so called donor substituents (D) tend to form preferably the head-to-tail product.⁶

Regarding the intramolecular [2+2]-PCA there are important classes of products that can be formed (**Scheme 2**).¹³



Scheme 2

In general, if possible, a five membered-ring is formed during the photochemical step (**Scheme 3**).



Scheme 3

Photochemical [2+2] cycloadditions can be used to synthesize the cyclobutane skeleton. Four membered rings are very versatile in organic chemistry, not only because it is a known precursor for natural products and various unique compounds. Cyclobutane rings can also undergo ring expansion reactions and originate other size rings in di- or tricyclic ring systems.¹⁴

The photochemical cycloadditions of α,β -unsaturated carbonyl, carboxyl, and related heterocyclic compounds to alkenes are important synthetic reactions, and the mechanisms of such processes have been the subject of controversy ever since the first reports by Eaton and Corey.¹⁵ Cycloaddition occurs in most cases, with excitation by light of relatively long wavelengths ($\lambda \geq 250$ nm), after intersystem crossing (ISC), from the lowest-lying triplet state (T_1), which has often a $\pi\pi^*$ character.¹⁶ In an extremely simplified fashion, using a valence bond description, the excited state can be written in biradical form (3D), to form the cyclobutane ring (**Figure 1**).

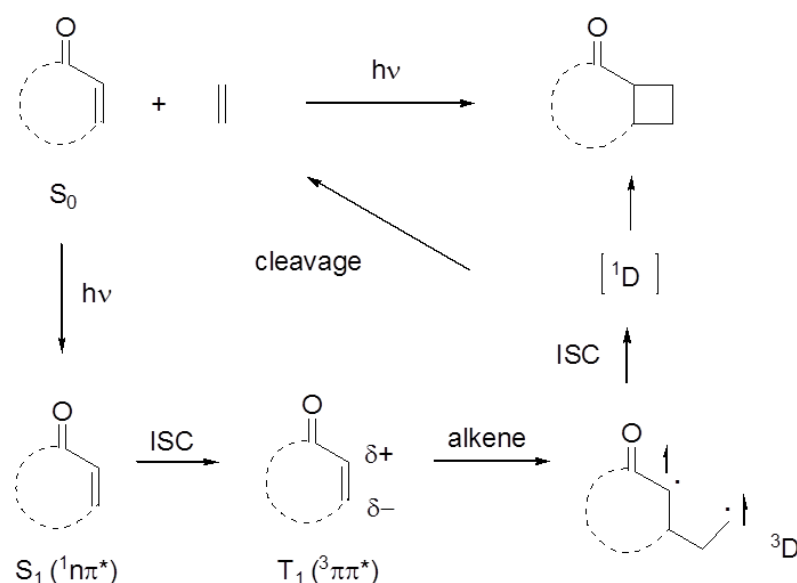


Figure 6: Mechanism proposed for the formation of the cyclobutane ring.⁶

The energy difference between the S_1 and the T_1 state of carbonyl compounds is low (both are np^* states).

In intramolecular reactions the pattern of substituents in the alkene has large influence in the regioselectivity of the reaction, with the general notion being that the T_1 state shows reverted polarity compared to the ground state.⁴

Most α,β -unsaturated compounds used in [2+2] photocycloadditions reactions are cyclic compounds of five- or six-membered rings. This choice avoids the rotation around the C-C single bond in intermediate 3D , which would act as rapid decay pathway to the ground-state via ultrafast intersystem crossing. The photochemistry of enones seems insensitive as to whether the excited enone is obtained by direct irradiation or triplet sensitization.¹⁵

There are various types of α,β -unsaturated carbonyl substrates according to the type of substituents. In the **Figure 7** general structures from A1 to A6 are described such as the R represents carbon and hydrogen, while Q represents oxygen, nitrogen and sulfur substituents.

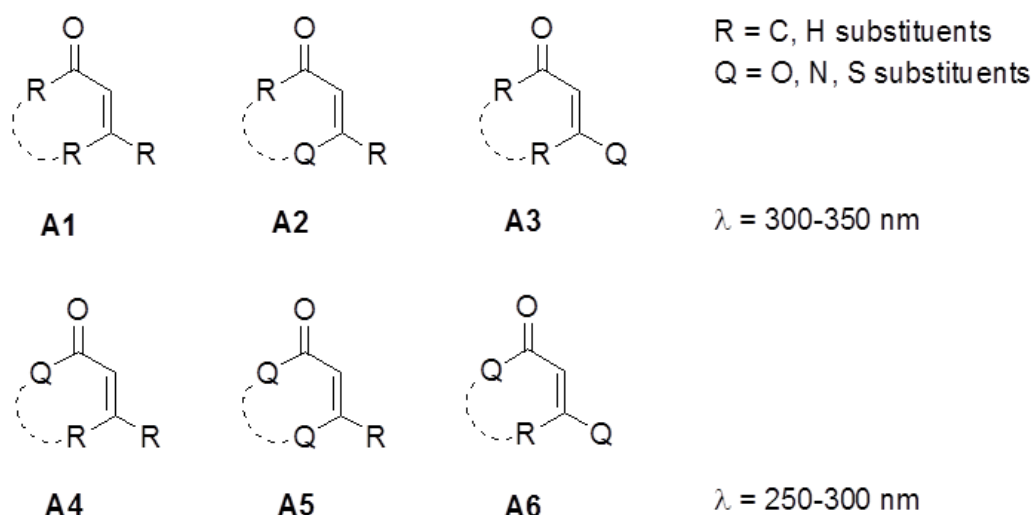
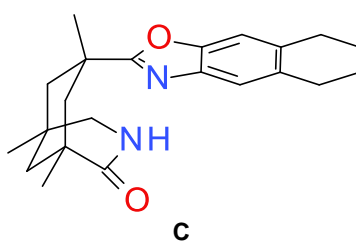


Figure 7: Types of substrates for [2+2]-photocycloaddition according to the type of substituents.

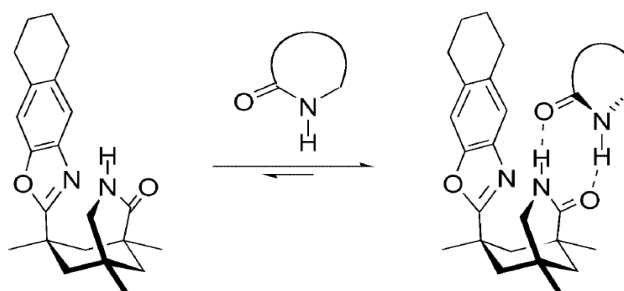
According to the different substituents and heteroatoms the wavelength of irradiation varies. The presence of sulfur substituents is not widely explored.

Photochemical enantioselective approaches to chiral molecules have been pursued along different lines of research. For a reaction to proceed in an enantioselective manner one way can be the use prochiral substrates. However this will only work if the photo-precursor has enantiotopic groups or faces that are recognized by the chiral entity. Providing a chiral environment in a photochemical reaction can be done in several ways, such as the use of homochiral crystals, inclusion complexes and chiral complexing agents (**Scheme 1**).



Scheme 4: Example of a chiral complexing agent.

A chiral complexing agent usually binds to the substrate by non-covalent interactions, establishing a fast and reversible equilibrium. Most chiral templates have motifs capable of establishing hydrogen bonding, and since light does not interfere with hydrogen bonds this has been considered a promising approach to enantiocontrol of photoreactions (**Scheme 2**).¹⁷



Scheme 5: Association behavior of a lactam substrate in the presence of complexing agent **C**

Photochemistry, and in particular [2+2]-PCA are underestimated tools in synthetic organic chemistry. Therefore to prove the versatility and accessibility of the [2+2]-PCA in the establishment of the cyclobutane rings in complex moieties is one the aims of this work.

1.3-Compact Modules in Medicinal Chemistry

Compact modules are essentially novel molecular scaffolds that provide access to specific molecular topologies with a set of diverse functional groups. These building blocks have been playing important roles in synthetic chemistry in the drug discovery processes.

Medicinal chemistry relies on the generation of new leads that discriminate among biological targets, promote selectivity and enhance the safety profile of a drug candidate. An ideal compact module is a polyfunctional scaffold with tunable polarities that affect physico-chemical and safety parameters in a beneficial way. The vectorization of the scaffold plays an important role in the access of a diverse collection of derivatives.¹⁸

Despite the fact that cyclobutanes have a three-dimensional vectorised topology which is a relevant feature in the core of drug structures their use is far from reaching the use of the phenyl group. Even though almost every over-the-counter drug possesses one or more phenyl rings, the higher complexity of recent targets is requiring a more versatile and architectural core.

One of the main goals of this particular work is the synthesis of innovative and complex compact modules containing a cyclobutane ring.

Screening compounds generated from such novel scaffolds readily overcome the molecular 'flatness' (low sp^3 character) which has become prevalent in the industry in recent years, driven by sp^2 - sp^2 aryl couplings emerging as favored synthetic steps. Low alkyl sp^3 character in compounds can have a negative effect on aqueous solubility and formulation, whilst increased aromaticity can increase undesired properties, such as CYP inhibition, plasma-protein binding and hERG binding, which negatively impact drug development.¹⁹

1.4. Alzheimer's disease and BACE1

In the beginning of the 20th century the German psychiatrist and pathologist Alois Alzheimer identified the presence of cellular abnormalities in *post-mortem* brain tissue. The patient had showed progressive memory loss and signs of confusion, which Alzheimer attributed to the formation of these abnormal deposits in the brain

Alzheimer's disease (AD) has become one of most common chronic neurodegenerative diseases and has fast becoming a serious economic and social burden. Characterized by memory and brain function loss this disease interferes with the ability to perform simple daily tasks. Besides affecting the patient itself this degenerative disease has a high impact on the life of the patient's loved ones. The progressive brain degeneration is followed side by side by visible deterioration of the patient's condition.

AD is a prevalent disease globally with a high unmet medical need. Large investments in scientific research have led to the dramatic increase in the comprehension of the pathology over the last 20 years. However, due to the complexity of the molecular pathways in the brain, the mechanisms causing AD are still not fully understood.

1.4.1-The Amyloid cascade hypothesis

AD is pathologically characterized by the existence of two types of structures in the brain of the patients: extracellular deposits known by amyloid plaques and intracellular structures known as neurofibrillary tangles. Both these structures are composed by misfolded proteins/peptides that form neurotoxic aggregates.

Amyloid plaques consist of aggregates of A β peptides. These peptides are formed by the cleavage of the amyloid precursor protein (APP) on the β -site APP

cleaving enzyme (BACE) followed by γ -secretase cleavage. Neurofibrillary tangles consist of aggregates of the TAU protein that suffered hyperphosphorylation leading to conformational changes that inactivate the protein. Even though the hyperphosphorylation of TAU is also a subject of study, deposition of the amyloid β -peptides in the brain is considered the central event towards Alzheimer's disease.

The amyloid cascade hypothesis is based on the accumulation of amyloid- β aggregates ($A\beta$) in the brain that are toxic to neurons. To date the amyloid cascade has not been fully validated however, is the most supported theory.

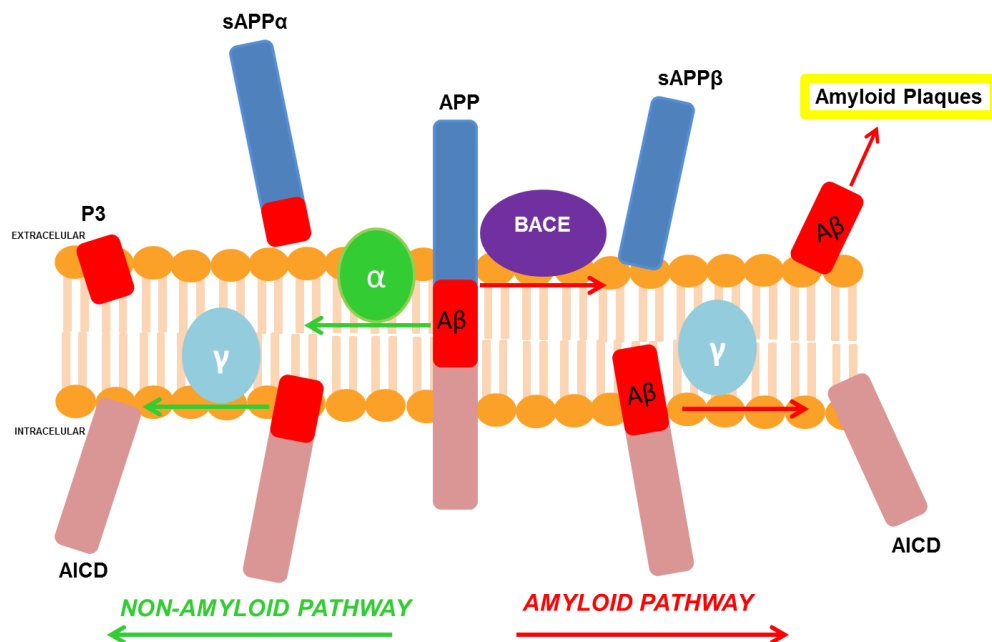


Figure 8: Illustration of the amyloid cascade hypothesis.

The role of APP peptide in the cell is not fully understood. It is known that in a normal person the APP peptides are cleaved by the protease α -secretase, releasing sAPP α and a peptide that is a substrate for the γ -secretase that forms P3 and AICD (APP intracitoplasmatic domain). These peptides are expected to play roles in cell signaling pathways. BACE1 cleaves APP in its β -site leading to the formation of a substrate that when cleaved by γ -secretase releases $A\beta$ peptides that tend to accumulate in brain tissue (**Figure 8**). The cleavage of APP by BACE1 also occurs in healthy organisms. However, in healthy organisms the clearance of $A\beta$ peptides does not allow the accumulation of amyloid. If the clearance mechanisms of $A\beta$ peptides stop working properly there is accumulation. There are two isoforms of $A\beta$: $A\beta_{40}$ and $A\beta_{42}$. The isoform that is more likely to adopt a fibril conformation and accumulate is

A β ₄₂. In familiar cases of AD is known that there is a genetically guided unbalance of the two isoforms in favor of the A β ₄₂. The presence of more A β ₄₂ in the cell makes the formation of amyloid plaques more favorable. Cases of AD with no genetic association usually are caused by the failure of mechanisms of clearance of A β peptides.

Through the years several different hypotheses about the role of the amyloid pathway have been proposed but none of them was completely validated.²⁰

Several mutations in APP have been identified. One of the identified mutations (on Ala-673) leads to the synthesis of an APP analogue that is a less efficient substrate for BACE1. People with this specific mutation have a higher chance to achieve the age of 85 years without Alzheimer's disease as well as slowing the natural cognitive decline in the elderly.²¹ This finding is responsible for reinforcing that BACE1 maybe the therapeutic target of choice when developing anti-Alzheimer's drugs.

Much research has gone into understanding the amyloidogenicity of the A β peptides. Preventing their formation is considered the most promising way to stop the evolution of Alzheimer's disease. Therefore drugs that might induce dissolution of the amyloid aggregates in plaque or inhibit the action of the β -or γ -secretase would be desired for Alzheimer's disease therapy.

1.4.2-BACE1 as a target in Alzheimer's disease therapy.

The few drugs available on the market for the symptomatic treatment and slowing down the progression of AD are targeting the cholinesterase pathway. These inhibitors block the breakdown of acetylcholinesterase that is a messenger in pathways that regulate memory. These drugs only delay the appearance of symptoms without making them regress or stop their progression. Therefore new targets to Alzheimer's disease treatment have to be discovered and explored.

Through the years several evidences have showed that keeping low levels of A β peptides is key to prevent the advance of AD.

BACE1 initiates APP processing in the amyloid pathway, and thus serves as rate-limiting step in production of A β . This together with the fact that BACE1

structural and physiological characteristics are known contributed to the fact that BACE1 was rapidly promoted as a prime target in drug discovery.

BACE1 is the isoform of the β -secretase peptidase expressed in the brain. The other isoform BACE2 is expressed in other tissues and plays different roles in the organism.

Validation of BACE1 as a target in Alzheimer's disease treatment came from observations generated from BACE1 knockout mice. The knockout mice also showed that complete inhibition of BACE1 might severe side effects like muscular contraction atrophy. Therefore only 50% of inhibition is the goal in the drug discovery process.

BACE1 is a more favorable target than γ -secretase due to the fact that the second one is involved in several pathways in the cell being crucial to the formation of transcription factors. Inhibition of γ -secretase would lead to more undesirable side effects and would require a more challenging and careful regulation mechanisms.

The aim of this work is the synthesis of novel tricyclic scaffolds that could be potentially functionalized to obtain compounds that potentially have activity as BACE1 inhibitors.

1.5- References

- ¹ <http://goldbook.iupac.org/P04588.html> (Last consulted at 1st December 2014)
- ² P. Klán, J. Wirz, "Photochemistry of Organic Compounds-From concepts to practice" Wiley, Chichester, **2009**
- ³ A. G. Griesbeck, J. Mattay, "Molecular and Supramolecular Photochemistry-Synthetic Organic Photochemistry", Volume 12, Marcel Dekker, New York, **2005**
- ⁴ K.H. Pfoertner, *J. Photochem.* **1984**, 25, 91-97
- ⁶ A. Albini, M. Fagnoni, 'Handbook of Synthetic Photochemistry' Wiley-VCH, Weinheim, **2010**
- ⁷ <http://www.britannica.com/EBchecked/topic/457736/photochemical-reaction> (Last consulted at 2nd December 2014).
- ⁸ E. Hückel, *Z. Physik*, **1931**, 71, 204-286
- ⁹ <http://www.firstlightlamps.co.uk/flowtubes-materials-selection.html> (last consulted at 6th of May 2015)
- ¹⁰ <http://www.rayonet.org/graphscharts.htm> (last consulted in the 6th of May 2015)
- ¹¹ L. Kürti, B. Czakó, E. J. Corey, K. C. Nicolaou "Strategic Applications of Named Reactions in organic Synthesis" Elsevier Academic Press, **2005**
- ¹² E. J. Corey, J. D. Bass, R. Le Mathiew, R. B. Mitra, *Can. J. Chem.*, **1963**, 41, 440-449
- ¹³ D. Becker, N. Haddad, *Org. Photochem.*, **1989**, 10, 1-162
- ¹⁴ R. Brimioulle, T. Bach. *Angew. Chem. Int. Ed.*, **2014**, 53, 12921-12924.
- ¹⁵ S. Wilsey, L. González, M. A. Robb, K. N. Houk, *J. Am. Chem. Soc.*, **2000**, 122, 5866-5876
- ¹⁶ D. I. Schuster, G. Lem, N. A. Kaprinidis, *Chem Rev.*, **1993**, 93, 3-22
- ¹⁷ B. Grosch, C. N. Orlebar, E. Herdweck, M. Kaneda, T. Wada, Y. Inoue, T. Bach, *Chem.-Eur.-J.*, **2004**, 10, 2179-2189
- ¹⁸ M. Rogers-Evans, H. Knust, J. Plancher, E. M. Carreira, G. Wuitschik, J. Burkhard, D. B. Li, C. Guérot, *Chimia*, **2014**, 68, 492-499
- ¹⁹ W. P. Walters, J. Green, J. R. Weiss, M. A. Murcko, *J. Med. Chem.*, **2011**, 54, 6405-6416
- ²⁰ J. Varghese, 'BACE: Lead Target for Orchestrated Therapy of Alzheimer's Disease', Wiley, **2010**

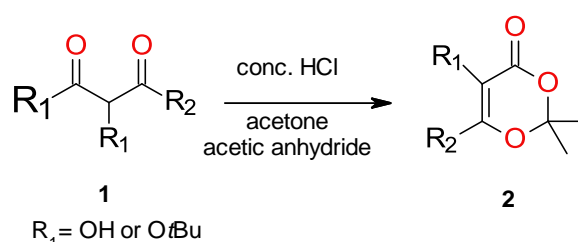
-
- ²¹ D. Oehrich, H. Prokopcova, H. J. M. Gijsen, *Bioorg. Med. Chem. Lett.*, **2014**, 24, 2033-2045

2-[2+2]-Photocycloaddition of 1,3-dioxin-4-ones vs 1,3-oxathiin-6-ones.

2.1-1,3-Dioxin-4-ones

1,3-Dioxin-4-ones have been used extensively in synthetic organic chemistry, representing ideal substitutes for β -ketocarboxylic acids. The potential use of 1,3-dioxin-4-ones derivatives as scaffolds in natural product synthesis has been widely explored.¹

In the second half of the 20th century the synthesis of 1,3-dioxin-4-ones was based on a 1,4-cycloaddition of ketones to acylketenes. In 1983 Sato *et al.*² reported a facile and general synthetic method using β -keto acid derivatives to obtain 1,3-dioxin-4-ones that have been used until recent times (**Scheme 1**).



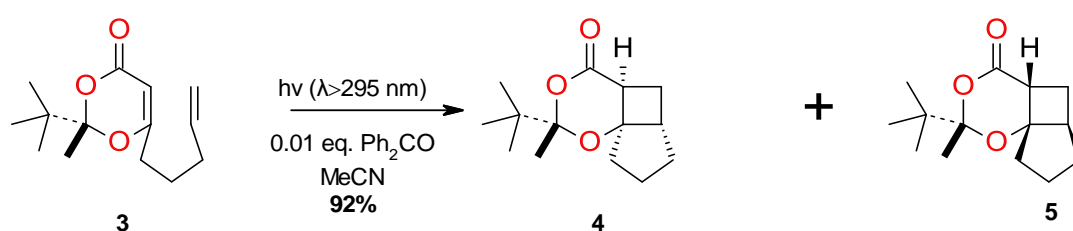
Scheme 1

Since the 1980's 1,3-dioxin-4-ones have been used as substrates in photoreactions. The first studies began with the [2+2]-photocycloaddition of cyclopentene and cyclohexene to form cyclobutane adducts. Several studies tried to propose mechanistic hypotheses to explain and predict the stereochemistry of the formed products.³ Various studies led to the conclusion that the facial selectivity achieved in the photocycloaddition of 1,3-dioxin-4-ones is opposite to the selectivity observed in the ground state reactions, hence the photoaddition tends to occur from the apparently most hindered face. To explain this stereochemical outcome has been proposed some explanations that imply the different conformation of the carbon atom C-6.^{4,9} [2+2]-Photocycloaddition of 1,3-dioxin-4-ones leads to the formation a new stereogenic center in which diastereofacial control can be achieved.

Winkler *et al.*⁵ used intramolecular [2+2]-PCA of 1,3-dioxin-4-ones in the synthesis of several complex natural products. The use of acetone as co-solvent in the reaction provided sensitization allowing the access to the product in higher yield.

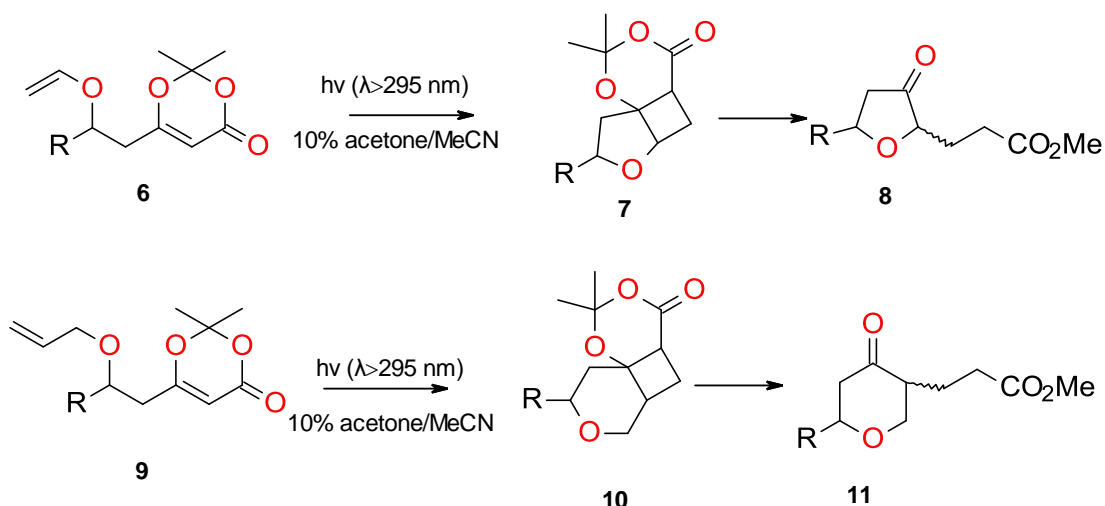
In order to develop methods with high stereoselectivity for the synthesis of spiro-ketals, Haddad *et al.*⁶ used a diastereoselective intramolecular photocycloaddition of a chiral 1,3-dioxin-4-one that allowed the generation of four stereogenic centers. The dioxinone functionality had several advantages, such as providing the required carbon-carbon double bond, enabling the selective fragmentation of the produced four-membered ring for further functionalization, introducing ketone functionality in the spiro ring, necessary for oxidative enlargement for the synthesis of spiro-ketals and allowing asymmetric induction.

From the 2-*tert*-butyl-2,6-dimethyl-1,3-dioxin-4-one through an alkylation reaction using LDA as the deprotonation agent and the required homoallylic halide it is possible to obtain the photoprecursor **3**. Irradiation of **3** in a Pyrex filter flask ($\lambda > 295$ nm in MeCN) in the presence of benzophenone as a sensitizer afforded the tricyclic isomers **4** and **5** in 92% yield. Haddad and his team reported that the temperature at which the reaction was performed had an influence in the facial selectivity of the [2+2]-PCA. The increase of the temperature from -70 °C to 0 °C caused a decrease in selectivity, however in both cases the major product was **5**. This shows a preference for the less hindered face of the dioxinone (**Scheme 2**).⁶



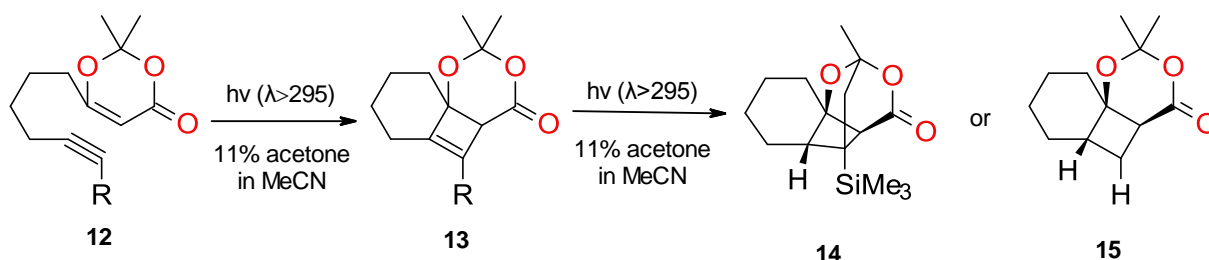
Scheme 2

Increasing of the chain by one carbon it is possible to form 6-membered rings through the intramolecular [2+2]-PCA. Carreira *et al.*'s *O*-allyl and *O*-vinyl dioxinone ethers (**6** and **9**) gave tricyclic ring systems, that under alkaline conditions fragments into 2,5-disubstituted tetrahydrofuran-3-ones and 2,5-disubstituted tetrahydropyran-4-ones – both are common building blocks in natural product synthesis (**Scheme 3**).⁷



Scheme 3

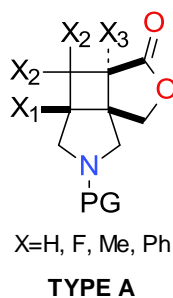
More recently in 2005, Winkler *et al.*⁸ reported the intramolecular photocycloaddition of dioxinones with alkynes leading to the formation of cyclobutene adducts, which are unstable under the photochemical reaction conditions and afforded secondary photoproducts, whose structure differed by the substituent on the alkyne photoprecursor (**Scheme 4**).



Scheme 4

Given the potential use of 1,3-dioxin-4-ones as new scaffolds for medicinal chemistry, the synthesis of novel spiroketals with a tricyclic skeleton seemed the right step towards the formation of complex compact modules being interesting for drug discovery.

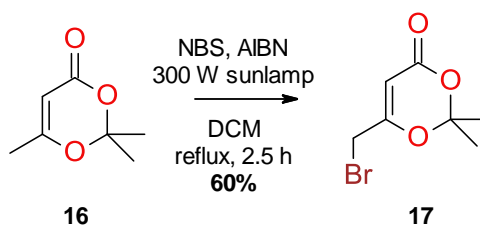
Since previous studies have shown that lactones of the type **A** (**Scheme 5**) can be generated by intramolecular [2+2]-photocycloaddition reactions of appropriately substituted 4-aminomethyl-2(5*H*)-furanones, a similar approach to synthesize the corresponding 1,3-dioxin-4-ones substrates for the intramolecular [2+2]-PCA reaction was used.



Scheme 5

6-Bromomethyl-2,2-dimethyl-1,3-dioxin-4-one has been described in the literature since the early 1990's,⁹ and has been employed in phosphonium salt generation reactions,¹⁰ substitution with soft carbon nucleophiles,⁶ and worked as an activated β -ketoester in several experiments.¹¹ Despite its easy access there is no record of substitution of the bromide with nitrogen nucleophiles. The synthesis of a novel photoprecursor combining a 1,3-dioxin-4-one moiety and a pyrrolidine ring was planned.

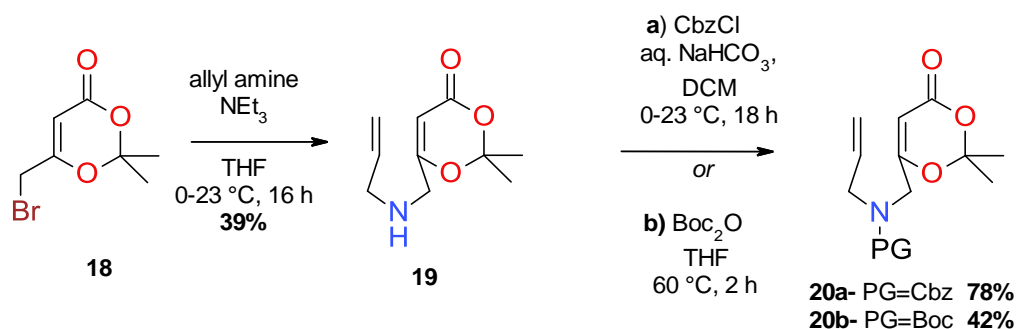
Although several routes to access compound **17** can be found in the literature,¹² the one that proved to be the most reliable in our hands started from the commercially available 2,2,6-trimethyl-4*H*-1,3-dioxin-4-one. Through a Wohl-Ziegler bromination, exposing a mixture of the substrate **16**, NBS and AIBN as a radical initiator to sun lamp irradiation, we were able to obtain the 6-bromomethyl-2,2-dimethyl-1,3-dioxin-4-one in 60% yield. The replacement of CCl_4 , used in the procedure described by Sato *et al.*,⁹ by CH_2Cl_2 , allowed a more environmental friendly approach without compromising the yield (**Scheme 6**).



Scheme 6

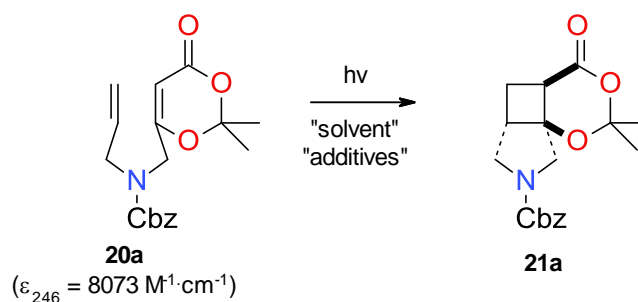
In order to access the desired photoprecursor nucleophilic substitution with allyl amine was performed, followed by Cbz-protection under Schotten-Baumann conditions to afford photoprecursor **20a**. Regardless of the moderate yields achieved

in the bromination and alkylation reactions, this 3-step route allows an easy access to the photoprecursor and can be reliably scaled up. To further investigate the influence of a different protecting group the photoprecursor **20b** was also synthesized using a standard protocol of amine protection with Boc₂O (**Scheme 7**).



Scheme 7

The unique photoprecursors **20a** and **20b** were successfully synthesized. The UV spectrum of **20a** was measured as well as the extinction coefficient (ϵ) determined, showing the maximum absorption at 246 nm ($\epsilon_{246} = 8073 \text{ M}^{-1} \cdot \text{cm}^{-1}$). With this data in hand it was predicted that irradiation of **20a** at 254 nm would lead to a lot of uptake of energy, hence short reaction times necessary to avoid large extent of photodecomposition (**Scheme 8**).



Scheme 8

Results showed that irradiation at a wavelength of 254 nm for only 1 hour in acetonitrile furnished the desired photoproducts in very good yield (**Table 1**). The Boc group proved to be more stable and “photofriendly” than the Cbz group resulting in a higher yield (75% (Boc) vs. 57% (Cbz)). This can be rationalized by the presence of the π system and the benzylic position in the Cbz protecting group that at high energy wavelengths can be excited and cause increase of the energy in the molecule leading to decomposition. Sensitization with acetone and benzophenone lead to very slow reactions and decomposition of starting material.

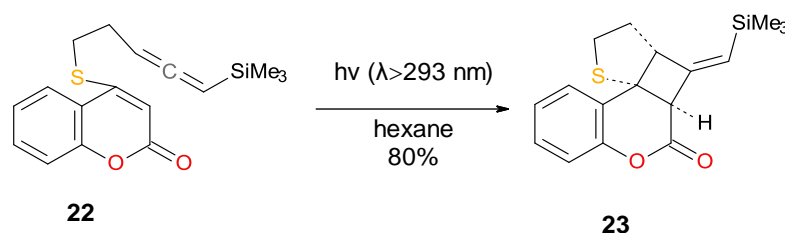
Table 1: Optimization of reaction conditions for the intramolecular [2+2]-PCA.

#	s.m.	PG	λ [nm]	Solvent	Additives	[c] [mM]	Reaction time	P	Yield [%]
1	20b	Boc	254	MeCN	none	5	1 h	21b	75
2	20a	Cbz	254	MeCN	none	5	1 h	21a	57
3	20a	Cbz	300	acetone	none	5	5 days	21a	decomposition
4	20a	Cbz	350	MeCN	0.1 equiv. Ph ₂ CO	5	5 days	21a	decomposition

The synthesis of complex photoproducts **21a** and **21b** was reported. Optimization of the intramolecular [2+2]-PCA reaction was accomplished. The unique 1,3-dioxin-4-ones derivatives can be used as molecular scaffolds given the variety of opportunities of further functionalization. The dioxinone ring can be cleaved in basic conditions providing two new exit vectors with a defined regiostereochemistry. These novel and easy accessed scaffolds have a vast potential in the synthesis of complex natural products.

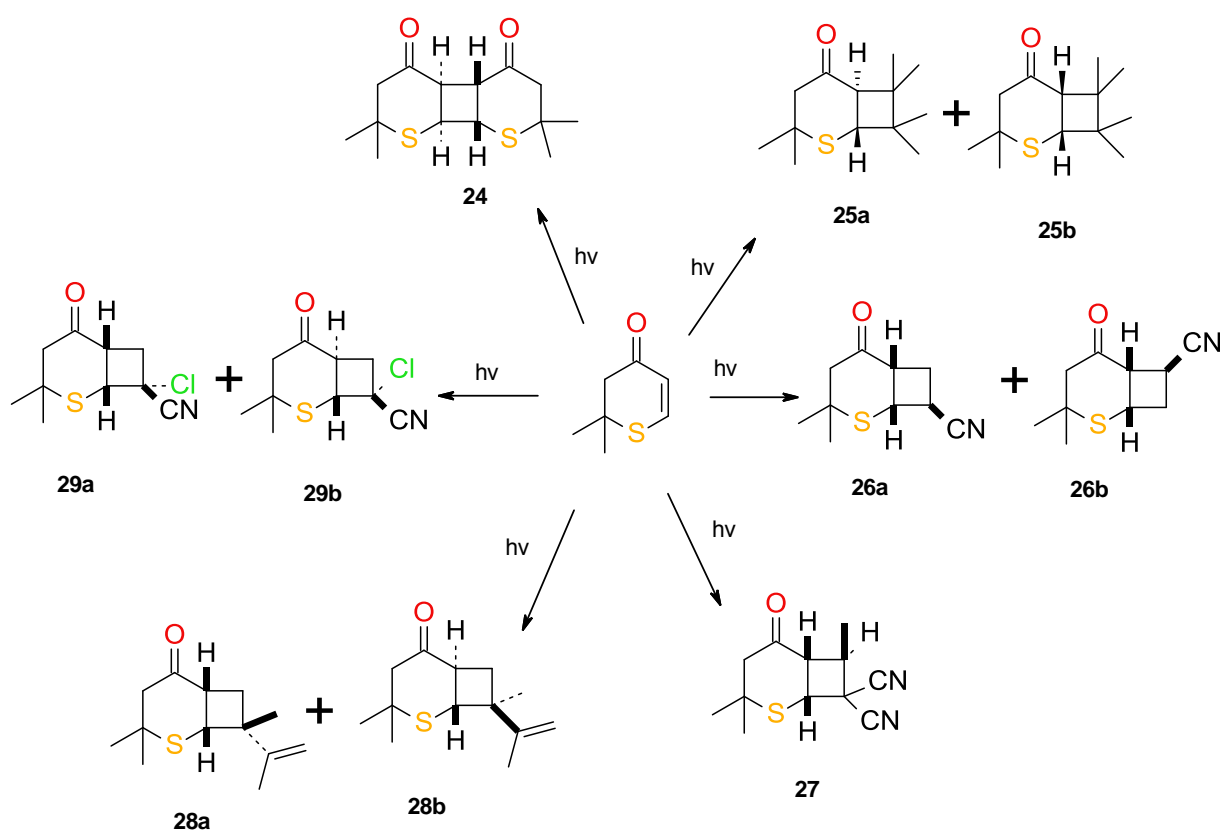
2.2-1,3-Oxathiin-6-ones

Coumarins with an exocyclic sulfur have been used by Carreira *et al.* in [2+2] PCA. Active allenylsilane **22** undergoes intramolecular [2+2]-PCA with enone to form cyclobutane adduct **23** which can further undergoes a protodesilylation. This was a step forward to the use of sulfur in intramolecular [2+2]-PCA (**Scheme 9**).¹³

**Scheme 9**

Cyclobutane rings with a sulfur atom attached are compounds exhibiting interesting properties. Although [2+2]-PCA reactions have been proven to be a useful synthetic tool to form the cyclobutane moiety, there is not much precedence about the use of this photochemical step in the formation of cyclobutane ring substituted with sulfur atoms.

Margaretha *et al.*¹⁴ have reported several experiments regarding intermolecular photocycloaddition of 2,2-dimethyl-3*H*-thiopyran-4-one (**Scheme 10**). Irradiation of 2,2-dimethyl-3*H*-thiopyran-4-one at a wavelength of 350 nm in benzene in the presence of substituted alkenes afforded several different photoadducts with specific stereochemistry. While with 2-chloroacrylonitrile there was only formation of [2+2]-photocycloadducts, in the presence of isoprene [2+4]-photocycloadducts were also isolated. This research group has described that the regio- and stereospecificity as well as the type of adducts formed strongly depended on the chosen alkene to react with the thiopyranone.

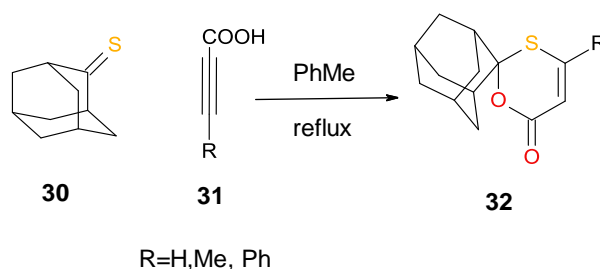


Scheme 10

The sulfur derived 1,3-oxathiine-6-ones are known,**Erro! Marcador não definido.** however they have not been employed in [2+2]-PCA.

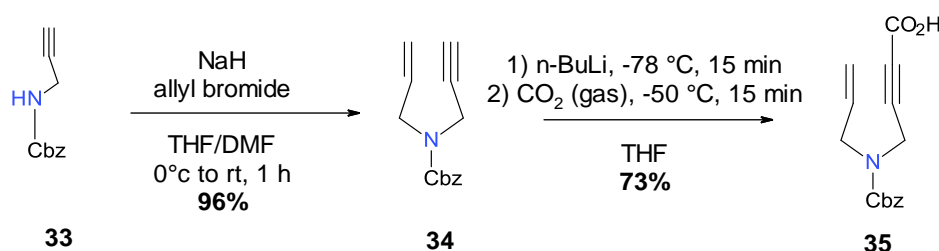
In the 1970's the condensation of thiobenzophenone with acetylenes was reported with good yields.¹⁵ Years later the same approach was used by Okuma *et al.***Erro! Marcador não definido.** to condense thioketones with propiolic acids. The successful treatment of adamantane-2-thione with propiolic acid in refluxing toluene to form the correspondent spiro derivative with high yields served as inspiration for

the synthesis of a new and unique photoprecursor with a spiro adamantane residue connected to a 1,3-oxathiin-6-one (**Scheme 11**).



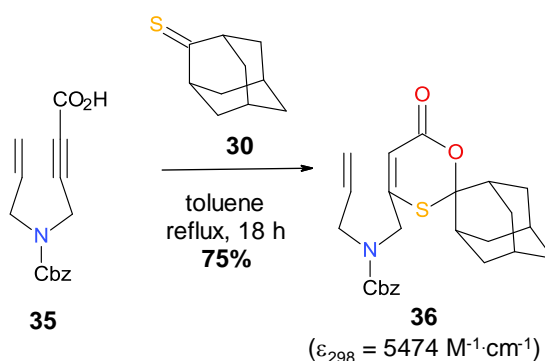
Scheme 11

The desired propiolic acid was synthesized from commercially available propargylamine by protection with CbzCl to furnish the protected amine **33**. Alkylation with allyl bromide using NaH as base gave benzyl allyl(prop-2-yn-1-yl)carbamate **34**; further deprotonation of the terminal alkyne with *n*-BuLi followed by the carboxylation with CO₂ gas originated the novel propiolic acid **35** (**Scheme 12**).



Scheme 12

The propiolic acid **35** was condensed with the known adamantane-2-thione.¹⁵ The photoprecursor **36** was obtained by simply refluxing in toluene for 18 h in 75% yield (**Scheme 13**). In contrast to the large excess of propiolic acid (3 equiv.) described by Okuma *et al.*, equimolar amounts of propiolic acid and adamantane-2-thione were sufficient to obtain **36** in 75% yield.



Scheme 13

The UV spectrum of compound **36** exhibited a strong absorption at 298 nm what predicted that direct irradiation of the photoprecursor at 300 nm would result most likely in quick photodecomposition. Considering the UV spectrum of **20a**, the sulfur derivative **36** showed a strong bathochromic shift (~50 nm) (**Figure 1**).

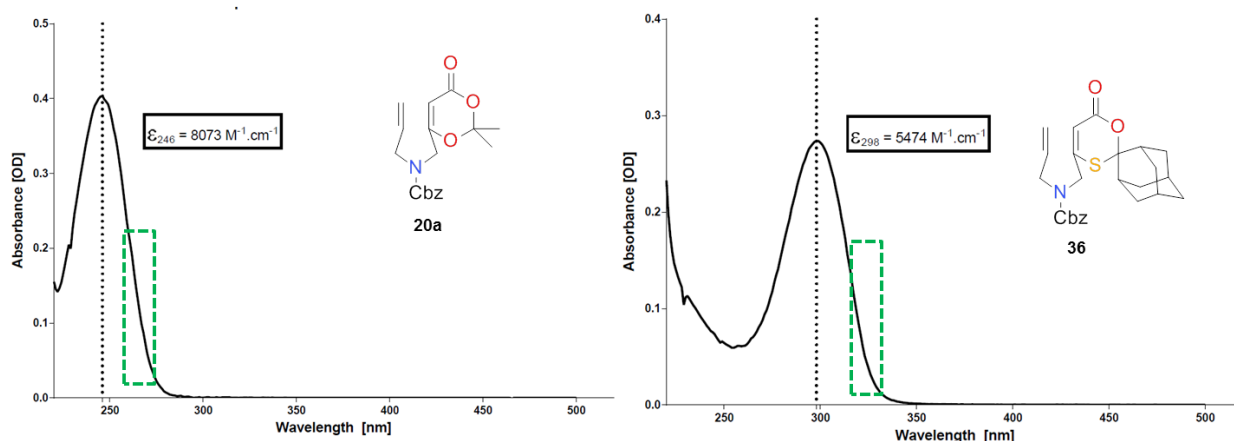
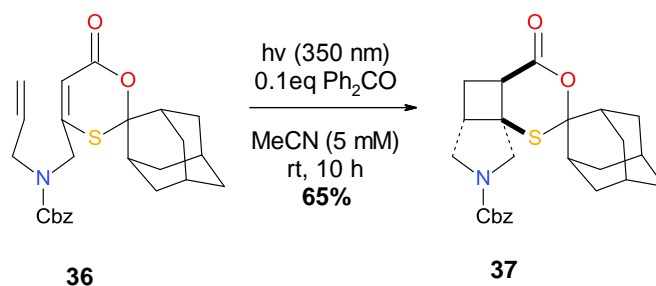


Figure 1: UV-spectrum of compounds **20a** and **36** measured in 50 μM in acetonitrile. The green dashed box represents the ideal wavelength of irradiation to perform a photoreaction

A first attempt to synthesize compound **37** was done by simple irradiation at 350 nm at room temperature using diethyl ether as a solvent (5 mM for 18 h). Although there was a significant consumption of starting material **36**, full conversion was not achieved and no product could be isolated. As expected increasing the energy by irradiation at 300 nm using diethyl ether as solvent (5 mM) resulted in full photodecomposition in less than 30 min.

While the direct irradiation at 350 nm did not result in desired product formation, irradiation at 300 nm was too high in energy leading to a quick decomposition of the starting material. Therefore the possibility of triplet sensitization was considered. A first test reaction was performed by irradiating the substrate at 350 nm in acetonitrile (5 mM) in the presence of 0.1 equiv. of benzophenone at room temperature. After 10 hours there was full consumption of starting material and the product **36** was isolated in 65% yield (**Scheme 14**).



Scheme 14

Another test reaction was performed to assess the efficacy of acetone as a solvent but also as triplet sensitizer. After 10 hours of irradiation at 350 nm at room temperature there was complete consumption of starting material but the isolated yield was just 35%. These results showed that triplet sensitization using 0.1 eq. of benzophenone in acetonitrile were the better conditions to perform this particular [2+2]-PCA (**Table 2**).

Table 2: Optimization of reaction conditions for the intramolecular [2+2]-PCA.

#	s. m.	PG	λ [nm]	Solvent	Additives	[c] [mM]	Reaction time	Yield of 37 [%]
1	36	Cbz	300	Et ₂ O	none	9	12 h	decomposition
2	36	Cbz	350	Et ₂ O	none	9	0.5 h	decomposition
3	36	Cbz	350	acetone	none	5	10 h	35
4	36	Cbz	350	MeCN	0.1 eq. Ph ₂ CO	5	10 h	65

The complex product **37** was successfully synthesized from a novel propiolic acid (**35**) and the known thioadamantanone followed by a [2+2]-PCA. Using reliable and known procedures the innovative photoproduct **37** has proven, once again, that sulfur and photochemistry are not incompatible.

Once again a complex novel tricyclic moiety was accessed. To our knowledge this is the first example where a *cis*-relationship of a carboxyl group and a low valent sulfur has been accessed by [2+2]-PCA. The optimization of the reaction conditions showed that in this case triplet sensitization is the key to the success of using low valent sulfur in photocycloadditions.

2.3-Conclusion

The synthesis of exciting novel photoproducts has been reported. For the first time an approach towards the functionalization of the easy accessible 6-(bromomethyl)-2,2-dimethyl-4H-1,3-dioxin-4-one (**17**) with nitrogen nucleophiles was described. A novel heterocyclic moiety fused with the dioxin-4-one ring was achieved by a common procedure of [2+2]-PCA reaction. A variety of exciting new complex tricyclic skeletons were synthesized. Studies of optimization of the synthesis proved that Boc was the preferred protecting group and that photosensitization had no beneficial impact in the synthesis of the photoproduct.

Significant differences between the UV absorption of the 1,3-dioxin-4-ones and its sulfur analogs (1,3-oxathiin-6-ones) were verified. A strong bathochromic shift (~50 nm) was observed in the UV-spectrum of the sulfur compound in comparison to the 1,3-dioxin-4-one. The light absorption characteristics of the compounds have consequences in the choice of the reactions conditions, such as the wavelength of irradiation and presence or absence of sensitizers. Sensitization in the photocycloaddition of the sulfur derivatives was key to success

Despite the limited number of literature examples in this area, a [2+2]-PCA was performed successfully with a sulphur derivative. 1,3-Oxathiin-6-one derivatives can be used as substrates in [2+2]-PCA to access novel scaffolds with potential interest in medicinal chemistry. The regio- and diastereoselective *cis* conformation of the fused 1,3-oxathiin-6-one cyclobutane ring, with sulfur substituents, is completely groundbreaking in this field.

The condensation of adamantane-2-thione with propiolic acids has proven to be efficient in the synthesis of 1,3-oxathiin-6-ones derivatives.

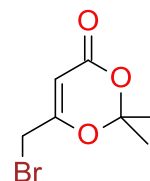
In summary, the set of reactions described provide a convenient access to various derivatives of 1,3-dioxin-4-ones and 1,3-oxathiin-6-ones that were employed successfully in [2+2]-PCA reactions. Completely novel complex photoproducts have shown versatility as molecular scaffolds allowing a great number of opportunities for further decoration.

2.4-Experimental section:

General: For the photoreactions a Rayonet RPR 200 merry-go-round reactor, equipped with 16 Rayonet RPR-2537 Å lamps ($\lambda = 254, 300$ and 350 nm) was used. Unless otherwise stated, the reactions were stopped when the starting material was fully consumed according to thin layer chromatography (TLC) and/or LC/MS analysis. Compounds were detected by UV ($\lambda = 254$ nm), CAM (cerium ammonium molybdate solution) or KMnO_4 . ^1H NMR: Bruker AV-300, AV-400 and AV-600 recorded at 300 K unless otherwise indicated. Chemical shifts are reported relative to the solvent [CHCl_3 : δ (^1H) = 7.26 ppm, DMSO δ (^1H) = 2.50 ppm as reference. The relative configuration of the products was determined by two-dimensional NMR spectra (COSY, NOESY, HSQC, HMBC). The UV-spectrum and extinction coefficient (ϵ) were conducted on a UV-Vis Thermo Evolution 220 spectrophotometer. HRMS data were recorded by electron spray ionization (ESI) on an ion trap mass spectrometer.

6-(Bromomethyl)-2,2-dimethyl-4*H*-1,3-dioxin-4-one (17):

A mixture of 2,2,6-trimethyl-4*H*-1,3-dioxin-4-one (2.97 g, 20.9 mmol, equiv: 1), *N*-bromosuccinimide (4.09 g, 23 mmol, equiv: 1.1) and AIBN (105 mg, 637 μmol , Eq: 0.0305) in dichloromethane (105 mL) was irradiated with a 300 W sunlamp (Osram Ultra-Vitalux). The mixture refluxed for 2.5 h. All volatiles were removed under vacuum and the crude material was purified by flash chromatography (silica gel, 100 g, 0% to 5% EtOAc in heptane) to give the 6-(bromomethyl)-2,2-dimethyl-4*H*-1,3-dioxin-4-one (3.95 g, 58% yield) as a light yellow liquid.

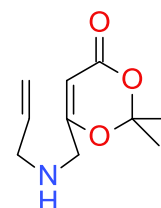


According to literature:¹¹

^1H NMR (600 MHz, CDCl_3) δ ppm 1.72 (s, 6H), 3.88 (s, 2H), 5.53 (s, 1H).

6-((Allylamino)methyl)-2,2-dimethyl-4*H*-1,3-dioxin-4-one (19):

6-(Bromomethyl)-2,2-dimethyl-4*H*-1,3-dioxin-4-one (500 mg, 2.26 mmol, equiv: 1.0) was dissolved in THF and cooled to 0 °C. A solution of prop-2-en-1-amine (129 mg, 170 μL , 2.26 mmol, equiv: 1.0) and NEt_3 (252 mg, 347 μL , 2.49 mmol, equiv: 1.1) in THF was added, and the reaction mixture was stirred at 23 °C during 18 h. All volatiles



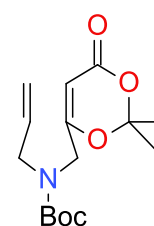
were removed under vacuum. The crude material was purified by flash chromatography (silica gel, 20 g, 0% to 100% EtOAc in heptane) to give 6-((allylamino)methyl)-2,2-dimethyl-4*H*-1,3-dioxin-4-one (446 mg, 40% yield) as a colorless oil.

¹H NMR (600 MHz, CDCl₃) δ ppm 1.70 (s, 6 H) 3.27 (dt, *J*=6.0, 1.4 Hz, 2 H) 3.36 (d, *J*=0.9 Hz, 2 H) 5.11 - 5.25 (m, 2 H) 5.47 (s, 1 H) 5.80 - 5.91 (m, 1 H)

HRMS *m/z*=198.1124 [M+H]⁺ calculated from C₁₀H₁₅NO₃ (M=197.10519)

Benzyl allyl((2,2-dimethyl-4-oxo-4*H*-1,3-dioxin-6-yl)methyl)carbamate (20a):

To a mixture of 6-((allylamino)methyl)-2,2-dimethyl-4*H*-1,3-dioxin-4-one (82 mg, 416 μmol, equiv: 1.0) and sodium bicarbonate (559 mg, 6.65 mmol, equiv: 16) in dichloromethane (245 μl) at 23 °C. Cbz-Cl (213 mg, 178 μl, 1.25 mmol, equiv: 3) was added dropwise. The mixture was stirred at 23°C during 16 h, poured into H₂O and extracted with dichloromethane. The organic layers were collected and dried over Na₂SO₄. All volatiles were removed under vacuum. The crude material was purified by flash chromatography (silica gel, 10 g, 0% to 100 %, EtOAc in heptane) to give benzyl allyl((2,2-dimethyl-4-oxo-4*H*-1,3-dioxin-6-yl)methyl)carbamate (110 mg, 80% yield) as a colorless oil.

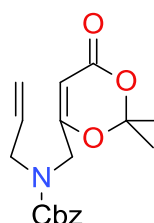


¹H NMR (600MHz, CDCl₃) δ ppm 1.52 (s, 3 H) 1.68 (s, 3 H) 3.86 (s, 4 H) 3.92 (br d, 2 H) 5.13 - 5.20 (m, 2 H) 5.32 (s, 1 H) 5.70 - 5.83 (m, 1 H)

LCMS (ESI) *m/z*=314.9 [M+NH₄]⁺ calculated from C₁₅H₂₃NO₅ (M=297)

***tert*-Butyl allyl((2,2-dimethyl-4-oxo-4*H*-1,3-dioxin-6-yl)methyl)carbamate (20b):**

6-((Allylamino)methyl)-2,2-dimethyl-4*H*-1,3-dioxin-4-one (180 mg, 913 μmol, equiv: 1.0) was dissolved in THF (2.28 mL), and Boc₂O (219 mg, 233 μl, 1.00 mmol, equiv: 1.1) was added. The reaction mixture was heated at 40 °C during 2 hours. All volatiles were removed under vacuum. The crude material was purified by flash chromatography (silica gel, 10 g, 0% to 100 % EtOAc in heptane) to give *tert*-butyl allyl((2,2-dimethyl-4-oxo-4*H*-1,3-dioxin-6-yl)methyl)carbamate (113 mg, 42% yield) as an orange oil.

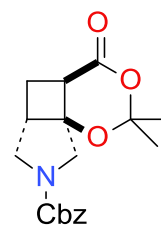


¹H NMR (600 MHz, CDCl₃) δ ppm 1.28 - 1.79 (m, 7 H) 3.74 - 4.14 (m, 4 H) 5.06 - 5.25 (m, 4 H) 5.26 - 5.41 (m, 1 H) 5.57 - 5.96 (m, 1 H) 7.29 - 7.48 (m, 5 H)

HRMS m/z = 332.14875 [M+H]⁺ calculated from C₁₈H₂₁NO₅ (M=331.1418)

(4aRS,5aSR,8aSR)-Benzyl 2,2-dimethyl-4-oxotetrahydro-4H-[1,3]dioxino[4',5':1,4]cyclobuta[1,2-c]pyrrole-7(8H)-carboxylate (21b):

In a 100 ml Kjeldahl quartz vessel a solution of benzyl allyl((2,2-dimethyl-4-oxo-4H-1,3-dioxin-6-yl)methyl)carbamate (905 mg, 2.73 mmol, equiv: 1.0) in acetonitrile (546 mL) was degassed bubbling argon through the solution, under sonication, for 30 min. Then the mixture was irradiated in a Rayonet RPR-200 reactor (16 x 8 W lamps) at 254 nm for 1 h. LC/MS indicated total consumption of starting material. All volatiles were removed under vacuum. The crude material was purified by flash chromatography (silica gel, 20 g, 0% to 100% EtOAc in heptane) to give (4aRS,5aSR,8aSR)-benzyl 2,2-dimethyl-4-oxotetrahydro-4H-[1,3]dioxino[4',5':1,4]cyclobuta[1,2-c]pyrrole-7(8H)-carboxylate (547 mg, 60% yield) as a colorless oil.

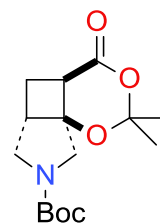


¹H NMR (600 MHz, CDCl₃) δ ppm 1.52 (s, 3 H) 1.59 (s, 3 H) 2.05 (br s, 1 H) 2.54 – 2.59 (m, 1 H) 2.82 - 2.86 (m, 1 H) 3.08 (br s, 1 H) 3.38 – 3.46 (m, 3 H) 4.08 7.33 – 7.41 (m, 5 H)

LC/MS (ESI) m/z = 230.6 [M-Boc]⁺ calculated from C₁₈H₂₁NO₅ (M=331.1419)

(4aRS,5aSR,8aSR)-tert-Butyl 2,2-dimethyl-4-oxotetrahydro-4H-[1,3]dioxino[4',5':1,4]cyclobuta[1,2-c]pyrrole-7(8H)-carboxylate (21a):

tert-Butyl allyl((2,2-dimethyl-4-oxo-4H-1,3-dioxin-6-yl)methyl)carbamate (20 mg, 67.3 μmol, equiv: 1.0) was dissolved in acetonitrile (13.5 mL) and irradiated at 254 nm during 1 hour. LC/MS indicated total consumption of starting material. All volatiles were removed under vacuum. The crude material was purified by flash chromatography (silica gel, 20 g, 0% to 100% EtOAc in heptane) to give (4aRS,5aSR,8aSR)-*tert*-Butyl 2,2-dimethyl-4-oxotetrahydro-4H-[1,3] dioxino[4',5':1,4] cyclobuta[1,2-c]pyrrole-7(8H)-carboxylate (15 mg, 75% yield) as a colorless oil.

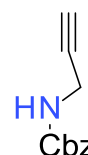


¹H NMR (600 MHz, CDCl₃) δ ppm 1.49 (s, 9 H) 1.53 (s, 6 H) 2.05 (br s, 1 H) 2.56 (ddd, *J* = 13, 9.9, 4.7 Hz, 1 H) 2.82 (br dd, *J* = 13, 9.9 Hz, 1 H) 3.15 (br dd, *J* = 13, 9.9 Hz, 1 H) 3.31 – 3.38 (m, 4 H)

GC/MS (EI): *m/z* = 198 [M-Boc]⁺ calculated from C₁₅H₁₃NO₅ (M = 297.1576)

Benzyl prop-2-yn-1-ylcarbamate (33):

A vigorously stirred mixture of prop-2-yn-1-amine (12.85 g, 233 mmol, equiv: 1.0) combined with a saturated solution of sodium bicarbonate (19.6 g, 300 ml, 233 mmol, equiv: 1.0) in dichloromethane (200 mL) was cooled down to - 10 °C. Cbz-Cl (41.8 g, 35 mL, 245 mmol, equiv: 1.05) was added via syringe within 2 min. The mixture was stirred at 23 °C during 18 h. The reaction mixture was extracted with dichloromethane washed with water and brine. The organic layers were collected and dried over Na₂SO₄. All volatiles were removed under vacuum. The crude material was purified by flash chromatography (silica gel, 200 g, 0% to 25% EtOAc in heptane) to give benzyl prop-2-yn-1-ylcarbamate (34.7 g, 78.6 % yield) as a light yellow oil.



According to literature:¹⁶

¹H NMR (400MHz, CDCl₃, 60 °C) δ ppm 7.36-7.29 (m, 5H), 5.14 (s, 2H), 4.85 (s, 1H), 3.99 (dd, *J* = 5.7, 2.6 Hz, 2H), 2.23 (t, *J* = 2.6 Hz, 1H);

HRMS: *m/z* = 189.0790 [M⁺] calculated from C₁₁H₁₁NO₂ (M = 189.0786)

Benzyl allyl(prop-2-yn-1-yl)carbamate (34):

To a solution of benzyl prop-2-yn-1-ylcarbamate (1.08 g, 4.71 mmol, equiv: 1.0) and allyl bromide (767 mg, 549 μl, 6.34 mmol, equiv: 1.2) in a mixture of tetrahydrofuran (15 mL) and *N,N*-dimethylformamide (15 mL) at 0 °C. NaH (254 mg, 6.34 mmol, equiv: 1.2) was added carefully. This mixture was stirred at 23 °C during 1 h the reaction was carefully quenched with H₂O. The product was extracted with EtOAc. The organic layers were collected and dried over Na₂SO₄. All volatiles were removed under vacuum. The crude material was purified by flash chromatography (silica gel, 20 g, 0% to 30 % EtOAc in heptane) to give benzyl allyl(prop-2-yn-1-yl)carbamate (1.08 g, 89% yield) as a colorless oil.



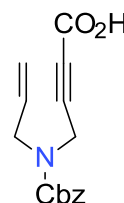
According to literature:¹⁶

¹H NMR (400MHz, CDCl₃, 60 °C) δ ppm 7.38-7.28 (m, 5H), 5.81 (ddt, *J* = 16.7, 10.7, 5.9 Hz, 1H), 5.23-5.17 (m, 2H), 5.18 (s, 2H), 4.11 (br. d, *J* = 1.4 Hz, 2H), 4.04 (br. dt, *J* = 5.9, 1.3 Hz, 2H), 2.20 (t, *J* = 2.5 Hz, 1H)

HRMS: *m/z* = 252.0994 [M+ Na]⁺ calculated from C₁₄H₁₅NO₂ (M=252.0995).

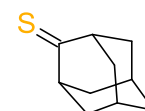
4-(Allyl((benzyloxy)carbonyl)amino)but-2-ynoic acid (35):

To a stirred solution of benzyl allyl(prop-2-yn-1-yl)carbamate (7.32 g, 31.9 mmol, equiv: 1.0) in tetrahydrofuran (22 ml) at -78 °C, *n*-butyllithium (20 ml, 31.9 mmol, equiv: 1.0) was added and the solution became slight yellow. The reaction mixture was stirred for 15 min at -78 °C. An excess of CO₂ gas (14.1 g, 319 mmol, equiv: 10) was bubbled into the reaction during 15 minutes. When the CO₂ gas was added the temperature raised until 50 °C. Consumption of starting material verified by LC/MS. Poured onto HCl 1 M and NaCl solid was added. The mixture was extracted with EtOAc. The organic layers were collected and dried over Na₂SO₄. All volatiles were removed under vacuum. The crude material was purified by flash chromatography (silica gel, 100 g, 0% to 100% EtOAc in heptane) to give the 4-(allyl((benzyloxy)carbonyl)amino)but-2-ynoic acid (6.4 g, 73% yield) as a brown oil.



(1R,3R,5R,7R)-Adamantane-2-thione¹⁷(30):

(1R,3R,5R,7R)-Adamantan-2-one (19.44 g, 129 mmol, equiv: 1.0) in pyridine (120 mL) was heated to 90°C, and phosphorus pentasulfide (7.02 g, 31.6 mmol, equiv: 0.244) was added. The reaction mixture was stirred at 90°C for 2h, and heating was turned off. The reaction mixture was cooled slowly until 23 °C and stirred during 18 h. A gum phase and a solution phase were formed. The pyridine solution phase was decanted and concentrated to dryness. The residual semi-solid was treated with heptane to give an orange solution containing a light-brown suspension. The suspension was removed by filtration. The filtrate was concentrated to dryness to give an orange solid. After the solid was dissolved in dichloroethane and purified by flash chromatography (silica gel, 100 g, 100% heptane) to give (1R,3R,5R,7R)-adamantane-2-thione (18 g, 84% yield) as an orange solid.

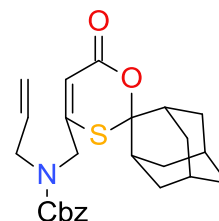


According to literature:**Erro! Marcador não definido.**

^1H NMR (CDCl_3) δ ppm 1.9-2.1 (m, 12 H), 3.43 (s, 2 H).

Benzyl.allyl(((1R,3R,5R,7R)-6'-oxo-6'H-spiro[adamantane-2,2'-[1,3]oxathiin]-4'-yl)methyl)carbamate (36):

4-(Allyl((benzyloxy)carbonyl)amino)but-2-ynoic acid (6.41 g, 23.5 mmol, equiv: 1.0) was added in one portion to a solution of (1R,3R,5R,7R)-adamantane-2-thione (1.3 g, 7.82 mmol, equiv: 1.0) in toluene (58.8 mL). After the mixture had been heated at reflux for 18 h, all volatiles were removed under vacuum to give an orange oil. The crude material was purified by flash chromatography (silica gel, 100 g, 0% to 100% EtOAc in heptane) to give the benzyl allyl(((1R,3R,5R,7R)-6'-oxo-6'H-spiro[adamantane-2,2'-[1,3]oxathiin]-4'-yl)methyl)carbamate (2.57 g, 75 % yield) as an orange oil.

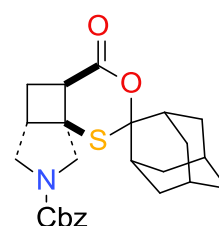


^1H NMR (600 MHz, DMSO, 120 °C) δ ppm 1.59-1.89 (m, 9 H) 1.95 (d, $J=13.3$ Hz, 2 H) 2.19 (d, $J=10.9$ Hz, 2 H) 2.39 (s, 2 H) 3.92 (dt, $J=5.8$, 1.4 Hz, 2 H) 4.22 (d, $J=1.2$ Hz, 2 H), 5.04-5.26 (m, 5 H) 5.83 (ddt, $J=17.2$, 10.2, 5.9, 5.9 Hz, 1 H) 6.06 (t, $J=1.3$ Hz, 1H) 7.17-7.49 (m, 6 H).

HRMS $m/z=440.1899$ $[\text{M}+\text{H}]^+$ calculated from $\text{C}_{25}\text{H}_{29}\text{NO}_4\text{S}$ ($M=439.1827$)

(1'SR,3'SR,4aSR,5aSR,5'SR,7'SR,8aSR)-Benzyl4-oxotetrahydro-4H-spiro[[1,3]oxathiino[4',5':1,4]cyclobuta[1,2-c]pyrrole-2,2'-adamantane]-7(8H)-carboxylate (37):

In a 100 ml Kjeldahl quartz vessel a solution of benzyl allyl(((1R,3R,5R,7R)-6'-oxo-6'H-spiro[adamantane-2,2'-[1,3]oxathiin]-4'-yl)methyl)carbamate (100 mg, 227 μmol , equiv: 1.0) and benzophenone (4.15 mg, 22.7 μmol , equiv: 0.1) in acetonitrile (45.5 mL) was degassed bubbling argon through the solution under sonication for 30 min. Then the mixture was irradiated in a Rayonet RPR-200 reactor (16 x 8 W lamps) at 350 nm for 10 h. All the volatiles were removed under vacuum. The crude material was purified by flash chromatography (silica gel, 20 g, 0% to 100% EtOAc in heptane) to give (1'SR,3'SR,4aSR,5aSR,5'SR,7'SR,8aSR)-benzyl-4-oxotetrahydro-4H-



spiro[[1,3]oxathiino[4',5':1,4]cyclobuta[1,2-*c*]pyrrole-2,2'-adamantane]-7(8*H*)-carboxylate (64 mg, 64% yield) as a colorless oil.

¹H NMR (600 MHz, CDCl₃) δ ppm 1.60-2.14 (m, 11 H) 2.15-2.40 (m, 3 H) 2.47 (d, *J*=12.8 Hz, 1 H) 2.69-2.86 (m, 2 H) 3.05 (s, 1 H), 3.27-3.45 (m, 2 H) 3.51-3.83 (m, 1 H) 3.92-4.47 (m, 1 H) 5.18 (s, 2 H) 7.28-7.53 (m, 5 H).

HRMS *m/z*=440.1892 [M+H]⁺ calculated from C₂₅H₂₉NO₄S (M=439.1818)

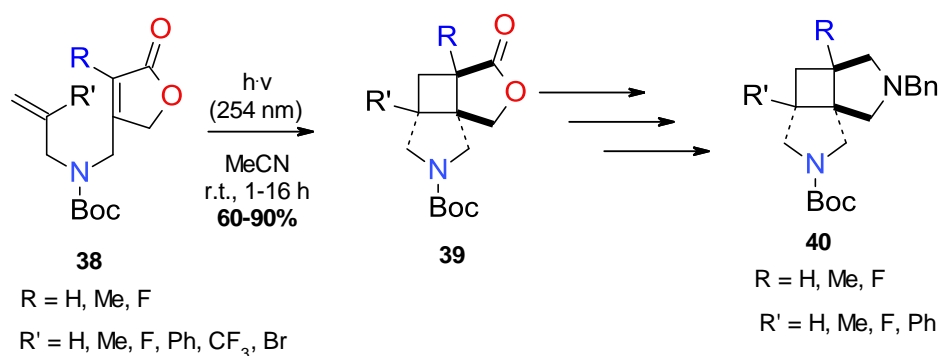
2.5-References

- ¹ E. Chorell, C. Bengtsson, T. S. Banchelin, P. Das, H. Uvell, A. K. Sinha, *Eur. J. Med. Chem.*, **2011**, 46, 1103-1116
- ² M. Sato, H. Ogasawara, K. Oi, T. Kato, *Chem. Pharm. Bull.*, **1983**, 31, 6, 1896-1901
- ³ G. L. Lange, M. G. Organ, *Tetrahedron Lett.*, **1993**, 34, 9, 1425-1428
- ⁴ A. Albin, M. Fagnoni, 'Handbook of Synthetic Photochemistry' Wiley-VCH, Weinheim, **2010**
- ⁵ J. D. Winkler, S. J. Harrison, M. F. Greaney, M. B. Rouse, *Synthesis*, **2002**, 14, 2150-2154
- ⁶ N. Haddad, I. Rukhman, Z. Abramovich, *J. Org. Chem.*, **1997**, 62, 7629-7636
- ⁷ J. H. Dritz, E. M. Carreira, *Tetrahedron Lett.*, **1997**, 38, 32, 5579-5582
- ⁸ J. D. Winkler, E. C. McLaughlin, *Org. Lett.*, **2005**, 7, 2, 227-229
- ⁹ M. Sato, J. Sakaki, K. Takayama, S. Kobayashi, M. Suzuki, C. Kaneko, *Chem. Pharm. Bull.*, **1990**, 38, 1, 94-98
- ¹⁰ R. C. F. Jones, M. Tankard, *J. Chem. Soc. Perkin, Trans. 1*, **1991**, 1, 240-241
- ¹¹ E. Chorell, C. Bengtsson, T. S. Banchelin, P. Das, H. Uvell, A. K. Sinha, J. S. Pinkner, S. J. Hultgren, F. Almqvist; *Eur. J. Med. Chem.* **2011**, 46, 1103-1116
- ¹² P. Cheruku, A. Peptchikhine, M. Ali, J. Neudörf, P. G. Andersson, *Org. Biomol. Chem.*, **2008**, 6, 366-373
- ¹³ M. S. Shepard, E. M. Carreira, *J. Am. Chem. Soc.*, **1997**, 119, 11,
- ¹⁴ a) K. Schmidt, J. Kopf, P. Margaretha, *Helv. Chim. Acta.*, **2005**, 88, 1922-1930; b) B. Lohmeyer, K. Schmidt, P. Margaretha, *Helv. Chim. Acta.*, **2006**, 89, 854-860; c) P. Margaretha, K. Schmidt, J. Kopf, V. Sinnwell, *Synthesis*, **2007**, 9, 1426-1433; d) K. Schmidt, P. Margaretha, *Helv. Chim. Acta.*, **2012**, 95, 423-427
- ¹⁵ a) A. Ohno, T. Kozumi, Y. Ohnishi, G. Tsuchihashi, *Tetrahedron Lett.*, **1970**, 2025; b) H. Gotthaldt, S. Nieber, *Tetrahedron Lett.*, **1976**, 3617; c) A. C. Brouwer, H. J. T. Bos, *Tetrahedron Lett.*, **1976**, 210
- ¹⁶ H. Teller, M. Corbet, L. Mantilli, G. Gopakumar, R. Goddard, W. Thiel, A. Fürstner, *J. Am. Chem. Soc.*, **2012**, 134, 15331-15342
- ¹⁷ C. Lin, D. S. Garvey, D. R. Janero, G. Letts, P. Marek, S. K. Richardson, D. Serebryanik, M. J. Shumway, S. W. Tam, A. M. Trocha, D. V. Young, *J. Med. Chem.*, **2004**, 47, 2276-2282

3-[2+2]-Photocycloaddition in the synthesis of novel conformationally restricted *bis*-pyrrolidines

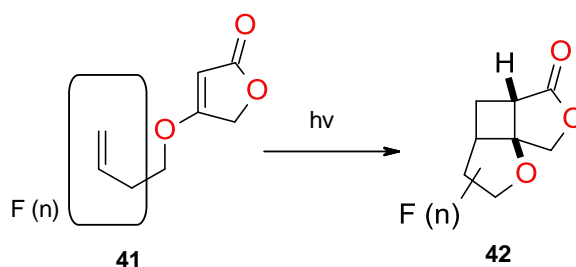
3.1- α,β -unsaturated lactones.

Photochemical reactions, in particular the [2+2]-photocycloaddition of α,β -unsaturated lactones has been widely explored. In recent years access to novel bridged *bis*-pyrrolidines has been studied. The interest in these moieties is related to their versatility as scaffolds in medicinal chemistry and the [2+2]-photocycloaddition reaction (PCA) was described as the key approach (**Scheme 1**).^{1,2} The synthesis of *bis*-pyrrolidines bearing angular methyl groups and fluorine atoms was achieved with good yields. However the [2+2]-PCA to get angular aryl substituents in the lactone part was described with low yields and long reaction times.



Scheme 1

Fluorinated compounds have been playing a huge role in medicinal chemistry in recent years. In an attempt to synthesize interesting fluorinated building blocks for medicinal chemistry Fort *et al.*³ used the intramolecular [2+2]-photocycloaddition of enones. The influence of the electron-withdrawing character of fluorine atoms that are directly attached to the double bond was studied (**Scheme 2**).



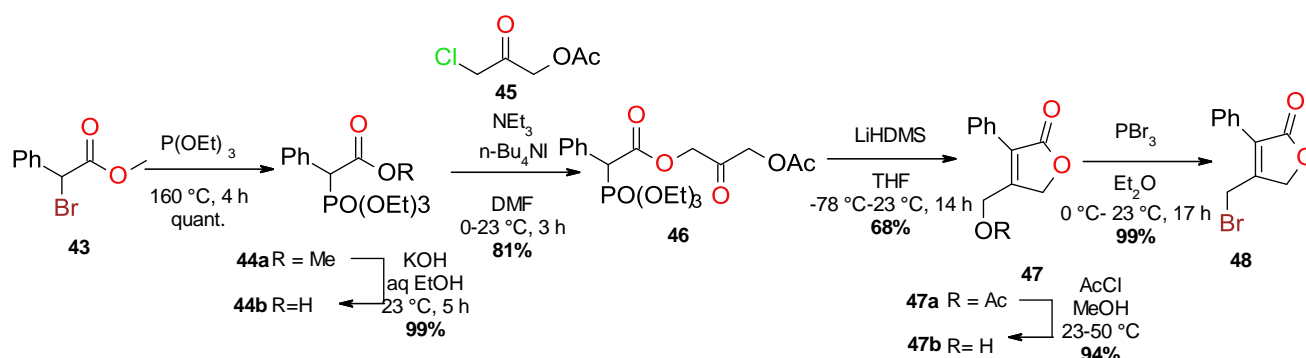
Scheme 2

In most cases irradiation at 254 nm at room temperature in diethyl ether allowed to obtain the product with yields around 70%. These experiments proved that the fluorine-substitution in a position adjacent to double bond is compatible with [2+2]-photocycloaddition.

The same research group also recently described the use of [2+2]-photocycloaddition in 4-substituted furanones to diastereoselectively form building blocks with potential application in medicinal chemistry.

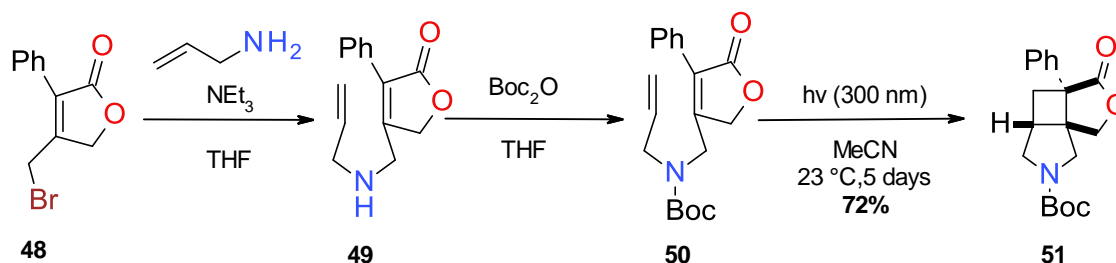
The experiments showed that Boc and Cbz both are good protecting groups for 4-(allylaminomethyl)-2(5*H*)-furanones in photocycloaddition reactions. The Cbz group can be more useful because there is a larger variety of cleavage procedures and is more efficient in the protection of bulkier substrates. In some cases of the [2+2]-PCA acetonitrile has shown to be superior as a solvent than diethyl ether improving the yields for particular substrates.

Fort *et al.*² reported the synthesis of 7-phenyl-substituted 3-aza-9-oxatricyclo[5.3.0.0^{1,5}]-decan-8-one from the alkylation of the bromide **48**. The bromide **48** was obtained through a synthetic route that started with the conversion of methyl-2-bromo-2-phenylacetate **43** to the corresponding diethoxy phosphonoacetate **44a** by an Arbuzov reaction.⁴ Saponification to the acid **44b** followed by the alkylation with 3-chloro-2-oxopropyl acetate **45** gave the 3-acetoxy-2-oxopropyl 2-(diethoxyphosphoryl)-2-phenylacetate **46** with 81% yield. An intramolecular Horner-Emmons-Wadsworth reaction using LiHMDS delivered the corresponding lactone **47a** which was deacetylated to the alcohol **47b**. A bromodehydroxylation with PBr₃ allowed access to the desired bromide **48** (Scheme 3).



Scheme 3

Alkylation of the bromide **48** with allylamine, followed by a protection of the intermediate **49** with Boc_2O gave the substituted lactone **50**, the substrate for the [2+2]-PCA reaction (**Scheme 4**).

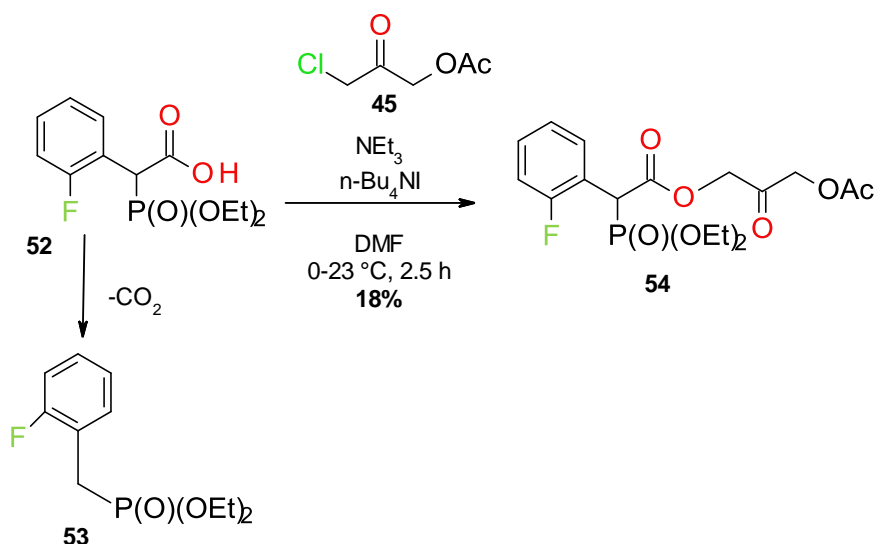


Scheme 4

The [2+2]-PCA reaction was performed in MeCN as solvent, irradiating **50** at 300 nm for 5 days. Although a yield of 72% was achieved the reaction time was very long in order to obtain full conversion. Attempts to diminish the reaction time were described, but the increase of energy by lowering the wavelength of irradiation (254 nm) caused formation of side products. Therefore research towards the optimization and differentiation of angular substituents was still to be performed.

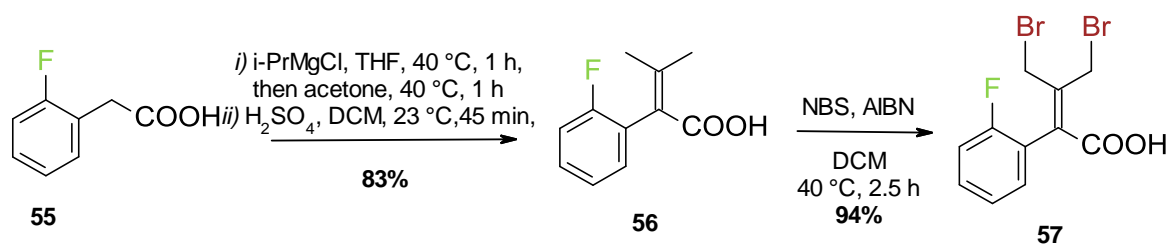
Fluorinated aromatic rings are quite frequently present in compounds useful in medicinal chemistry. Within the aim of producing new medicinal chemistry scaffolds and with the knowledge obtained with the synthesis of 7-phenyl-substituted 3-aza-9-oxatricyclo[5.3.0.0^{1,5}]-decan-8-one an attempt to synthesize the corresponding 2-fluoro-phenyl derivative was made.

The 2-fluoro-phenyl equivalent of the alkyl bromide **48** was required as a starting material. In order to achieve the synthesis of bromide **58**, a similar synthetic approach as the previous done for the alkyl bromide **48** was initially employed. However the yield of the Arbuzov reaction was low due to the fast decomposition of the starting material **52** by decarboxylation (**Scheme 5**).



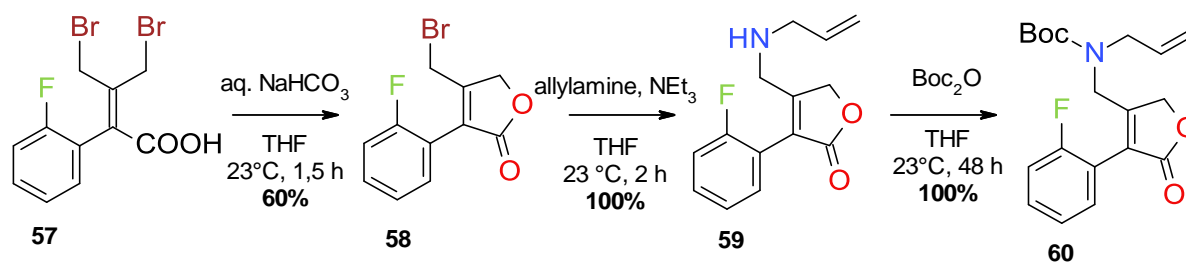
Scheme 5

Due to the low yield in the first step of the route and considering that the planned synthetic route had a projected length of more than 15 steps, an alternative approach was planned. The commercially available 2-(2-fluorophenyl)acetic acid **55** was condensed with acetone using *iso*-propylmagnesium chloride as a base to form 2-(2-fluorophenyl)-3-methylbut-2-enoic acid **56**, followed by a double Wohl-Ziegler bromination to give the dibromide **57** (**Scheme 6**).



Scheme 6

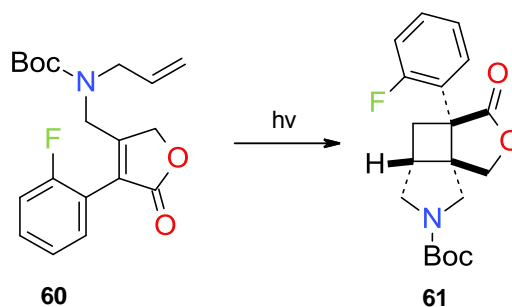
Lactonization to give **58** occurred in the presence of 5 eq. of aqueous sodium bicarbonate in tetrahydrofuran at 23°C . An increase of the temperature from 40°C to 60°C in the Wohl-Ziegler bromination lead to the *in situ* lactonization of some of the dibromide material. However, the complete cyclization of the dibromide did not occur due to equilibrium establishment. The bromination at 40°C , followed by the lactonization under mildly basic conditions has been established as the most beneficial approach, since the yields were higher and purification process easier (**Scheme 7**).



Scheme 7

The bromide **58** was alkylated with allyl amine then subsequently protected, using Boc anhydride, to obtain the photosubstrate **60**.

Several studies regarding the [2+2]-PCA reaction (**Scheme 8**) conditions with the aim of establishing good yields with reduced reaction times were performed (**Table 1**).



Scheme 8

Table 1: Optimization of reaction conditions

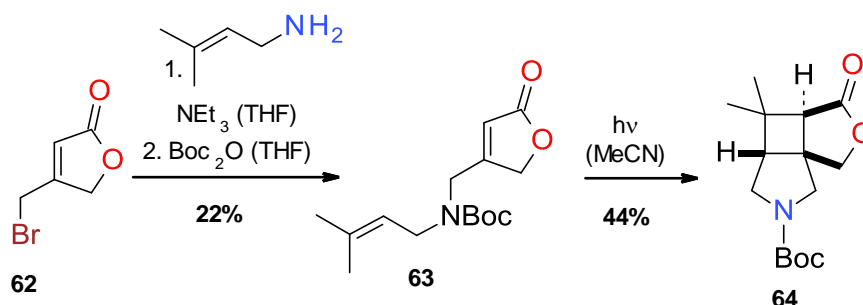
#	s.m.	λ [nm]	Solvent	c [mM]	Additives	Reaction time	Yield of 61 (%)
1	60	300	Et ₂ O	20	none	22 h	No conversion
2	60	300	MeCN	7	none	22 h	30%
3	60	300	MeCN	20	none	22 h	53%
4	60	300	MeCN	42	none	22 h	36%
5	60	300	Acetone	75	none	4-16 h	60%
6	60	300	MeCN	20	0.1 eq. Ph ₂ CO	4 days	30%

Initially a set of conditions similar to the ones described in the literature for the phenyl compound were used. Irradiation at 300 nm in MeCN, at various concentrations provided the product (**61**) with modest yields and long reaction times. In collaboration with Chembiotek, the synthesis of the photoproduct **61** was optimized to achieve a better yield in the [2+2]-PCA. Using the concept of triplet sensitization,

the photoprecursor **60** was irradiated at 300 nm in acetone as solvent and triplet sensitizer resulting in an increase of yield from 30% to 60% and a reduction of the reaction time from 144 h (6 days) to a maximum of 16 h in larger scale reactions (~12 g). A method of achieving high yields, as well as a major decrease of reaction time in the [2+2]-PCA to access conformationally restricted *bis*-pyrrolidines was described. The use of sensitization besides novel is a highly versatile method of increasing the success of these type of reactions. The sensitization approach has proven to be a tool that can determine the success of [2+2]-PCA.

3.2- Novel Spiro Compact Module

The synthesis of the dimethyl derivative **64** has already been described.² The alkylation reaction of the bromo-furanone **62** was performed with low yields. The sensitivity of the lactone to strongly basic conditions and the low nucleophilicity of the desired amine limited the success of the reaction (**Scheme 9**).

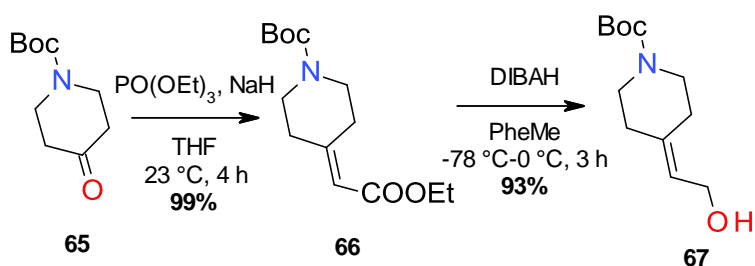


Scheme 9

To improve the previously published work by increasing the complexity of the scaffolds a new synthesis route to access a novel photoprecursor was developed. The synthesis of novel BACE1 inhibitors is one of the goals of this work. By functionalization of the cyclobutane in order to obtain heterocyclic spiro motifs, a deep penetration of the S2' pocket was expected. The first approach was towards the functionalization with a piperidine scaffold. Hence the right amine building block had to be accessed in order to be used as nucleophile to alkylate the bromo-furanone **62** in a similar approach to the previous work.

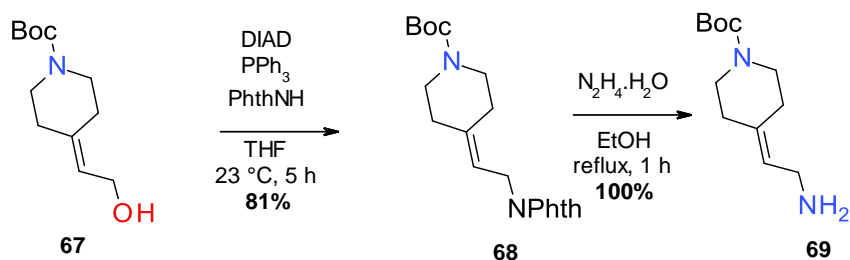
From the commercially available *tert*-butyl 4-Boc-piperidone **65** a standard Horner–Wadsworth–Emmons reaction using triethyl phosphonoacetate and sodium hydride as base produced the α,β -unsaturated ethyl ester **66** in quantitative

yield. **Erro! Marcador não definido.** Reduction of the ester with diisobutylaluminum hydride⁵ allowed the access to the correspondent allylic alcohol **67** (Scheme 10).



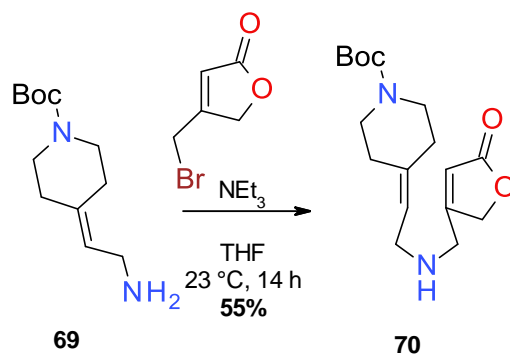
Scheme 10

By a Mitsunobu approach using phthalimide as a nitrogen nucleophile intermediate **68** was produced.⁶ Hydrazinolysis of **13** in refluxing ethanol gave the desired primary amine **69** (Scheme 11).⁷



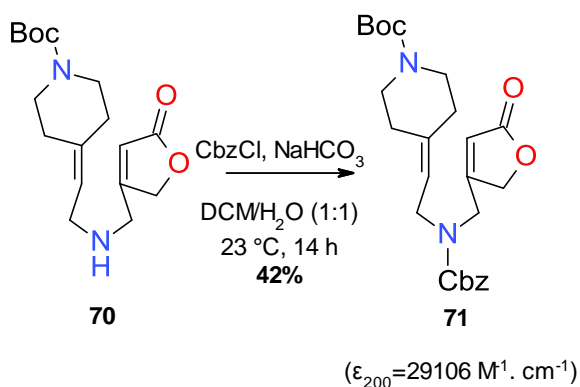
Scheme 11

In order to form the desired substrate for the [2+2]-PCA the amine **69** was used as the nucleophile in an alkylation reaction with the known bromo-furanone **62**. The yield of the alkylation with the bromo-furanone **62** - although low - is higher in comparison to the alkylation reaction used in the synthesis of dimethyl photoprecursor **63** (Scheme 12). In an attempt to optimize the yield of the alkylation reaction the conditions were altered, replacing triethylamine in THF with a biphasic system of aqueous potassium carbonate in dichloromethane⁸. Yet the yield using triethylamine as base was still higher (55% vs 32%). The di-alkylated product was also isolated from the reaction what lead to the conclusion that the occurrence double-alkylation was the cause for the moderate yields. A reductive amination between the allylic amine and the 4-formylfuran-2(5H)-one (synthesized from oxidation of the 4-hydroxymethylfuran-2(5H)-one⁹) was performed as an alternative route to obtain **70**. However the reaction mixture was unclean, and there was still formation of a mixture of mono- and di-substituted, in a higher ratio of the di-substituted product than in the alkylation procedures.



Scheme 12

The free amine group was further protected with Cbz under Schotten-Baumann conditions to form **71**. Due to the fact that Cbz has proven to have a nice behavior in [2+2]-PCA reactions and because the nitrogen in the piperidine was protected with Boc, Cbz appeared to be the best option as a protecting group. The fact that both nitrogen atoms in the molecule are protected with orthogonal protecting groups allowed the possibility of selective cleavage which would allow further functionalization (**Scheme 14**).



Scheme 13

The UV spectrum of **71** was measured and the extension coefficient for the maximum wavelength (200 nm) was determined ($\epsilon_{200}=29106 \text{ M}^{-1} \cdot \text{cm}^{-1}$). From the previous knowledge of the relation between the maximum wavelength of absorption the ideal interval of wavelength of irradiation was established (**Figure 1**). The starting point was 254 nm due to the fact that UV lamps with higher energy were not available.

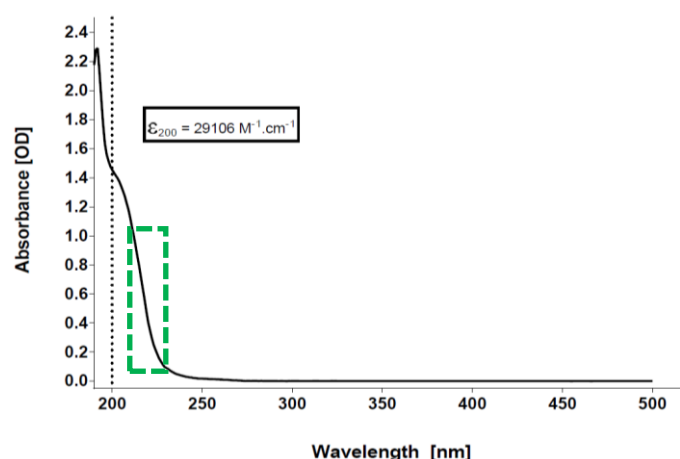
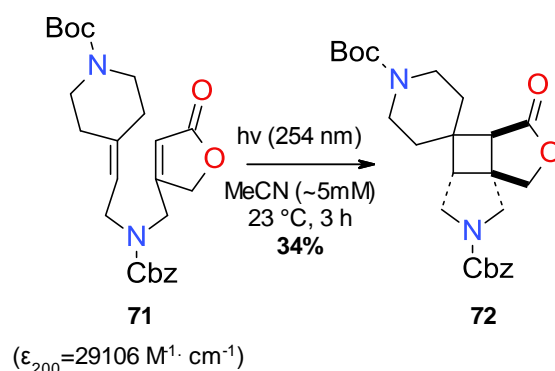


Figure 1: UV-spectrum of **71** measured at 50 μM in acetonitrile. The green dashed box represents the ideal wavelength of irradiation to perform a photoreaction

Although, from the UV spectrum it seems that the molecule would not uptake any energy at 254 nm, the UV lamps have a spectral distribution of wavelength and therefore emit radiation in an interval of wavelengths. The 254 nm lamps also emit radiation at lower wavelengths that provided sufficient energy for the photochemical process to occur.

The photoprecursor **71** was irradiated at 254 nm in MeCN for 3 h to give a new conformationally restricted pyrrolidine **72** with a *spiro*-piperidine moiety in 34% yield. Steric hindrance is most likely the cause of the moderate yield (**Scheme 14**).



Scheme 14

The synthesis of the desired complex spiro-piperidine photoproduct **72** was successful. This novel building block has an enormous level of complexity, compromising a tricyclic skeleton with a spiro-piperidine functionalization, which possesses a large variety of exit vectors that can be selectively functionalized. The

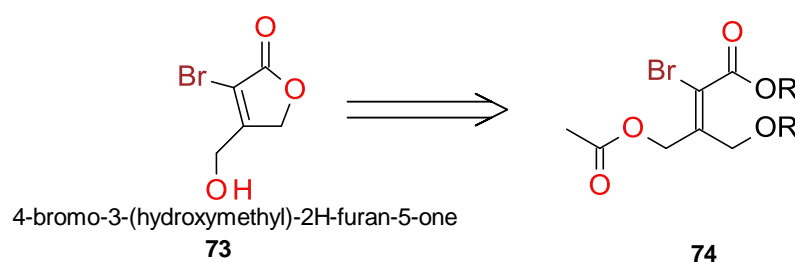
key step in allowing the establishment of the intricate moiety in a regioselective manner was the [2+2]-PCA.

3.3-Synthesis of versatile 3-(hydroxymethyl)-2H-furan-5-ones derivatives bearing a leaving group in 4-position

The success of the [2+2]-PCA of functionalized α,β -unsaturated lactones and the possibility of their use as molecular scaffolds served as inspiration towards the synthesis of multipurpose functionalized lactones for achieving a more modular approach.

In recent years cross-coupling reactions have played an important role in synthetic organic chemistry. Bromides are extremely versatile in cross coupling reactions, therefore, a lactone with a bromide functionality at the 4-position was proposed as a convenient scaffold. Furthermore, the installation of a hydroxymethyl group in the 3-position would allow differential functionalization. It was expected that the combined functionalization of the 3- and 4-positions would enable the formation of a highly versatile building block, which can access a broad range of products suitable for the subsequent intramolecular [2+2]-PCA reaction.

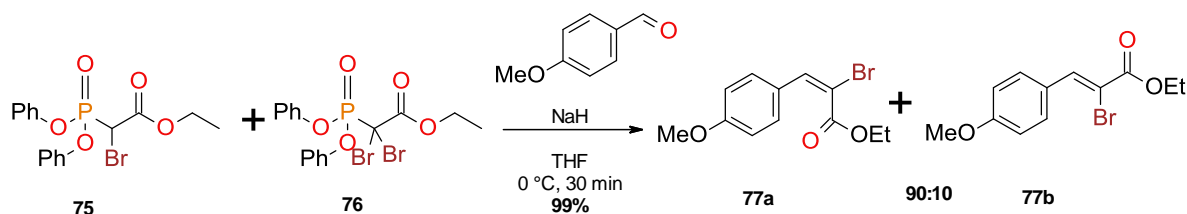
From the knowledge acquired in the synthesis of the different 2-substituted lactones it was predicted that the lactone type **73** would be accessible through the intermediate of the type **74** (Scheme 15).



Scheme 15

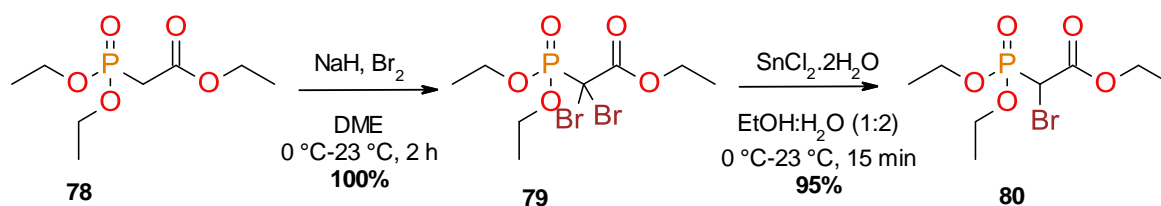
In 2004, Brückner *et al.* described the stereoselective preparation of trisubstituted double bonds from the condensation of brominated phosphonoacetate esters with aldehydes. The preparation of the α -brominated α,β -unsaturated esters was optimized with the use of several bases and solvents. The use of NaH in THF at

0 °C provided the better yield and selectivity in the condensation of a mixture of mono-dibromophosphonates and anisaldehyde (**Scheme 16**).¹⁰



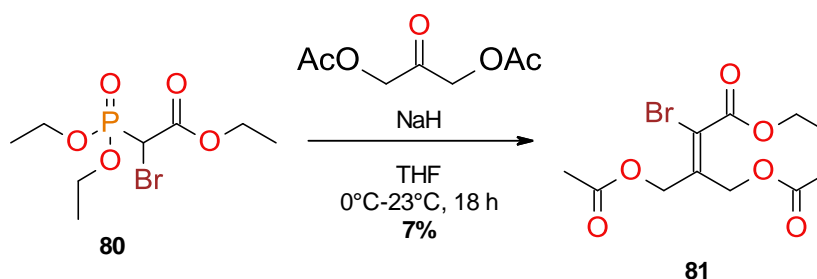
Scheme 16

In order to avoid selectivity problems condensation of the ethyl 2-bromo-2-(diethoxyphosphoryl)acetate with the symmetric 2-oxopropane-1,3-diyl diacetate was planned. The ethyl 2-bromo-2-(diethoxyphosphoryl)acetate **80** was synthesized by the double dehydrobromination of commercially available triethyl phosphonoacetate followed by selective reductive elimination of one bromine with tin(II)chloride dihydrate (**Scheme 17**).¹¹



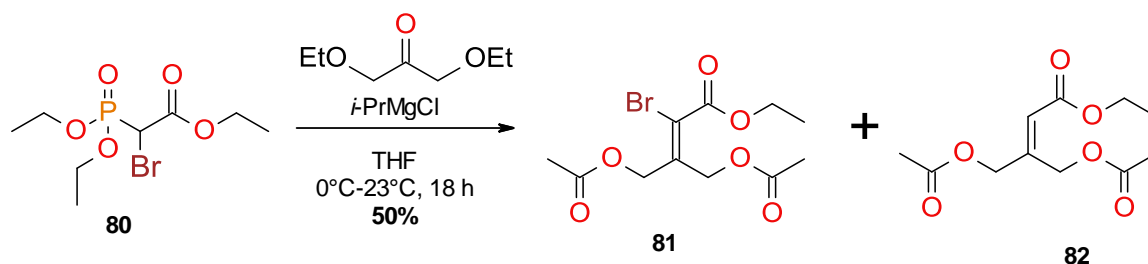
Scheme 17

The condensation of the bromo-phosphonate **80** with the diacetoxylacetone in the presence of sodium hydride gave the desired product with a very low yield after a tedious purification process (**Scheme 18**).



Scheme 18

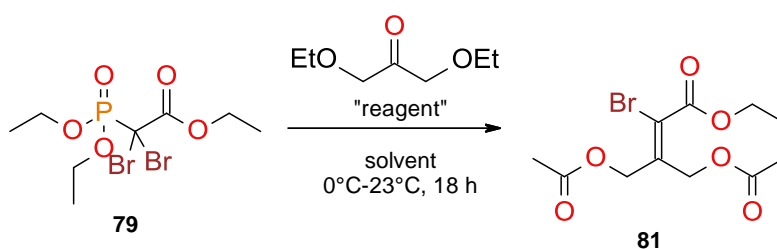
An attempt to do the previous reaction with *i*-PrMgCl as base instead of NaH was made (**Scheme 19**).



Scheme 19

With the use of *i*-PrMgCl and the bromide **80** the elimination product **82** was formed in a 1:1 proportion with the bromide **81**. The formation of the elimination product and the fact that a mixture of both the mono- and dibromo phosphonates were used by Brückner *et al.* lead to the rationalization of using the dibromide instead of the monobromide as starting material.

Knochel *et al.* reported the use of functionalized magnesium carbenoids in the synthesis of unsaturated esters. A bromine-magnesium exchange that can further be quenched with several electrophiles provided the corresponding unsaturated esters.¹² The dibromide **79** was reacted with *i*-PrMgCl resulting in the formation of the mono bromide **80** *in situ*; this was verified by quenching a sample with water and analyzing using LC/MS. The bromide-magnesium exchange is driven by the difference of pK_a of starting material and product. Upon completed conversion of the dibromide **79** to corresponding monobromide **80**, the reaction mixture was quenched with diacetoxyacetone (**Scheme 20**).



Scheme 20

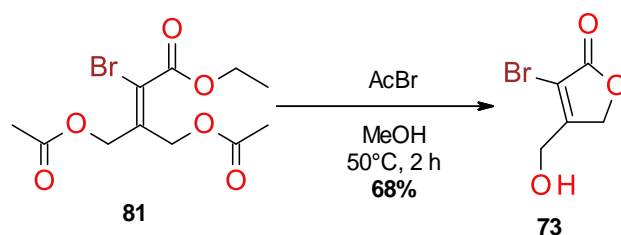
Although higher than the yield of the reaction with the mono-bromide **80**, the yield of this reaction was still low. Furanone **73** was an interesting building block for further derivatization. With that in mind a low yield synthesis was not convenient because larger quantities of furanone **73** were necessary for further plans. Therefore an attempt to optimize this particular step was performed (**Table 2**).

Table 2: Optimization of the synthesis of **81**.

#	s.m.	Solvent	Reagent	scale	Reaction time	P	Yield of 26 (%)	Side products
1	80	THF	<i>i</i> -PrMgCl	500 mg	18 h	81	20%	82 (elimination) (1:1)
2	80	THF	NaH	500 mg	18 h	81	7%	none
3	79	THF	<i>i</i> -PrMgCl	1 g	18 h	81	24 %	none
4	79	THF	NaH	200 mg	18 h	81	No product	Not identified
5	79	THF	<i>i</i> -PrMgCl·LiCl	1 g	18 h	81	32%	none
6	79	THF	<i>i</i> -PrMgCl·LiCl	25 g	18 h	81	10 %	none

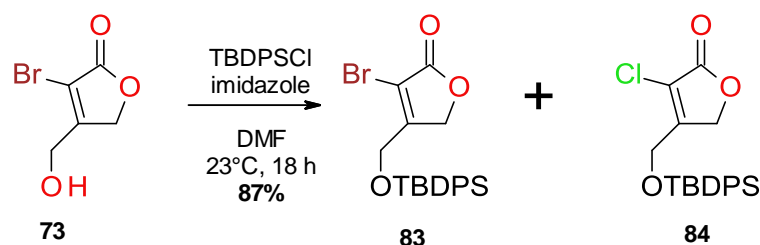
After 18 h the reaction with sodium hydride was not finished and there was no product formation. Then an attempt using *iso*-propylmagnesiumchloride lithium chloride complex was made, and there was an increase of the yield. However when the scale up was done the yield was much lower. The use of lithium salts as additives, in particular LiCl, has shown to increase the rate of the bromine-magnesium exchange. LiCl has the ability to cleave polymeric aggregates of *iso*-propylmagnesiumchloride and thus increasing the reactivity of the magnesiate species.¹³

The lactonization reaction occurred in the presence of acetyl bromide in methanol and gave the lactone **73** with 68% yield (**Scheme 21**).

**Scheme 21**

After the synthesis of a small amount of the bromo-furanone **73** the protection of the hydroxy group was done. A bulky silyl ether such TBDPS was chosen due to an increase of lipophilicity that would turn the compound easier to handle. The silyl ethers are stable in most of the cross coupling procedures. The protection reaction was conducted using the classic procedure of TBDPSCl, imidazole in DMF.

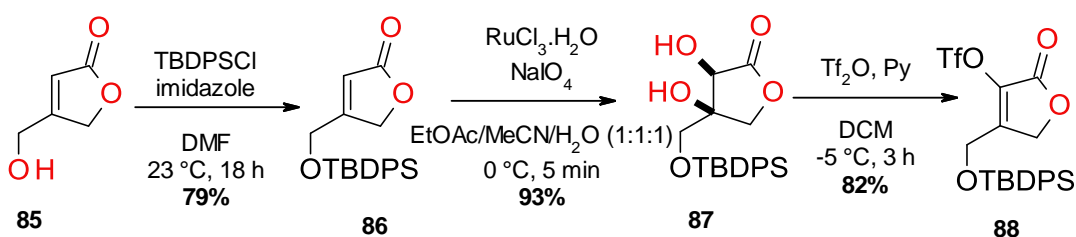
Unfortunately a bromine-chlorine exchange happened. The exchange lead to a formation of a 1:1 ratio between the chloride and the bromide that had overlapping retention times which did not allow separation by flash chromatography. In order to solve this issue TBDPSOTf should be used instead of the silyl chloride (**Scheme 22**).



Scheme 22

The synthetic route to obtain the bromide **73** was low yielding, inefficient and difficult to reproduce on a larger scale. An alternative route had to be found. The main goal of the bromide **73** was to access an intermediate with versatility in cross-coupling reactions. Although bromides are one of the most used functionalities in cross-coupling reactions, triflates have been widely used as well.^{14,15} The synthesis of the triflate equivalent was planned

The commercially available 3-(hydroxymethyl)-2*H*-furan-5-one (**85**) was protected with TBDPS. The rapid vicinal dihydroxylation by catalytic ruthenium tetroxide gave the diol **87** compound in a high yielding procedure.¹⁶ The triflate was installed by a double sulfonylation and concomitant elimination procedure using triflic anhydride and pyridine to give the desired furanone **88**.¹⁷



With a high yielding three step synthesis, access to the triflate **88** was successfully achieved.

3.4-Conclusion

The behavior displayed by molecules interacting and absorbing light greatly varies. Understanding this behavior was key in order to determine the success of [2+2]-PCA. The comprehension and utilization of triplet sensitization has the potential to transform the use of photochemistry in organic synthesis.

Several novel molecular scaffolds were successfully synthesized. Optimization of the intramolecular [2+2]-PCA reaction of the 2-fluoro-phenyl derivative **61** led to the establishment of conditions that allow fast, clean high yielding reactions at larger scale.

A novel complex spiro compound was successfully synthesized. The position of the piperidine ring in the cyclobutane is innovative and pioneering. The establishment of the success of this [2+2]-PCA is cutting-edge when it comes to validate photochemistry as a way of achieving complexity. In the future attempts to higher levels of substitution of the cyclobutane moiety can be studied, knowing that steric hindrance does not fully prevent the [2+2]-PCA.

Two new versatile furanone-type building blocks were accessed. The bromide **73** however isolated, the yields of the synthetic route were moderate for its purpose as a building block. Despite the low yields the synthesis was optimized. The bromine-magnesium exchange from the dibromide phosphonate **79** has proven to be the better mechanism. Sodium hydride failed to live up to the expectations.

The replacement of the bromine with a triflate group was a good solution. The synthesis of the triflate-furanone **88** is short with high yields. The versatility of the triflate **88** is at the same level as the bromide **73**. Several protocols of cross-coupling reactions are described with vinylic triflates.

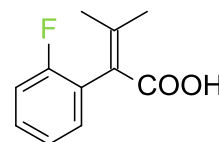
High level of complexity and innovation was reported. The synthesis and optimization of new [2+2]-PCA protocols has a massive contribution to the further work in this area. The level of the versatility of the reported photoproducts allows creative functionalization to give a huge variety of novel compounds.

3.5-Experimental section:

General: Unless otherwise stated, the reactions were stopped when the starting material was fully consumed according to thin layer chromatography (TLC) and/or LC/MS analysis. Compounds were detected by UV ($\lambda=254$ nm), CAM (cerium ammonium molybdate solution) or KMnO_4 . ^1H and ^{13}C NMR: Bruker AV-300, AV-400 and AV-600 recorded at 300 K unless otherwise indicated. Chemical shifts are reported relative to the solvent [CHCl_3 : δ (^1H) = 7.26 ppm, δ (^{13}C) = 77.0 ppm, DMSO δ (^1H) = 2.50 ppm, δ (^{13}C) = 39.5 ppm] as reference. The relative configuration of the products was determined by two-dimensional NMR spectra (COSY, NOESY, HSQC, HMBC). HRMS data were recorded by electron spray ionization (ESI) on an ion trap mass spectrometer.

2-(2-Fluorophenyl)-3-methylbut-2-enoic acid (56):

To a solution of isopropylmagnesium chloride 2M in THF (100 mL, 200 mmol, equiv: 2.0) in tetrahydrofuran (100 mL) at 23 °C was added dropwise a solution of 2-(2-fluorophenyl)acetic acid (15.4 g, 100 mmol, equiv: 1.0) in tetrahydrofuran (200 mL). The reaction mixture was stirred, with an overhead stirrer for 1 h at 40 °C. The reaction mixture was cooled to 0 °C and acetone (8.71 g, 11 mL, 150 mmol, equiv: 1.5) was added dropwise, without the temperature to go higher than 20 °C. After the complete addition, the reaction mixture was stirred for 1 h at 40 °C. The reaction was cooled to 0 °C and added 100 mL 14% H_2SO_4 , extracted with TBME, dried over Na_2SO_4 , filtered off and evaporated totally. The residue was dissolved in 100 mL dichloromethane and added under ice bath cooling H_2SO_4 conc. (50 g). Stirred at 23 °C for 45 minutes, the reaction mixture was poured onto ice water and extracted with dichloromethane. The organic layers were collected and dried over Na_2SO_4 . All volatiles were removed under vacuum. The crude material was dissolved in methanol (100 mL) and added charcoal (1.6 g) was added and stirred at 50 °C for 30 min, filtered off and evaporated totally. Added heptane (50 mL) and stirred at 50 °C for 1 h, cooled to 23 °C and filtered off the solid, dried in high vacuum to give 2-(2-Fluorophenyl)-3-methylbut-2-enoic acid (13.51 g, 70% yield) as a white solid.

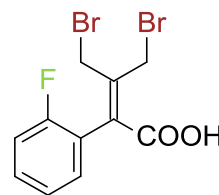


According to literature:¹⁸

^1H NMR (300 MHz, CDCl_3) δ ppm 1.74 (s, 3 H) 2.52 (s, 3 H), 7.68-8.26 (m, 4 H)

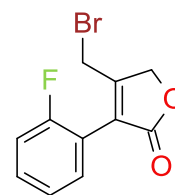
4-Bromo-3-(bromomethyl)-2-(2-fluorophenyl)but-2-enoic acid (57):

A mixture of 2-(2-fluorophenyl)-3-methylbut-2-enoic acid (10.84 g, 55.8 mmol, equiv: 1.0) with NBS (19.9 g, 112 mmol, equiv: 2.0) and AIBN (183 mg, 1.12 mmol, equiv: 0.02) in dichloromethane (283 mL) was stirred at reflux overnight. The mixture was cooled to 23 °C and evaporated totally. The crude material was purified by flash chromatography (silica gel, 20 g 0% to 40% EtOAc in heptane). The product fractions were combined and totally evaporated to give: 4-bromo-3-(bromomethyl)-2-(2-fluorophenyl)but-2-enoic acid (18.53 g, 94% yield) as a yellow solid. 3-(2-fluorophenyl)-5-hydroxy-4-methylfuran-2(5H)-one was isolated as a minor side product resulting of a double-elimination.



4-(Bromomethyl)-3-(2-fluorophenyl)furan-2(5H)-one (58):

To NaHCO₃ in water 1M (263 mL, 263 mmol, equiv: 5.0) and tetrahydrofuran (279 mL) was added a solution of 4-bromo-3-(bromomethyl)-2-(2-fluorophenyl)but-2-enoic acid (18.53 g, 52.6 mmol, equiv: 1.0) in tetrahydrofuran (92.9 mL), and the mixture was stirred for 1.5 h at 23 °C. The mixture was extracted with water and EtOAc. The organic layers were collected and dried over Na₂SO₄. All volatiles were removed under vacuum. The crude material was purified by flash chromatography (silica gel, 100 g, 0% to 30% of EtOAc in heptane) to give 4-(bromomethyl)-3-(2-fluorophenyl)furan-2(5H)-one (8.5 g, 60% yield) as a colorless oil.

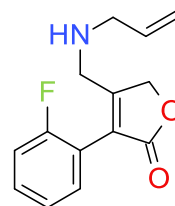


¹H NMR (600 MHz, CDCl₃) δ ppm 4.25 (d, *J*=0.6 Hz, 2 H) 5.10 (s, 2 H) 7.18 (ddd, *J*=9.9, 8.5, 1.0 Hz, 1 H) 7.26 - 7.30 (m, 1 H) 7.41 - 7.49 (m, 2 H)

GCMS (EI): *m/z*=269.969 [M•]⁺ calculated from C₁₁H₈BrFO₂ (M=269.969)

4-((Allylamino)methyl)-3-(2-fluorophenyl)furan-2(5H)-one (59):

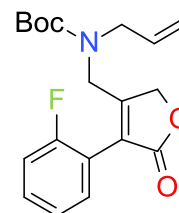
Dropwise addition of allylamine (2.15 g, 2.82 mL, 37.6 mmol, equiv: 1.2) and triethylamine (3.17 g, 4.37 mL, 31.4 mmol, equiv: 1.0) in tetrahydrofuran (100 mL) to an ice bath cooled solution of 4-(bromomethyl)-3-(2-fluorophenyl)furan-2(5H)-one (8.5 g, 31.4 mmol, equiv: 1.0) in tetrahydrofuran (100 mL). The ice bath was removed allowing the reaction to warm up to 23 °C and stirred 2 hours. The solid was filtered



and the solution was evaporated totally. The crude material was purified by flash chromatography (silica gel, 100 g, 0% to 100% EtOAc in heptane) and gave 4-((allylamino)methyl)-3-(2-fluorophenyl)furan-2(5H)-one (5.43 g, 70% yield) as a light brown oil.

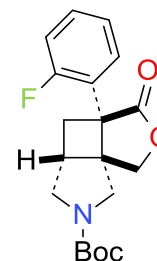
***tert*-Butyl allyl((4-(2-fluorophenyl)-5-oxo-2,5-dihydrofuran-3-yl)methyl)carbamate (60):**

A mixture of 4-((allylamino)methyl)-3-(2-fluorophenyl)furan-2(5H)-one (5.43 g, 22 mmol, equiv: 1.0) with Boc-anhydride (5.03 g, 5.35 mL, 23.1 mmol, equiv: 1.05) in tetrahydrofuran (162 mL) was stirred for 72 h at 23 °C. The reaction mixture was concentrated and purified by flash chromatography (silica gel, 100 g, 0% to 50% EtOAc in heptane) to give: *tert*-butyl allyl((4-(2-fluorophenyl)-5-oxo-2,5-dihydrofuran-3-yl)methyl)carbamate (7.63 g, 100% yield) as a light yellow oil.



(3aRS,4aRS,7aSR)-*tert*-Butyl 3a-(2-fluorophenyl)-3-oxohexahydrofuro[3',4':1,4]cyclobuta[1,2-c]pyrrole-6(1H)-carboxylate (61):

A solution of *tert*-butyl allyl((4-(2-fluorophenyl)-5-oxo-2,5-dihydrofuran-3-yl)methyl)carbamate (5 g, 14.40 mmol) in acetone (200 mL, 72 mM) was deoxygenated by bubbling argon through the solution under sonication for 1h and then irradiated in a Rayonet RPR-200 reactor (16 x 8 W lamps) ($\lambda=300$ nm) for 9 h. The solvent was removed in vacuum, and the crude material was purified by flash chromatography (silica gel, 100g, 15% to 30% EtOAc in hexane) to give (3aRS,4aRS,7aSR)-3a-(2-fluoro-phenyl)-3-oxo-tetrahydro-2-oxa-6-aza-cyclobuta[1,2:1,4]dicyclopentene-6-carboxylic acid *tert*-butyl ester (3.01g, 60%) as an off white solid.

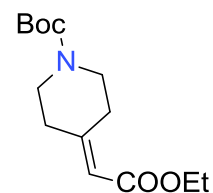


^1H NMR (600 MHz, CDCl_3) δ ppm 1.11 - 1.69 (m, 9 H) 2.53 (dd, $J=12.9, 6.6$ Hz, 1 H) 2.78 (dd, $J=12.8, 8.5$ Hz, 1 H) 2.87 - 3.10 (m, 2 H) 3.17 - 3.38 (m, 1 H) 3.46 - 3.82 (m, 2 H) 4.30 - 4.52 (m, 2 H) 7.09 (d, $J=8.5$ Hz, 1 H) 7.23 (d, $J=1.0$ Hz, 1 H) 7.28 (br. s., 1 H) 7.32 - 7.41 (m, 1 H)

HRMS: $m/z= 248.1003$ $[\text{M}+\text{H}]^+$ calculated from $\text{C}_{14}\text{H}_{14}\text{FNO}_2$ ($\text{M}=247.1003$)

***tert*-Butyl 4-(2-ethoxy-2-oxoethylidene)piperidine-1-carboxylate (66):**

To a solution of triethyl phosphonoacetate (70.75 g, 63.2 mL, 316 mmol, equiv: 1.26) in tetrahydrofuran (500 mL) at 0-5 °C. sodium hydride (60% in mineral oil) (12.1 g, 304 mmol, Eq: 1.21) was added portionwise, and the mixture was stirred for 30 min. Then a solution of *tert*-butyl 4-oxopiperidine-1-carboxylate (50 g, 251 mmol, equiv: 1.0) in tetrahydrofuran (500 mL) was added dropwise and the mixture was stirred at 23 °C for 4 h. After the completion of the reaction (verified by TLC), water (500 mL) was added, and the water layers were extracted with EtOAc. The organic layers were collected and dried over Na₂SO₄. All volatiles were removed under vacuum leaving a white solid. The crude material was triturated with n-pentane (200 mL) at 23 °C for 15 min, then at 0 °C for 1.5 h, the solid was filtered off, washed with cold n-pentane and dried in high vacuum to give the first crop of *tert*-butyl 4-(2-ethoxy-2-oxoethylidene)piperidine-1-carboxylate (62.16 g, 231 mmol, 92 % yield) as a white solid. The mother liquor was evaporated to give 18 g of yellow oil, which was purified by flash chromatography (silica gel, 100 g, 0% to 15% EtOAc in heptane) to give a second crop of *tert*-butyl 4-(2-ethoxy-2-oxoethylidene)piperidine-1-carboxylate (4.95 g, 18.4 mmol, 7.32 % yield) as a white solid. Overall the *tert*-butyl 4-(2-ethoxy-2-oxoethylidene)piperidine-1-carboxylate (67.11 g, 99% yield) was obtained as white solid.

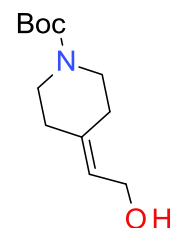


According to literature:¹⁹

¹H NMR (600 MHz, CDCl₃) δ ppm: 1.26 (t, *J* = 7.0 Hz, 3 H) 1.46 (s, *t*Bu, 9 H) 2.1-2.4 (m, 2 H) 2.8-3.1 (m, 2 H) 3.1-3.6 (m, 4 H) 4.12 (q, *J* = 7.0 Hz, 2 H) 5.68 (br s, 1 H)

***tert*-Butyl 4-(2-hydroxyethylidene)piperidine-1-carboxylate (67):**

To a solution of *tert*-butyl 4-(2-ethoxy-2-oxoethylidene)piperidine-1-carboxylate (3.5 g, 13 mmol, equiv: 1.0) in toluene (30 mL) at -78 °C was added diisobutylaluminum hydride (~1.7 M in toluene, 25%) (19.1 mL, 32.5 mmol, equiv: 2.5) keeping the internal temperature below -50 °C. Stirring was continued at -78 °C slowly warming up to 0 ° for 3 h. MeOH (2 mL) was added, followed by a saturated aqueous solution of Seignette's salt (30 mL), and the mixture was warmed up to 23



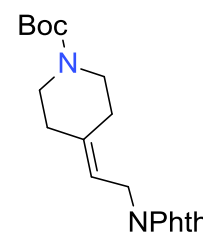
°C. Extraction with EtOAc. The organic layers were collected and dried over Na₂SO₄. All volatiles were removed under vacuum. The crude material was purified by flash chromatography (silica gel, 50 g, 0% to 60% EtOAc in heptane) to give the *tert*-butyl 4-(2-hydroxyethylidene)piperidine-1-carboxylate (2.737 g, 93% yield) as a colorless oil.

According to literature:²⁰

¹H NMR (400 MHz, CDCl₃) δ ppm 5.49 (t, *J* = 7.0 Hz, 1 H) 4.17 (d, *J* = 7.0 Hz, 2 H) 3.42 (m, 4H) 2.26 (t, *J* = 5.8 Hz, 2 H), 2.18 (t, *J* = 5.8 Hz, 2 H) 1.57 (br s, 1H) 1.47 (s, 9 H)

***tert*-Butyl 4-(2-(1,3-dioxoisindolin-2-yl)ethylidene)piperidine-1-carboxylate (68):**

tert-Butyl 4-(2-hydroxyethylidene)piperidine-1-carboxylate (1 g, 4.4 mmol, equiv: 1.0) was dissolved in THF (8.8 mL). Then triphenylphosphine (1.15 g, 4.4 mmol, equiv: 1.0) and phthalimide (647 mg, 4.4 mmol, equiv: 1.0) were added, and the system was covered with aluminum foil. Dropwise addition of diisopropyl azodicarboxylate (890 mg, 855 µl, 4.4 mmol, equiv: 1.0). The mixture was stirred at 23 °C during 5h. The reaction mixture was washed with sodium bicarbonate and brine, extracted with ethyl acetate. The organic layers were collected and dried over Na₂SO₄. All volatiles were removed under vacuum. The crude material was purified by flash chromatography (silica gel, 40 g, 0% to 50% EtOAc in heptane) to give *tert*-butyl 4-(2-(1,3-dioxoisindolin-2-yl)ethylidene)piperidine-1-carboxylate (1.27 g, 81% yield) as a light yellow oil.



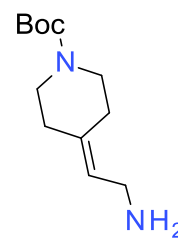
¹H NMR (600 MHz, CDCl₃) δ ppm 1.46 (s, 9 H) 2.14 (br t, *J*=5.0 Hz, 2 H) 2.45 (t, *J*=5.6 Hz, 2 H) 3.27 - 3.63 (m, 4 H) 4.29 (d, *J*=7.4 Hz, 2 H) 5.36 (s, 1 H) 7.64 - 7.76 (m, 2 H) 7.80 - 7.91 (m, 2 H)

HRMS: *m/z*= 257.1287 [M-BOC]⁺ calculated from C₂₀H₂₄N₂O₄ (M=356.1736)

***tert*-Butyl 4-(2-aminoethylidene)piperidine-1-carboxylate (69):**

To a solution of *tert*-butyl 4-(2-(1,3-dioxoisindolin-2-yl)ethylidene)piperidine-1-carboxylate (1.27 g, 3.56 mmol, Eq: 1) in ethanol (23 mL) hydrazine hydrate was

added (535 mg, 519 μ l, 10.7 mmol, equiv: 3.0) was added and mixture was refluxed for 1 h. After cooling down to 23 $^{\circ}$ C, the resulting precipitate (phthalide) was filtered off and washed with a small amount of ethanol. The residue was concentrated and extracted with dichloromethane. The organic layers were washed with brine and dried with Na_2SO_4 . The solvents were removed to give *tert*-butyl 4-(2-aminoethylidene)piperidine-1-carboxylate (808 mg, 100% yield) as a light yellow oil.

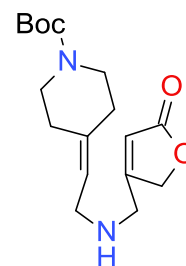


^1H NMR (600 MHz, CDCl_3) δ ppm 1.47 (s, 10 H) 1.98 - 2.40 (m, 4 H) 3.30 (d, $J=7.0$ Hz, 2 H) 3.35 - 3.50 (m, 4 H) 5.34 (t, $J=7.0$ Hz, 1 H)

HRMS: $m/z=227.1759$ $[\text{M}+\text{H}]^+$ calculated from $\text{C}_{12}\text{H}_{22}\text{N}_2\text{O}_2$ ($M=226.1681$)

***tert*-Butyl 4-(2-(((5-oxo-2,5-dihydrofuran-3-yl)methyl)amino)ethylidene)piperidine-1-carboxylate (70):**

To a solution of *tert*-butyl 4-(2-aminoethylidene)piperidine-1-carboxylate (808 mg, 3.57 mmol, equiv: 1.0) in tetrahydrofuran (17.9 mL), was added triethylamine (434 mg, 597 μ l, 4.28 mmol, equiv: 1.2). At 0 $^{\circ}$ C 4-(bromomethyl)furan-2(5*H*)-one (632 mg, 3.57 mmol, equiv: 1.0) was added and were left at 23 $^{\circ}$ C overnight. The reaction mixture was filtered and the solvents evaporated. The crude material was purified by flash chromatography (silica gel 20g, 0% to 100% EtOAc in heptane) to give *tert*-butyl 4-(2-(((5-oxo-2,5-dihydrofuran-3-yl)methyl)amino)ethylidene)piperidine-1-carboxylate (628 mg, 55% yield) as an orange oil.

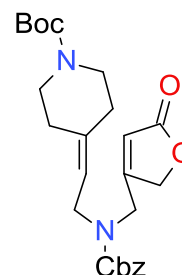


^1H NMR (600 MHz, CDCl_3) δ ppm 1.43 - 1.50 (m, 20 H) 2.10 - 2.35 (m, 9 H) 3.12 (d, $J=7.0$ Hz, 2 H) 3.28 (d, $J=7.1$ Hz, 2 H) 3.33 - 3.50 (m, 12 H) 3.60 - 3.66 (m, 2 H) 4.79 (d, $J=1.7$ Hz, 3 H) 4.83 (d, $J=1.8$ Hz, 2 H) 5.21 - 5.27 (m, 1 H) 5.29 - 5.35 (m, 3 H) 6.00 (quin, $J=1.7$ Hz, 1 H) 6.04 (t, $J=1.6$ Hz, 2 H)

HRMS: $m/z=223.1454$ $[\text{M}-\text{Boc}]^+$ calculated from $\text{C}_{17}\text{H}_{26}\text{N}_2\text{O}_4$ ($M=322.1892$)

***tert*-Butyl 4-(2-(((benzyloxy)carbonyl)((5-oxo-2,5-dihydrofuran-3-yl)methyl)amino)ethylidene)piperidine-1-carboxylate (71):**

A mixture of *tert*-butyl 4-(2-(((5-oxo-2,5-dihydrofuran-3-yl)methyl)amino)ethylidene)piperidine-1-carboxylate (628 mg, 1.95 mmol, equiv: 1.0) and sodium bicarbonate (818 mg, 9.74 mmol, equiv: 5.0) in dichloromethane (1.15 mL) and water (1.15 mL) was stirred at 0 °C. Dropwise addition of CBZ-Cl (498 mg, 417 μ l, 2.92 mmol, equiv: 1.5), was followed by stirring at 23 °C during 18 h.



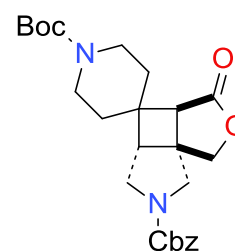
The reaction mixture was extracted with water and EtOAc. The organic layers were collected and dried over Na₂SO₄. All volatiles were removed under vacuum. The crude material was purified by flash chromatography (silica gel, 20 g, 0% to 100% EtOAc in heptane) to give *tert*-butyl 4-(2-(((benzyloxy)carbonyl)((5-oxo-2,5-dihydrofuran-3-yl)methyl)amino)ethylidene)piperidine-1-carboxylate (368 mg, 41% yield) as a colorless oil.

¹H NMR (400 MHz, DMSO, 120 °C) δ ppm 1.20 - 1.51 (m, 13 H) 1.97 - 2.23 (m, 6 H) 3.13 - 3.41 (m, 6 H) 3.93 (d, J =7.1 Hz, 3 H) 4.11 - 4.32 (m, 3 H) 4.64 - 4.83 (m, 2 H) 5.11 (s, 3 H) 5.22 - 5.34 (m, 1 H) 5.89 (t, J =1.8 Hz, 1 H) 7.01 - 7.56 (m, 5 H)

LC/MS m/z = 357.1832 [M-Boc]⁺ calculated from C₂₅H₃₂N₂O₆ (M=456.2260)

(3aRS,4aRS,7aSR)-6-Benzyl 1'-*tert*-butyl 3-oxotetrahydro-1H-spiro[furo[3',4':1,4]cyclobuta[1,2-c]pyrrole-4,4'-piperidine]-1',6(7*H*)-dicarboxylate (72):

In a quartz flask *tert*-butyl 4-(2-(((benzyloxy)carbonyl)((5-oxo-2,5-dihydrofuran-3-yl)methyl)amino)ethylidene)piperidine-1-carboxylate (100 mg, 219 μ mol, equiv: 1.0) was dissolved in acetonitrile (45 mL) and bubbled argon through, under ultrasound for 20 min. This mixture was irradiated in a Rayonet



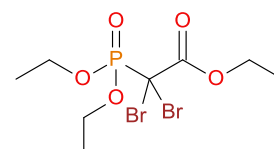
RPR-200 reactor (16 x 8 W lamps) at λ =254 nm for 3 h. All the volatiles were removed under vacuum. The crude material was purified by flash chromatography (silica gel, 12 g, 0% to 100% EtOAc in heptane) to give (3aRS,4aRS,7aSR)-6-benzyl 1'-*tert*-butyl 3-oxotetrahydro-1H-spiro[furo[3',4':1,4]cyclobuta[1,2-c]pyrrole-4,4'-piperidine]-1',6(7*H*)-dicarboxylate (34 mg, 34% yield) as an orange oil.

¹H NMR (400 MHz, DMSO 120 °C) δ ppm 1.44 (s, 13 H) 1.53 - 1.66 (m, 3 H) 2.59 (s, 1 H) 2.79 (s, 1 H) 3.13 - 3.55 (m, 7 H) 3.85 (d, *J*=12.2 Hz, 1 H) 3.95 (d, *J*=12.4 Hz, 1 H) 4.23 (d, *J*=9.7 Hz, 1 H) 4.49 (d, *J*=9.7 Hz, 1 H) 5.01 - 5.26 (m, 2 H) 7.39 (d, *J*=4.3 Hz, 4 H)

HRMS: *m/z*=357.1819 [M-Boc]⁺ calculated from C₂₅H₃₂N₂O₆ (M=456.2260)

Ethyl 2,2-dibromo-2-(diethoxyphosphoryl)acetate (79):

Ethyl 2-(diethoxyphosphoryl)acetate (45 g, 40 mmol, equiv: 1.0) was dissolved in DME (400 mL). The reaction was cooled down with a water bath and sodium hydride (60% in mineral oil) (14 g, 350 mmol, equiv: 1.74) was added carefully (exothermic reaction). The temperature was left to rise until 23 °C and stir for one hour. Cool down the reaction until 0 °C with an ice bath and add bromine (64.2 g, 20.7 mL, 401 mmol, equiv: 2.0). The reaction stirred at 23 °C during 2 hours. Extract with water/EtOAc. All the volatiles were removed. The crude material was purified by flash chromatography (silica gel) first with 3:1 and then 1:1 Heptane: EtOAc to give ethyl 2,2-dibromo-2-(diethoxyphosphoryl)acetate (71.1 g, 93% yield) as a light yellow oil.



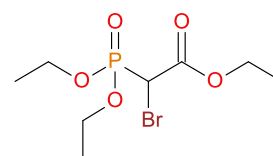
According to literature:¹¹

¹H NMR (600 MHz, CDCl₃) δ ppm: 1.32 – 1.47 (m, 12 H) 4.28 – 4.46 (m, 8 H)

³¹P NMR (300 MHz, CDCl₃) δ ppm: 8.4 (s) 7.0 (s)

Ethyl 2-bromo-2-(diethoxyphosphoryl)acetate (80)

Ethyl 2,2-dibromo-2-(diethoxyphosphoryl)acetate (7.64 g, 20 mmol, equiv: 1.0) was dissolved in ethanol (19.3 mL) in a ice bath. A solution of in water (38.5 mL) was added, maintaining the temperature lower than 10 °C. When the addition was complete, the reaction mixture was stirred for an additional 15 min at 23 °C. The mixture was extracted with DCM and dried over Na₂SO₄. All the volatiles were removed. The crude material was purified by flash chromatography (silica gel, 40 g, 0% to 100% EtOAc in heptane) to give ethyl 2-bromo-2-(diethoxyphosphoryl)acetate (5.73 g, 95% yield) as a light yellow oil.



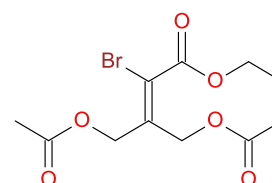
According to literature:¹¹

¹H NMR (600 MHz, CDCl₃) δ ppm: 1.32 (t, *J*= 7.1 Hz, 3 H) 1.38 (t, *J*= 7.1 Hz, 6 H) 4.23 – 4.33 (m, 8 H)

³¹P NMR (300 MHz, CDCl₃) δ ppm 13.2 (m).

2-(1-Bromo-2-ethoxy-2-oxoethylidene)propane-1,3-diyl diacetate (81):

To a solution of ethyl 2,2-dibromo-2-(diethoxyphosphoryl)acetate (2.41 g, 6.32 mmol, equiv: 1.1) in THF (14.9 mL) at 0° C was added dropwise *iso*-propylmagnesium chloride-lithium chloride complex (4.86 mL, 6.32 mmol, equiv: 1.1), and the mixture was stirred at



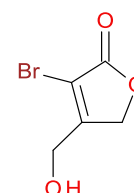
0° C for 30 minutes (conversion of the di-bromo to the mono-bromo compound checked by LC/MS). 2-Oxopropane-1,3-diyl diacetate (1 g, 5.74 mmol, equiv: 1.0) was added. The reaction was stirred at 23 °C during 18 h. There was no full conversion of starting material. The reaction mixture was poured into sat NH₄Cl, extracted with TBME and the organic layer were dried over Na₂SO₄. All the volatiles were removed by vacuum. The crude material was purified by flash chromatography (silica gel, 20 g, 0% to 100% EtOAc in heptane). There was isolation of as light yellow oil. (588 mg, 32% yield).

¹H NMR (600 MHz, CDCl₃) δ ppm 1.30 - 1.40 (m, 3 H) 2.04 - 2.12 (m, 6 H) 4.32 (q, *J*=7.1 Hz, 2 H) 4.91 (d, *J*=11.4 Hz, 4 H)

HRMS *m/z*= 325.0095 [M+H]⁺ calculated from C₁₁H₁₅BrO₆ (M=322.0038)

3-Bromo-4-(hydroxymethyl)furan-2(5H)-one (73):

In a flask with a condenser 2-(1-bromo-2-ethoxy-2-oxoethylidene)propane-1,3-diyl diacetate (4.75 g, 14.7 mmol, equiv: 1.0) was dissolved in methanol (45 mL). Add acetyl bromide (181 mg, 109 μL, 1.47 mmol, equiv: 0.1) and stirred at 23 °C during 18 h. The TLC



showed still starting material, so 10 mL of AcBr were added and the reaction mixture was warmed until 50 °C during 1,5 h. The reaction mixture was evaporated and azeotroped 3 times with toluene to give the 3-bromo-4-(hydroxymethyl)furan-2(5H)-one (1.92 g, 9.95 mmol, 67.7 % yield) as a brown oil. The crude material was purified

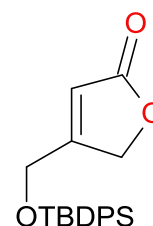
by flash chromatography (silica gel, 40 g, 0% to 100% EtOAc in heptane) to give 3-bromo-4-(hydroxymethyl)furan-2(5H)-one (1.92 g, 68% yield) as a yellow oil.

¹H NMR (600 MHz, CDCl₃) δ ppm 2.26 (br s, 1 H) 4.69 (s, 2 H) 4.98 (t, *J*=1.1 Hz, 2 H)

GCMS (EI): *m/z* = 192.1 [M•]⁺ calculated from C₅H₅BrO₃ (M=192.995)

4-(((*tert*-Butyldiphenylsilyl)oxy)methyl)furan-2(5H)-one (86):

In a flask, 4-(hydroxymethyl)furan-2(5H)-one (5.041 g, 44.2 mmol, equiv: 1.0) was combined with DMF (58.9 mL) to give a light brown solution. Imidazole (4.51 g, 66.3 mmol, equiv: 1.5) was added. TBDPS-Cl (14.6 g, 13.6 mL, 53 mmol, equiv: 1.2) was added dropwise. The reaction mixture was stirred at 23 °C during 18 h and extracted with TBME and water. The organic layer was dried with Na₂SO₄ and the solvents removed. The crude material was purified by flash chromatography (silica gel, 80 g, 0% to 50% EtOAc in heptane) to give 4-(((*tert*-butyldiphenylsilyl)oxy)methyl)furan-2(5H)-one (12.25 g, 79% yield) as a white solid.

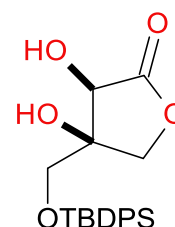


¹H NMR (600 MHz, CDCl₃) δ ppm 1.08 (s, 9 H) 4.50 - 4.61 (m, 2 H) 4.74 - 4.82 (m, 2 H) 6.03 (t, *J*=1.9 Hz, 1 H) 7.38 - 7.43 (m, 4 H) 7.45 - 7.49 (m, 2 H) 7.61 - 7.66 (m, 4 H)

HRMS *m/z* = 353.1564 [M+H]⁺ calculated from C₁₂H₂₄O₃Si (M=352.1491)

(3*RS*,4*SR*)-4-(((*tert*-Butyldiphenylsilyl)oxy)methyl)-3,4-dihydroxydihydrofuran-2(3*H*)-one (87):

To a vigorously stirred solution of 4-(((*tert*-butyldiphenylsilyl)oxy)methyl)furan-2(5*H*)-one (4.97 g, 14.1 mmol, equiv: 1.0) in ethyl acetate (89.5 mL)/acetonitrile (89.5 mL) at 0 °C was added a solution of ruthenium(III) chloride hydrate (223 mg, 987 μmol, equiv: 0.07) and sodium periodate (4.52 g, 21.1 mmol, equiv: 1.5) in water (24.9 mL). The two-phase mixture was stirred vigorously for 3 min and quenched with a saturated solution of Na₂S₂O₃. The aqueous phase was extracted with EtOAc. The organic layers were collected and dried over Na₂SO₄. All volatiles were removed under vacuum. The crude material was purified by flash chromatography (silica gel, 20g, 0% to 50% EtOAc in heptane) to give (3*RS*,4*SR*)-4-



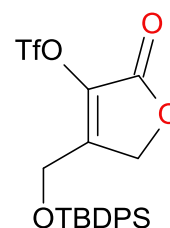
(((tert-butyldiphenylsilyl)oxy)methyl)-3,4-dihydroxydihydrofuran-2(3H)-one (5.10 g, 94% yield) as a light yellow foam.

¹H NMR (600 MHz, CDCl₃) δ ppm 1.05 - 1.14 (m, 9 H) 2.77 (d, *J*=4.4 Hz, 1 H) 2.88 (d, *J*=1.4 Hz, 1 H) 3.70 (s, 2 H) 4.23 (d, *J*=10.0 Hz, 1 H) 4.36 (dd, *J*=10.0, 1.3 Hz, 1 H) 4.53 (d, *J*=4.2 Hz, 1 H) 7.39 - 7.45 (m, 4 H) 7.48 (d, *J*=7.3 Hz, 2 H) 7.60 - 7.67 (m, 4 H)

HRMS *m/z*= 385.1479 [M-H]⁻ calculated from C₂₁H₂₆O₅Si 386.1551

4-(((tert-Butyldiphenylsilyl)oxy)methyl)-2-oxo-2,5-dihydrofuran-3-yl trifluoromethanesulfonate (88):

To a solution of (3RS,4SR)-4-(((tert-butyldiphenylsilyl)oxy)methyl)-3,4-dihydroxydihydrofuran-2(3H)-one (2 g, 5.17 mmol, equiv: 1.0) in dichloromethane (49 mL) held at -78 °C under argon were successively added pyridine (2.05 g, 2.09 mL, 25.9 mmol, equiv: 5.0) and a solution of trifluoromethanesulfonic anhydride (4.38 g, 2.62 mL, 15.5 mmol, equiv: 3.0) in dichloromethane (16.3 mL). After 15 min stirring at -78 °C, the reaction mixture was slowly warmed to -5 °C over a period of 3 h. The reaction was then poured into cold diethyl ether (40 mL). The precipitate was removed by filtration and the filtrate was evaporated in vacuum at 0 °C. The crude material was purified by flash chromatography (silica gel, 40 g, 0% to 50% EtOAc in heptane) to give 4-(((tert-butyldiphenylsilyl)oxy)methyl)-2-oxo-2,5-dihydrofuran-3-yl trifluoromethanesulfonate (2.13 g, 82% yield) a light yellow oil that further crystallized as white crystals .



¹H NMR (600 MHz, CDCl₃) δ ppm 1.00 - 1.13 (m, 9 H) 4.69 (s, 2 H) 4.96 (s, 2 H) 7.38 - 7.69 (m, 10 H)

GCMS (EI): *m/z*= 518.2 [M+NH₄]⁺ calculated from C₂₂H₂₃F₃O₆SSi (M=500.560)

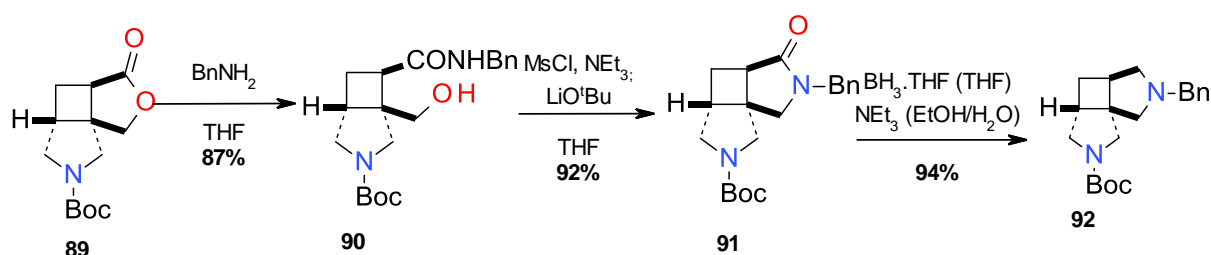
3.6-References

-
- ¹ D. A. Fort, T. J. Woltering, A. M. Alker, T. Bach, *Heterocycl.* **2014**, 88, 2, 1079-1100
 - ² D. A. Fort, T. J. Woltering, A. M. Alker, T. Bach, *J. Org. Chem.*, **2014**, 79, 7152-7162
 - ³ D. A. Fort, T. J. Woltering, M. Nettekoven, H. Knust, T. Bach, *Angew. Chem. Int. Ed.*, **2012**, 51, 10169-10172.
 - ⁴ A. Ianni, S. R. Waldvogel, *Synthesis*, **2006**, 2103-2112
 - ⁵ World patent: WO 2007/003964, **2007**
 - ⁶ United States patent: US 2006/0052359 A1, **2006**
 - ⁷ World patent: WO 97/40051, **1997**
 - ⁸ S. Mukherjee, B. List, *J. Am. Chem. Soc.*, **2007**, 129, 11336-11337
 - ⁹ E. Lattmann, H. M. R. Hoffman, *Synthesis*, **1996**, 155-163
 - ¹⁰ T. Olpp, R. Brückner, *Synthesis*, **2004**, 13, 2135-2152
 - ¹¹ C. E. McKenna, L. A. Khawli, *J. Org. Chem.*, **1986**, 51, 5467-5471
 - ¹² V. A. Vu, I. Marek, P. Knochel, *Synthesis*, **2003**, 12, 1797-1802
 - ¹³ A. Krasovskiy, P. Knochel, *Angew. Chem. Int. Ed.*, **2004**, 43, 25, 3333-3336
 - ¹⁴ S. Chassaing, S. Specklin, J. Weibel, P. Pale, *Tetrahedron*, **2012**, 36, 68, 7245-7273
 - ¹⁵ R. Jana, T. Pathak, M. Sigman, *Chem. Rev.*, **2011**, 111, 1417-1492
 - ¹⁶ T. Shing, V. Tai, E. Tam, *Angew. Chem. Int. Ed. Engl.*, **1994**, 33, 22, 2312-2313
 - ¹⁷ M. Valle, A. Tarrade-Matha, P. Dauban, R. Dodd, *Tetrahedron*, **2008**, 64, 419-432
 - ¹⁸ R. Raap, C. G. Chin, R. G. Micetich, *Can J. Chem.*, **1971**, 49, 2143-2151
 - ¹⁹ T. Sato, K. Okamoto, Y. Nakano, J. Uenishi, M. Ikeda, *Heterocycl.*, **2001**, 54, 747-755
 - ²⁰ A. Pohjakallio, P. M. Pihko, U. M. Laitinen, *Chem. Eur. J.*, **2009**, 15, 3960-3964

4-Further Functionalization of [2+2]-PCA products

4.1-Compact Modules

An approach to the synthesis of conformationally restricted bis-pyrrolidines has been described using as starting material the photoproduct **89**. The lactone ring was opened with benzylamine in THF forming the corresponding benzylamide and a primary alcohol **90**. Mesylation of the free hydroxyl group and subsequent treatment with LiO^tBu induced the nucleophilic substitution. Selective lactam reduction with borane-THF complex originated the corresponding borane-amine complex from which the free base 3,9-diazatricyclo[5.3.0.0^{1,5}]decane **92** was liberated (**Scheme 1**).¹



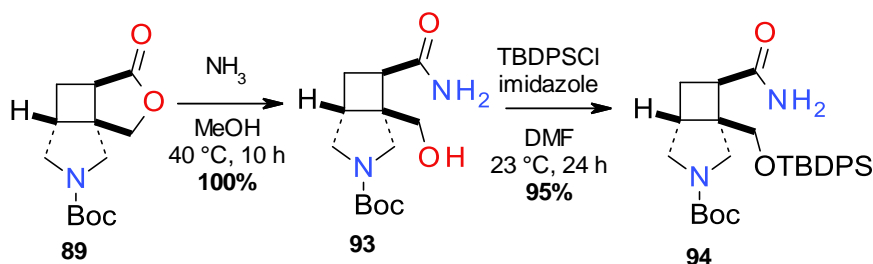
Scheme 1

This work shows an example of further functionalization of the photoproducts as a way of obtaining highly functionalized molecules with potential use in complex organic chemistry synthesis.

In extension to the work previously developed by Fort *et al.*¹, a different approach towards the functionalization of **89** was performed which demonstrated the versatility of the photoproducts by introducing different functionalities. The goal was the synthesis of an electrophilic building block rather than a nucleophilic one like **92**. However, all the intermediates used in the synthetic route can be considered useful compact modules. A route with classic and reliable procedures was proposed.

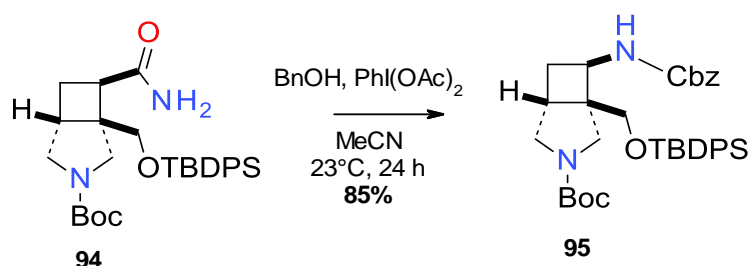
The lactone ring of **89** was quantitatively opened using ammonia as a nucleophile. The scaffold **94** possesses an amide and a primary alcohol in *cis* configuration. For the sequential rearrangement the hydroxyl group was protected

with TBDPS to give **94**. TBDPS was the favorable choice due to the fact that it is quite a resistant protecting group but can be cleaved selectively.



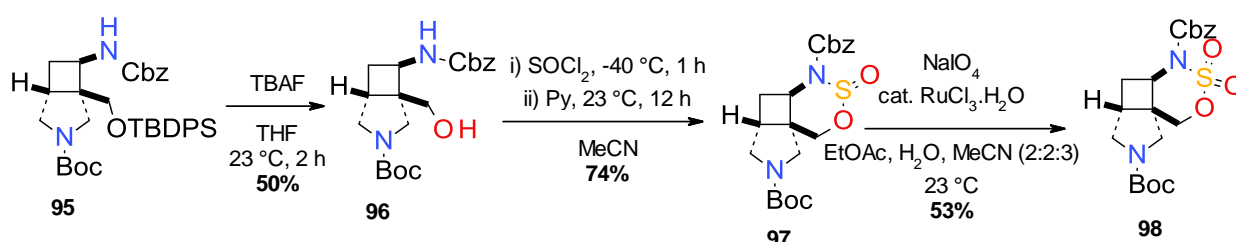
Scheme 2

Through a successful Hoffman rearrangement the amide was converted to the amine protected with Cbz (**95**). Contrary to a standard Hoffman rearrangement that is performed under highly basic conditions, the utilization of $\text{PhI}(\text{OAc})_2$ allowed the reaction to occur under mild conditions. The use of a reagent with a hypervalent iodine allowed the oxidation of the carboxamide to the corresponding isocyanate that later was trapped with benzyl alcohol as nucleophile.



Scheme 3

Cleavage of the TBDPS protecting group with TBAF, followed by the reaction with thionyl chloride followed by treatment with pyridine gave access to cyclic sulfamidite **97**. The rather low yield of the deprotection reaction can be justified by the formation of a cyclic carbamate. Further oxidation with catalytic ruthenium chloride and sodium periodate gave access to the cyclic sulfamidate **98**.



Scheme 4

Stable electrophilic building blocks are not widely available; however, this particular cyclic sulfamidate is an interesting example. Compact module **98** is a stable cyclic sulfamidate, which possesses two orthogonally protected nitrogen atoms allowing further selective functionalization. Of particular interest is the neopentyl carbon which is generally quite unreactive in substitution reactions but in the case of the sulfamidate **98** nicely set up for S_N2 reaction due to its cyclic structure. The synthetic potential of the complex cyclic sulfamidate **98** is beyond that which has been described, therefore delivering a great number of future synthetic opportunities.

4.2 BACE1 inhibitors:

An attempt to synthesize an active compound to be used as a BACE-1 inhibitor was made.

The initial examples of BACE1 inhibitors originated from substrate and transition-state analysis design. The compounds that were originated by this method possessed a large polar surface area making them prohibitive for permeability of the blood-brain barriers. Due to its large active site, the search for BACE1 inhibitors and their optimization has proved to be challenging. Small molecule inhibitors can be optimized for potency and potentially developed to be brain permeable and orally bioavailable and therefore allow a versatility that peptide mimetics do not offer.

Amidine or guanidine-containing moieties were identified early on to form an ideal hydrogen-bonding system with the catalytic aspartyl dyad in BACE1 active center.²

BACE can be prepared in highly purified forms and several of three - dimensional (3D) structures in complexation with a variety of inhibitors have been solved to contribute to rational drug design.

BACE belongs to the family of the aspartic proteases and therefore its catalytic center has a dyad of aspartate residues. At least eight specific pockets (S4-S1 and S1'-S4') appear to be required for binding of substrate to the active site. In general, the active site of BACE is dominated by hydrophobic residues. S4, S2 and S2' are more hydrophilic and solvent exposed (**Figure 1**).

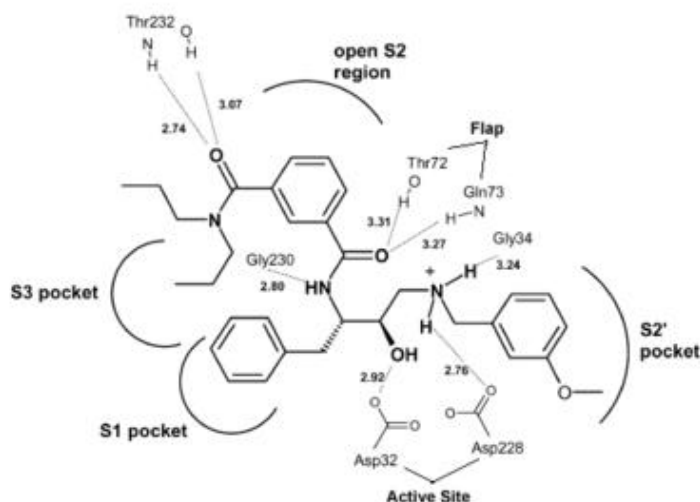


Figure 1: Simplified diagram of BACE1 active site³

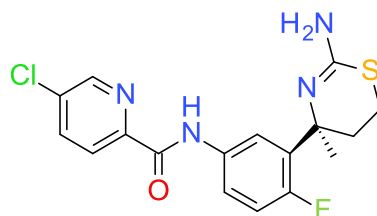
There are two main regions in BACE1 that can undergo conformational changes. The first, a β -harpin structure spans residues 70~76 known as the flap and the second one is a deep cleft adjacent to the S3 pocket, often referred to as the S3 subpocket. The conformational changes are highly dependent on the nature of the ligand. The flap is a region that can be potentially used in order to achieve selectivity between the two BACE isoforms 1 and 2. In the BACE2 flap there is a proline instead of tyrosine that rigidifies the structure. The fact that the BACE1 flap is more conformationally free may allow that a longer substituent can conduct a change in the BACE1 flap that would cost too much energy in the case of BACE2 and therefore lead to selectivity. Previous exploitation of the conformationally variable S3 had shown impressive gains of potency.⁴

The prime site of BACE has shown to be less restricted than the non-prime pockets. The S1' pocket is large enough to accommodate a cyclohexyl group however, in natural substrates it is often unoccupied.

One of the main challenges of the synthesis of BACE1 inhibitors is the fact that the active site is highly conserved among BACE1 and BACE2 making it difficult achieving selectivity. Besides the similarity among BACE1 and BACE2 there are some aspartyl proteases expressed in other tissues of the organism with a similar active site that its inhibition can cause undesirable side effects.

4.2.1 Molecular modeling and *de novo* design

One of the first highly potent and more drug-like small molecule non-peptide BACE1 inhibitors described was a 2-aminothiazine derivative synthesized by the Japanese pharmaceutical company Shionogi® (**Scheme 5**).⁵



108

Scheme 5

This compound shows good *in vitro* and *in vivo* activity and due to that soon became a reference compound for assays and molecular modeling. Through the years several x-rays structures were resolved of the BACE1 **108** complex. Low selectivity towards BACE2 and hERG channel inhibition are two of the main factors why the compound **108** did not became a drug.

Since then several pharmaceutical companies have been working in the synthesis of BACE1 inhibitors. In **Figure 2** there is an overview of several “head groups” that were synthesized and described by several companies.²

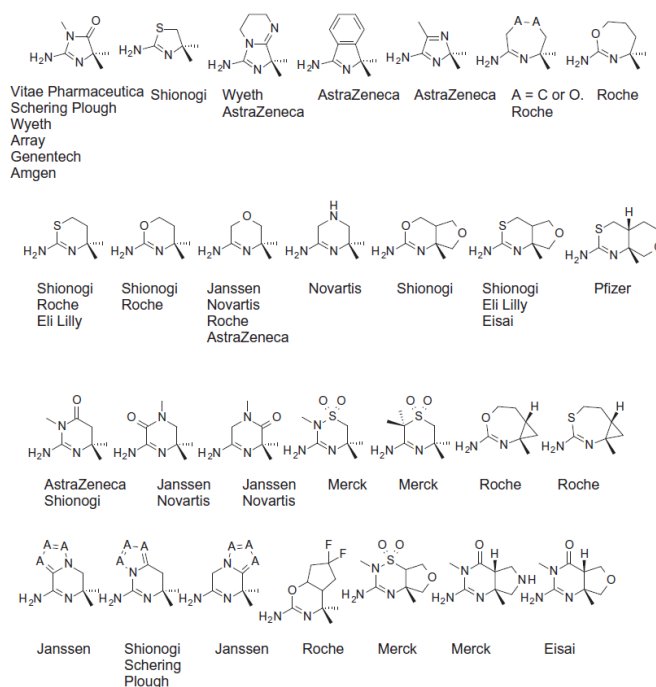
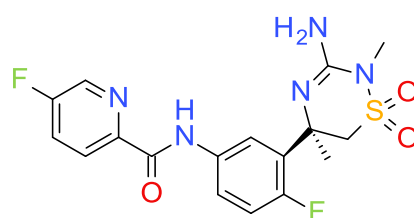


Figure 2: Overview of different “head groups” of BACE1 inhibitors that were described by several pharmaceutical companies.

The fact that several different companies have been working in the last years in the synthesis of BACE1 inhibitors reveals how complex the synthesis and discovery of active compounds is.

Although several new molecules were synthesized since the discovery of compound **108**, most of them failed to become a drug. In the present there is one compound, Verubecestat, from the pharmaceutical company Merck® in phase III clinical trials (**Scheme 6**).



Verubecestat

Scheme 6

The similarities among compound **108** and verubecestat are easily noticeable. Amide bonds, specially the ones whose cleavage could lead to formation of anilines are known to not be the most stable and safe motifs in drug compounds. Thus, verubecestat has not shown high metabolic instability.

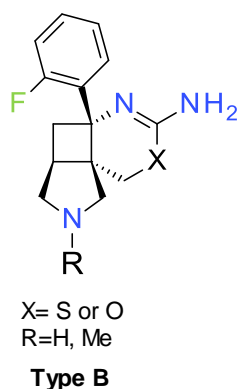
The 2-aminothiazine and 2-aminooxazine moieties are present in a lot of active compounds and increase the activity due to the establishment of a double hydrogen bonding network with the aspartatic dyad. The amidine moiety is responsible to ensure selectivity over other proteases.

Another interesting feature of compound **108** is the extended functionalization towards the S3 pocket with a 5-chloro-2-pyridyl residue. The 5-chloro penetrates deeply into the S3 pocket, and the nitrogen of the pyridyl forms a hydrogen bond with the amide and thereby is responsible for the alignment of the phenyl and pyridyl residues in an almost planar arrangement. The amide bond between the two aromatic heterocycles mimics the peptide bond present in the natural substrate forming a hydrogen bond with the glycine 291 of BACE1.

With this information in hand and some more acquired from other known inhibitors the design of novel series of potential BACE1 inhibitors was performed. The 2-aminothiazine or 2-aminooxazine moieties were kept due to the fact that these

have been shown to be important pharmacophores. The incorporation of a cyclobutane ring allowed the opportunity to have more exit vectors towards other pockets that are not explored in compound **108**. Aiming at gain of activity and selectivity, a functionalization towards the flap region was desired. The tricyclic scaffolds obtained by the intramolecular [2+2]-PCA of substituted furanones have a pyrrolidine ring that would be conformationally placed towards the flap. The pyrrolidine ring also permitted further functionalization of the nitrogen in order to have different substituents. Since the natural substrate of BACE1 has an aromatic residue lodged in S1 pocket an aryl ring into that position could also be a key point of the activity of the head group.

The synthesis of a head group of the type **B** was planned (**Scheme 7**).



Scheme 7

Computational molecular modeling, using the software Moloc,⁶ was performed for the head group to check its conformation in the active site of BACE1. **Figure 3** consists of the image of the modulation of the oxazine head group and the methylated pyrrolidine nitrogen in green, aligned with the x-ray structure of the Shionogi compound **108** (1bfg; in orange) in the BACE1 active site.

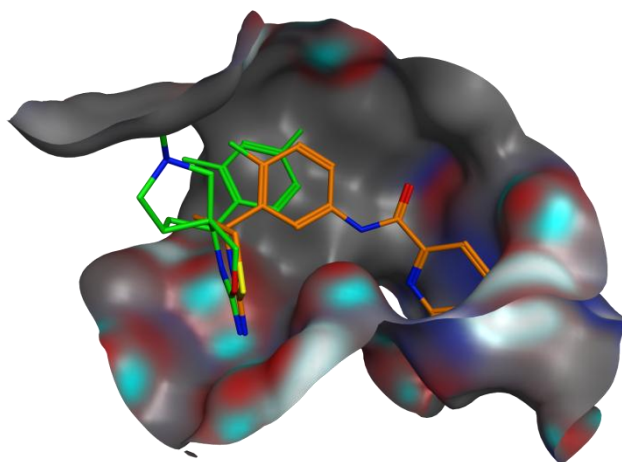


Figure 3: Computational molecular modeling image of the BACE1 active site and two ligands (orange: Shionogi compound (1bfgy); green: compound type B (with X=O and R= Me).

With the model it is possible to determine that the nitrogen of the pyrrolidine ring cannot be functionalized with a large substituent because most likely it would collide with the surface of the protein. So a methyl group would be the ideal substituent due to its small size and low hydrophilicity. There is still the chance of functionalization of the aryl ring in the *para*-position to the fluorine. By functionalization of this position there is the possibility to move slightly towards the S3 pocket. However, due to the different spatial conformation this functionalization would not go deeply into S3 pocket as the one in the Shionogi compound **108**.

After the information from computational molecular modeling was gathered the synthesis of the potential BACE1 inhibitors was planned. For that photoproducts previously described were used as starting point.

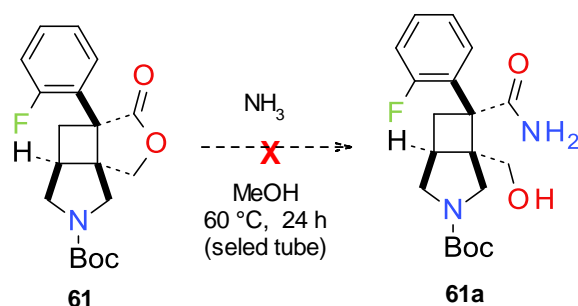
4.2.2- Synthesis of potential BACE1 inhibitors

The amidine moiety has been reported as a crucial functionality towards the activity in BACE1. To install the amidine group directly into the cyclobutane ring, the loss of one carbon atom was required. Regarding to this, a rearrangement of a suitable carboxylic acid derivative (e.g. amide *via* Hoffmann or hydrazide *via* Curtius rearrangement) to the correspondent amine was envisioned.⁷

From the previously described photoproduct **76** (*chapter 3*) the lactone ring was opened. Initially ammonia was chosen as the nucleophile. A similar approach

used in the synthesis of the cyclic sulfamidate **96** was planned. The ring open with ammonia would lead to the correspondent amide that would be a part of a Hoffman rearrangement to form the carbamate.

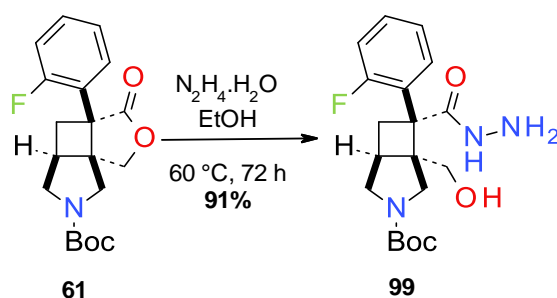
Although the ammonolysis of the lactone **89** was successful in the 2-fluorophenyl derivative **61** case it's nucleophilic character was not strong enough (**Scheme 8**). After 24 h there was no consumption of starting material **61**.



Scheme 8

Given that a stronger nitrogen nucleophile was required, hydrazine was considered as the way to go. From the corresponding hydrazide conversion towards the corresponding acyl azide was possible and therefore a Curtius rearrangement was planned to access the desired carbamate. Hydrazine has a higher nucleophilicity than ammonia due to the so called α -effect. This effect states that a presence of an adjacent (α) atom with lone pair of electrons increases the nucleophilic character of a molecule. This effect has been explained assuming that the alpha lone-pair and nucleophilic electron pair destabilize each other by electronic repulsion and thereby increase the ground state making it more reactive.

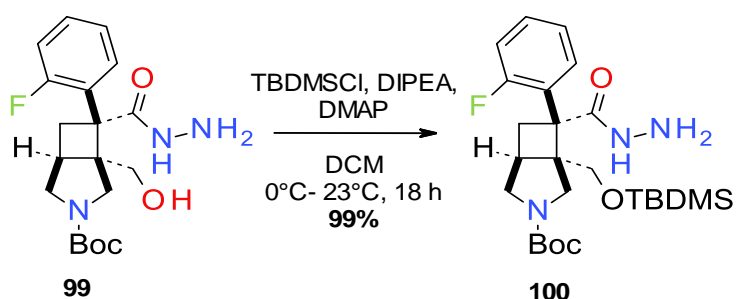
Reaction between **61** and excess hydrazine hydrate in ethanol in a pressure tube at 60 °C gave access to the corresponding hydrazide derivative **99** in almost quantitative yield (**Scheme 9**).



Scheme 9

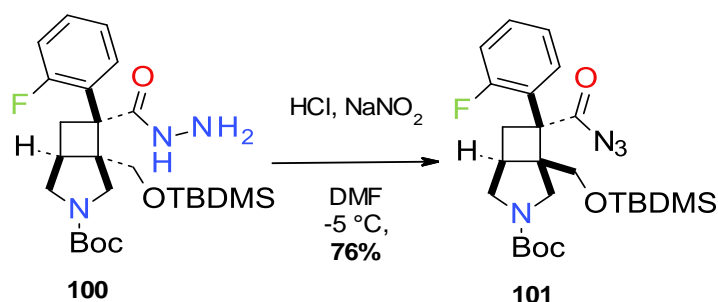
In consideration to the rearrangement the hydroxyl group had to be protected to avoid side reactions. In the Curtius rearrangement there is formation of the isocyanate as an intermediate. The free hydroxyl group could react with the isocyanate forming a cyclic carbamate which would be extremely hard to cleave. The first choice for protecting group was the TBDPS group since it has shown good performance in similar derivatives. However, the protection reaction occurred with low yields most likely due to high steric hindrance.

In an attempt to increase the yield of the transformation another protecting group was selected. A similar but yet less bulky option was found in the TBDMS group. The fact that the silyl ethers are easily formed and cleaved selectively under mild conditions are two of the most interesting characteristics of this family of protecting groups (**Scheme 10**).



Scheme 10

The following step was to convert the hydrazide into an acyl azide in the presence of the Boc group. Using a classic peptide synthesis procedure the conversion occurred with 76% yield on a reasonable scale.⁸ The acyl azide **101** was isolated and even chromatographed with no sign of decomposition (**Scheme 11**).

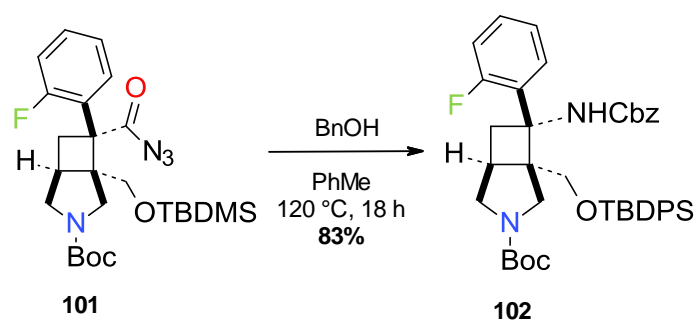


Scheme 11

With the acyl azide **101** in hand the Curtius rearrangement to obtain the corresponding carbamate was performed (**Scheme 12**). Although formation of the

free amine is necessary for a later step, direct isolation of this compound would prove difficult. In addition access to the free amine *via* the Curtius rearrangement would require strongly basic conditions leading to cleavage of the TBDMS group. Instead, accessing the corresponding carbamate afforded two orthogonally protected nitrogens and facilitated isolation and purification processes.

Mechanistically the Curtius rearrangement has two main parts: the formation of the isocyanate by refluxing the acyl azide in toluene followed by the carbamate formation in the presence of benzyl alcohol. Transformation from the acyl azide **101** to the corresponding carbamate **102** was performed using just two equivalents of benzyl alcohol with a high yield (**Scheme 12**).

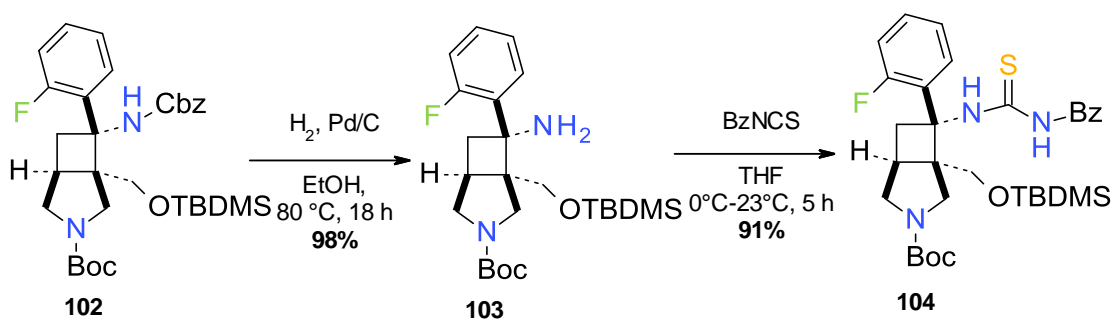


Scheme 12

The rearrangement was performed in the presence of an alcohol to avoid reaction between the isocyanates, forming stable urea derivatives which would be hard to cleave. The choice of benzyl alcohol allowed cleavage by hydrogenolysis; conditions to which the Boc and TBDMS protecting groups are inert in this substrate. However the high boiling point of benzyl alcohol also played an important role.

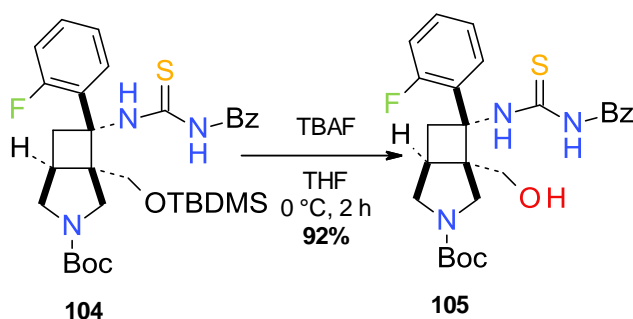
Cleavage of the Cbz group by hydrogenolysis provided the free amine in quantitative yield. As previously discussed the selectivity of the hydrogenolysis allowed that the pyrrolidine and the hydroxyl group remained protected. For the success of the synthesis of the thiourea it was crucial that the free amine was the only free functionality available to react with the benzoyl isothiocyanate.

With just 1.05 equiv. of benzoyl isothiocyanate the thiourea **104** was smoothly synthesized in 91% yield (**Scheme 13**).



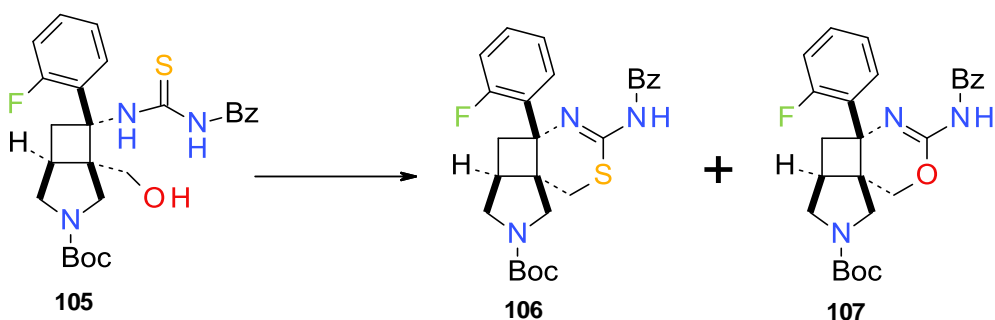
Scheme 13

For both - the oxazine and the thiazine compounds - the TBDMS group was cleaved to give the free hydroxy thiourea **105**.



Scheme 14

From scaffold **105** both oxazine and thiazine rings can be accessed. Although both compounds were interesting a set of reaction conditions that would be selective towards each one of the functional groups was desired. An initial set of experiments was performed.



Scheme 15

Table 1: Optimization of selectivity of the synthesis of **106** vs **107**.

#	s.m.	Reaction conditions	Reaction time	Products	Yield of (%)
1	105	Tf ₂ O, Py, DCM, -50 °C to -30 °C	2 h	106 and 107 (1:1)	106 -44% 107 -42%
2	105	CBr ₄ , PPh ₃ , DCM, 0°C	2 h	106 and 107 (3:1)	106 -77% 107 -22%
3	105	Ghosez's reagent, DCM, 0 °C to 23 °C	2.5 h	106	97%
4	105	EDC, MeCN, 75 °C	1.5 h	107	98%

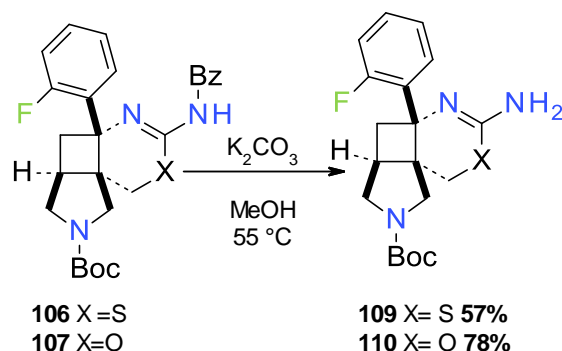
First triflic anhydride, pyridine in dichloromethane was used and led to the formation of both the oxazine and the thiazine in a 1:1 ratio.⁹ The 1:1 ratio is due to the formation of both the STf and the OTf in the reaction mixture. In the case of the formation of the OTf there is formation of the thiazine and consequently the formation of STf as a leaving group gives the oxazine.

In a second approach carbon tetrabromide, triphenylphosphine in dichloromethane also caused formation of both products in a 3:1 ratio in favor of the thiazine. Using carbon tetrabromide and triphenylphosphine it was expected that the phosphonium salt would activate the hydroxyl group. Therefore the bromine would be inserted in the hydroxyl position and act as a leaving group for the formation of the thiazine ring. However, there is also activation of the sulfur by the phosphonium salt, which leads to the formation of the oxazine ring. Due to the strong oxophilic character of phosphorous there is a preferential activation of the hydroxyl group. This justifies the higher ratio of thiazine formation.

In the continuous search for selective conditions towards the thiazine a procedure using Ghosez's reagent was performed. Mechanistically the Ghosez's reagent would lead to the replacement of the hydroxyl group by chlorine. The chlorine would act as a leaving group leading to the formation of the thiazine. Using Ghosez's reagent selectivity towards the thiazine synthesis was achieved.¹⁰

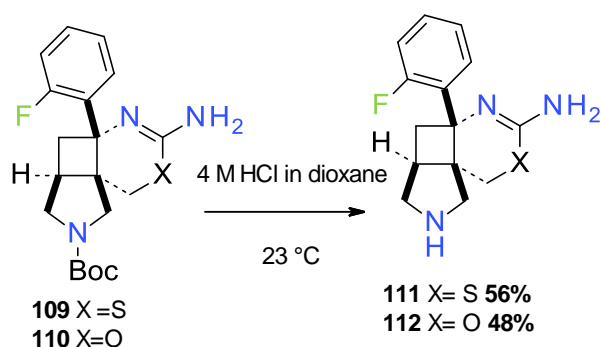
In the attempt to obtain selective conditions towards the synthesis of the oxazine moiety, EDC was used as reagent. EDC captures the sulfur and forms a carbodiimine that is attacked by the oxygen of the hydroxyl group closing the oxazine ring. The reaction was conducted using acetonitrile reflux, and 1.5 hour later the oxazine **107** was synthesized with 98% yield.

In order to enable BACE1 binding the free amidine is required. The benzoyl group was cleaved using potassium carbonate in methanol at 55 °C (**Scheme 16**).



Scheme 16

The next step consisted of cleaving the Boc group in order to have the free amines. The cleavage was performed by suspending the starting materials in a 4 M solution of HCl in dioxane and filtration of the HCl salt precipitate (**Scheme 17**).



Scheme 17

The head groups with the free amidine moiety were submitted to an *in vitro* assay. The compounds submitted were all racemic mixtures because a chiral synthesis was not discovered in this case. It is known that most likely only one enantiomer will be active. If the racemic mixtures show activity in the biological assays the enantiomers can be separated by chiral HPLC. Further functionalization to achieve a variety of new compounds was planned. The free pyrrolidine group increases the basicity of the molecule. In the other hand the Boc group is most likely too large and would collide with the surface of the protein. The molecular modeling showed that the methyl group could be a good choice.

4.2.3 MR121 BACE assay and results

The MR121 fluorescence assay is based on the fact that MR121 forms a non-fluorescent ground state complex with tryptophan. This principle can be used to design biochemical assays for proteases. In absence of protease activity, the substrate remains intact, and the MR121 fluorescence is reduced by the high *local* Trp-concentration. If the substrate is cleaved by the enzyme the MR121 fluorescence is recovered. In our case the protease is the aspartic protease 6his-BACE1. The enzymatic reaction can be followed in a kinetic measurement detecting an increase of MR121 fluorescence during the reaction time. If the enzyme is inhibited there is no increase of the MR121 fluorescence. Calculating the slope in the linear range of the kinetic provides a robust value for the activity of 6his-BACE1. This assay principle is suitable for inhibitor screens, looking for compounds which decrease the activity and thus the slope.

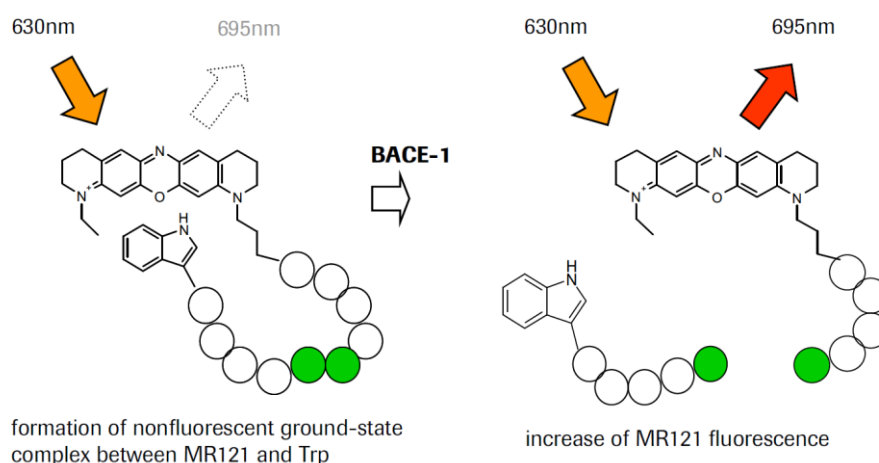


Figure 4: Schematic representation of the principle of an MR121 BACE assay.

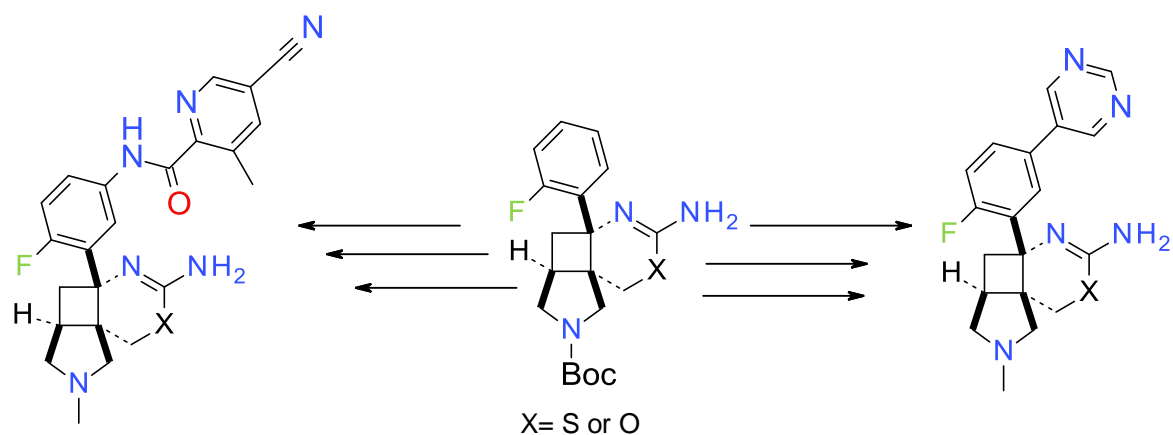
In order to evaluate the binding activity of the head groups **109**, **110** and **111** this groups were submitted to the MR121 BACE1 (**Table 2**). Head group **112** was not submitted early enough so the results were obtained to be part of this dissertation.

Table 2: Results of the MR121 BACE assays.

#	Compound no.	BACE1 IC ₅₀	BACE2 IC ₅₀
1	109	>200 (μM)	>200 (μM)
2	110	>200 (μM)	>200 (μM)
3	111	>200 (μM)	>200 (μM)

The results of the MR121 showed that the head groups have no inhibition activity towards BACE1 or BACE2. With an IC_{50} of over 200 μ M in the MR121 the compounds do not show promising potential to become BACE1 inhibitors. The lack of activity of compounds **109** and **110** was expected due to the fact that the Boc group on the pyrrolidine ring would be too bulky and collapse against the surface of the protein. The lack of activity of compound **111** can be explained by the high basicity of the free amine and amidine moieties that can compromise binding. Another explanation is that the pyrrolidine ring is just too big itself to fit in the active site of BACE. In order to try to understand the lack of activity further decoration of the head group was planned.

Further functionalization of the aryl ring has proven to be important in binding and selectivity towards BACE1. A methyl group would be small enough to fit in the active site without colliding with the surface of the active center. Several studies have showed that the functionalized pyridine group with the extension towards the S3 pocket has increased the selectivity. However, the head group conformation showed that such a big substituent would not fit since it would not be oriented towards the S3 pocket. (**Scheme 18**).



Scheme 18

The first set of experiments will consist in the methylation of pyrrolidinic nitrogen followed functionalization of the phenyl ring with a small heterocyclic rotasymmetric substituent. Parallel to the attempts of increasing activity by functionalization of the head groups the synthesis of similar derivatives without the pyrrolidine group is being conducted. This set of experiments will help to determine if the pyrrolidine group is the cause of lack of activity.

4.3-Conclusion

A novel electrophilic building block was successfully synthesized. The [2+2]-PCA was crucial to establish the cyclobutane moiety with the right regioselectivity. The versatility of photoproduct **89** was once again demonstrated. The exit vectors of the tricyclic moiety were successfully functionalized to obtain another complex and novel compact module.

Cyclic sulfamidate **98** is a stable electrophilic building block with a set of characteristics that provide an enormous synthetic versatility that is rarely found in such complex scaffolds. The two orthogonally protected nitrogens, the stable sulfamidate and the reactive neopentyl carbon provide several opportunities of decoration to achieve higher levels of complexity.

In recent years several technological advances have been achieved towards the optimization of computational chemistry. One of the biggest challenges is the accurate calculation of absolute free energies of binding. The underlying physics of a protein are best computed using rigorous statistical mechanisms methods. However, perfect prediction of protein-ligand interactions is not possible. *In vivo* and *in vitro* assays sometimes have completely different outcomes from what the computational chemistry predicted. This was demonstrated in the case of the head groups **109**, **110** and **111**. Although the compounds should have high probability of activity according to computational modeling in the *in vitro* assay the compounds showed to be inactive. Methylation of the pyrrolidinic nitrogen as well as functionalization of the aryl ring may cause increase of the activity.

Despite being inactive the novel head groups have a tricyclic moiety with a cyclobutane ring that has never been reported as potential BACE1 inhibitors. The topology of the cyclobutane ring forces the ligand into a conformation allowing the exploration of the S2 region and S2' pocket. Several approaches of functionalization of the cyclobutane ring are innovative and hopefully will be groundbreaking in the synthesis of BACE1 inhibitors.

The large number of companies and the time spent in BACE1 inhibitors research illustrate the dimension of the challenge. Several *in vitro* highly active compounds have been described however, most of them showed no *in vivo* activity.

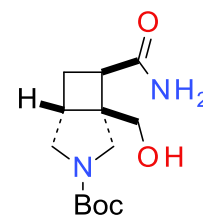
Blood Brain barrier penetration as well as Pgp efflux continue to be the main challenges in the design of BACE1 inhibitors. Other problems are related with safety risks because selectivity towards closely related aspartyl proteases is required in order to avoid several secondary effects.

4.4-Experimental section:

General: Unless otherwise stated, the reactions were stopped when the starting material was fully consumed according to thin layer chromatography (TLC) and/or LC/MS analysis. Compounds were detected by UV ($\lambda=254$ nm), CAM (cerium ammonium molybdate solution) or KMnO_4 . ^1H and ^{13}C NMR: Bruker AV-300, AV-400 and AV-600 recorded at 300 K unless otherwise indicated. Chemical shifts are reported relative to the solvent [CHCl_3 : δ (^1H) = 7.26 ppm, δ (^{13}C) = 77.0 ppm, DMSO δ (^1H) = 2.50 ppm, δ (^{13}C) = 39.5 ppm] as reference. The relative configuration of the products was determined by two-dimensional NMR spectra (COSY, NOESY, HSQC, HMBC). HRMS data were recorded by electron spray ionization (ESI) on an ion trap mass spectrometer.

(1SR,5RS,7RS)-*tert*-Butyl-7-carbamoyl-1-(hydroxymethyl)-3-azabicyclo[3.2.0]heptane-3-carboxylate (93):

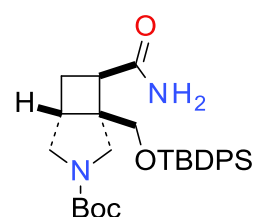
In a pressure tube, a mixture of (3aRS,4aRS,7aSR)-*tert*-butyl 3-oxohexahydrofuro[3',4':1,4]cyclobuta[1,2-c]pyrrole-6(1H)-carboxylate (6 g, 23.7 mmol, equiv: 1.0) and ammonia (7 M in methanol) (49.1 mL, 343 mmol, equiv: 14.5) was stirred at 40 °C for 24 h. All volatiles were removed in vacuum to give the (1SR,5RS,7RS)-*tert*-butyl 7-carbamoyl-1-(hydroxymethyl)-3-azabicyclo[3.2.0]heptane-3-carboxylate (6.4 g, 100 % yield) as a white foam.



^1H NMR (600 MHz, DMSO) δ ppm 1.42 (s, 9 H), 1.49-1.57 (m, 1 H), 2.32-2.49 (m, 2 H), 2.78-2.84 (m, 1 H), 3.13-3.27 (m, 2 H), 3.37-3.57 (m, 4 H), 4.66 (s, 1 H), 6.81 (s, 1 H), 7.24 (s, 1 H).

(1SR,5RS,7RS)-*tert*-Butyl 1-(((*tert*-butyldiphenylsilyl)oxy)methyl)-7-carbamoyl-3-azabicyclo[3.2.0]heptane-3-carboxylate (94):

(1SR,5RS,7RS)-*tert*-Butyl 7-carbamoyl-1-(hydroxymethyl)-3-azabicyclo[3.2.0]heptane-3-carboxylate (4.48 g, 16.6 mmol, equiv: 1.0) was combined with DMF (22.1 mL). Imidazole (1.69 g, 24.9 mmol, equiv: 1.5) was added. Dropwise addition of TBDPS-Cl (5.47 g, 5.11 mL, 19.9 mmol, equiv: 1.2) and the reaction mixture was stirred at 23 °C during 18 h. The reaction mixture was



extracted with EtOAc and water. The organic layers were collected and dried over Na₂SO₄. All volatiles were removed under vacuum. The crude material was purified by flash chromatography (silica gel, 40 g, 0% to 80% EtOAc in heptane). The major fraction was collected to give as a white crystal (1SR,5RS,7RS)-*tert*-butyl 1-(((*tert*-butyldiphenylsilyl)oxy)methyl)-7-carbamoyl-3-azabicyclo[3.2.0]heptane-3-carboxylate (7.286 g, 86% yield).

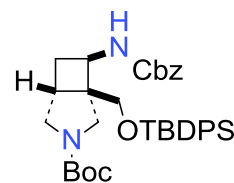
¹H NMR (600 MHz, DMSO) δ ppm 0.88-1.06 (m, 9 H), 1.43 (s, 9 H), 151-1.66 (m, 1 H), 2.38 (ddd, $J=11.9, 9.1, 7.4$ Hz, 1 H), 2.52-2.55 (m, 1 H), 2.83 (t, $J= 8.0$ Hz, 1 H) 3.29 (dd, $J= 11.4, 7.3$ Hz, 2 H) 3.42 (d, $J= 11.3$ Hz, 1 H), 3.51-3.87 (m, 3 H), 6.77 (s, 1 H), 7.12-7.32 (m, 1 H), 7.38-7.69 (m, 10 H)

HRMS $m/z=409.230$ [(M+H)+(-Boc)]⁺ calculated from C₂₉H₄₀N₂O₄Si (M=508.2768)

(1RS,5RS,7RS)-*tert*-Butyl 7-(((benzyloxy)carbonyl)amino)-1-(((*tert*-butyldiphenylsilyl)oxy)methyl)-3-azabicyclo[3.2.0]heptane-3-carboxylate (95):

A solution of (1SR,5RS,7RS)-*tert*-butyl 1-(((*tert*-butyldiphenylsilyl)oxy)methyl)-7-carbamoyl-3-

azabicyclo[3.2.0]heptane-3-carboxylate (7.286 g, 14.3 mmol, equiv: 1.0) in acetonitrile (57.3 mL) was stirred at 23 °C. Benzyl alcohol (3.1 g, 2.98 mL, 28.6 mmol, equiv: 2.0) was added, and



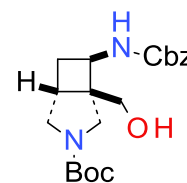
the mixture was stirred. The reaction was cooled down to 0 °C with an ice bath, and iodobenzene diacetate (5.07 g, 15.8 mmol, equiv: 1.1) was added carefully. The reaction was stirred overnight at 23 °C. The organic layer was extracted with TBME and water and NaCl. The organic layers were collected and dried over Na₂SO₄. All volatiles were removed under vacuum. The crude material was purified by flash chromatography (silica gel, 40 g, 0% to 50% EtOAc in heptane) to give (1RS,5RS,7RS)-*tert*-butyl 7-(((benzyloxy)carbonyl)amino)-1-(((*tert*-butyldiphenylsilyl)oxy)methyl)-3-azabicyclo[3.2.0]heptane-3-carboxylate (5.74 g, 65% yield) as a colorless oil.

¹H NMR (600 MHz, CDCl₃) δ ppm 1.02-1.16 (m, 6 H), 1.20-1.32 (m, 1 H), 1.37-1.55 (m, 6 H), 2.06-2.25 (m, 1 H), 2.76 (s, 2 H), 3.15-3.91 (m, 4 H), 4.29 (q, $J=8.2$ Hz, 1 H), 4.57-4.73 (m, 4 H), 4.95-5.19 (m, 1 H), 5.87 (s, 1 H), 7.27-7.51 (m, 13 H), 7.55-7.75 (m, 3 H)

HRMS m/z = 637.3075 $[M+Na]^+$ calculated from $C_{36}H_{46}N_{20}O_5Si$ (M =614.3179)

(1RS,5RS,7RS)-tert-Butyl 7-(((benzyloxy)carbonyl)amino)-1-(hydroxymethyl)-3-azabicyclo[3.2.0]heptane-3-carboxylate (96):

A solution of (1RS,5RS,7RS)-tert-butyl 7-(((benzyloxy)carbonyl)amino)-1-(((tert-butyldiphenylsilyl)oxy)methyl)-3-azabicyclo[3.2.0]heptane-3-carboxylate (5.74 g, 9.34 mmol, equiv: 1.0) in TBAF (9.34 mL, 9.34 mmol, equiv: 1.0) was stirred at 23 °C during 2 h. The reaction was extracted with water and EtOAc, the organic layers were collected and dried over Na_2SO_4 . All volatiles were removed under vacuum. The crude material was purified by flash chromatography (silica gel, 80 g, 0% to 100% EtOAc in heptane). The bottom spot was isolated and identified as (1RS,5RS,7RS)-tert-butyl 7-(((benzyloxy)carbonyl)amino)-1-(hydroxymethyl)-3-azabicyclo[3.2.0]heptane-3-carboxylate (1.91 g, 54% yield), as a colorless oil.

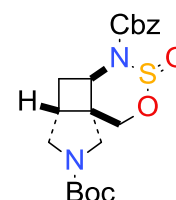


1H NMR (600 MHz, $CDCl_3$) δ ppm 1.47 (s, 9 H), 1.98 (s, 1 H), 2.18 (s, 1 H), 2.39 (s, 1 H), 2.57 (s, 1 H), 3.12 (d, J =10.0 Hz, 1 H), 3.29-3.75 (m, 4 H), 3.81 (s, 1 H), 4.03-4.25 (m, 1 H), 4.98-5.19 (m, 2 H), 5.38 (s, 1 H), 7.30-7.49 (m, 5 H).

HRMS m/z = 321.1447 $[(M+H)^+ - (C_4H_8)]$ calculated from $C_{20}H_{28}FN_2O_5$ (M =376.2013)

(4aRS,5aRS,8aRS)-4-Benzyl 7-tert-butyl tetrahydropyrrolo[3',4':2,3]cyclobuta[1,2-d][1,2,3]oxathiazine-4,7(1H,8H)-dicarboxylate 3-oxide (97):

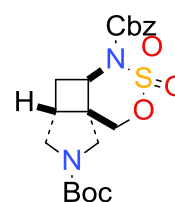
To a solution of thionyl chloride (1.51 g, 926 μ L, 12.7 mmol, equiv: 2.5) in acetonitrile (22.3 mL) at -40 °C was dropwise a solution of (1RS,5RS,7RS)-tert-butyl 7-(((benzyloxy)carbonyl)amino)-1-(hydroxymethyl)-3-azabicyclo[3.2.0]heptane-3-carboxylate (1.91 g, 5.07 mmol, equiv: 1.0) in acetonitrile (4.45 mL), the mixture was stirred at -40 °C for 1 h, then pyridine (2.01 g, 2.05 mL, 25.4 mmol, equiv: 5.0) was added dropwise, and the reaction was allowed to warm to 23 °C and stirred for 20 h. All volatiles were removed in vacuum, added diethyl ether, the solid was filtered off, the organic layer was washed with 0.5 M HCl and brine, dried over Na_2SO_4 . Filtration and removal of the solvent in vacuum



left the crude (4aRS,5aRS,8aRS)-4-benzyl 7-*tert*-butyl tetrahydropyrrolo[3',4':2,3]cyclobuta[1,2-d][1,2,3]oxathiazine-4,7(1*H*,8*H*)-dicarboxylate 3-oxide (1.87 g, 87.2 % yield) as a light yellow oil which was used without further purification.

(4aRS,5aRS,8aRS)-4-Benzyl-7-*tert*-butyl tetrahydropyrrolo[3',4':2,3]cyclobuta[1,2-d][1,2,3]oxathiazine-4,7(1*H*,8*H*)-dicarboxylate 3,3-dioxide (98):

To a solution of (4aRS,5aRS,8aRS)-4-benzyl 7-*tert*-butyl tetrahydropyrrolo[3',4':2,3]cyclobuta[1,2-d][1,2,3]oxathiazine-4,7(1*H*,8*H*)-dicarboxylate 3-oxide (1.87 g, 4.43 mmol, equiv: 1.0) in ethyl acetate (12.6 mL), acetonitrile (12.6 mL) and water (19 mL) at 5 °C was added sodium periodate (1.42 g, 6.64 mmol, equiv: 1.5) followed by ruthenium(II) chloride hydrate (9.98 mg, 44.3 µmol, equiv: 0.01) and the mixture was stirred at 23 °C for 1.75 h. Poured into water, extracted with EtOAc, the organic layer was washed with brine. The organic layers were collected and dried over Na₂SO₄. All volatiles were removed under vacuum. The crude material was purified by flash chromatography (silica gel, 100 g, 0% to 100% EtOAc in heptane) to give the (4aRS,5aRS,8aRS)-4-benzyl 7-*tert*-butyl tetrahydropyrrolo[3',4':2,3]cyclobuta[1,2-d][1,2,3]oxathiazine-4,7(1*H*,8*H*)-dicarboxylate 3,3-dioxide (1.19 g, 61.3 % yield) as a white foam.

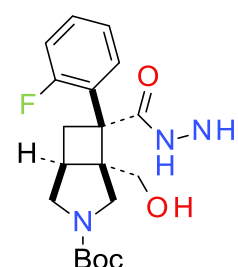


¹H NMR (600 MHz, CDCl₃) δ ppm 1.47 (s, 9 H), 2.18-2.65 (m, 2 H), 2.91 (d, *J*=12.0 Hz, 2 H), 3.39-3.78 (m, 3 H), 4.47-4.79 (m, 2 H), 4.91 (t, *J*= 8.2 Hz, 1 H), 5.26-5.41 (m, 3 H)

HRMS *m/z*= 483.1425 [M+HCOO]⁺ calculated from C₂₀H₂₆N₂O₇S (M=438.1429)

(1*S*,5*R*,7*R*)-*tert*-Butyl 7-(2-fluorophenyl)-7-(hydrazinecarbonyl)-1-(hydroxymethyl)-3-azabicyclo[3.2.0]heptane-3-carboxylate (99):

In 20mL pressure tubes, (3aRS4aRS,7aSR)-*tert*-butyl 3a-(2-fluorophenyl)-3-oxohexahydrofuro[3',4':1,4]cyclobuta[1,2-c]pyrrole-6(1*H*)-carboxylate (15.84 g, 45.6 mmol, equiv: 1.0) was combined with ethanol (76 mL). Hydrazine hydrate (14.3 g, 13.8 mL, 182 mmol, equiv: 4.0) was added. The mixture was stirred



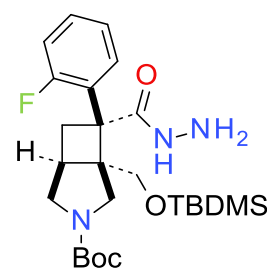
during 72 h at 60 °C. The solvents were evaporated. Extracted with water and EtOAc, dried over Na₂SO₄, filtered off and evaporated totally (18.2 g yellow foam). Trituration with dichloromethane and diethyl ether stirred for 10 minutes and filtered off the crystals. Washed with diethyl ether and dried in HV to give 13.57 g white crystals. The organic layers were collected and dried over Na₂SO₄. All volatiles were removed under vacuum. The crude material was purified by flash chromatography (silica gel, 50 g, 0% to 100% EtOAc in heptane). The product fractions were combined and totally evaporated to give (1*S*,5*R*,7*R*)-*tert*-Butyl 7-(2-fluorophenyl)-7-(hydrazinecarbonyl)-1-(hydroxymethyl)-3-azabicyclo[3.2.0]heptane-3-carboxylate (2.17 g, 91% yield) as a light yellow foam.

¹H NMR (600 MHz, DMSO) δ ppm 1.22 (s, 6 H), 1.34 (s, 10 H), 1.79-1.94 (m, 2 H), 2.17-2.22 (m, 1 H), 2.68-2.76 (m, 1 H), 2.71-2.76 (m, 1 H), 3.05-3.14 (m, 2 H), 3.22 (s, 3 H), 3.23-3.28 (m, 2 H), 3.30-3.31 (m, 1 H), 3.44-3.49 (m, 2 H), 3.47-3.52 (m, 1 H), 3.57 (d, *J*= 4.9 Hz, 2 H), 3.58 (d, *J*=5.1 Hz, 1 H), 4.29 (s, 4 H), 4.95 (d, *J*=18.2 Hz, 2 H), 7.10-7.15 (m, 2 H), 7.13-7.21 (m, 1 H), 7.28 (s, 1 H), 7.29-7.40 (m, 2 H), 8.09-8.35 (m, 2 H)

HRMS *m/z* =380.1977 [M+H]⁺ calculated from C₁₉H₂₆FN₃O₄ (M=379.1903)

(1*S*,5*R*,7*R*)-*tert*-Butyl 7-(2-fluorophenyl)-7-(hydrazinecarbonyl)-1-(hydroxymethyl)-3-azabicyclo[3.2.0]heptane-3-carboxylate (100):

To a solution of (1*SR*,5*RS*,7*RS*)-*tert*-butyl 7-(2-fluorophenyl)-7-(hydrazinecarbonyl)-1-(hydroxymethyl)-3-azabicyclo[3.2.0]heptane-3-carboxylate (5.34 g, 14.1 mmol, equiv: 1), DIPEA (2.55 g, 3.44 mL, 19.7 mmol, equiv: 1.4), DMAP (172 mg, 1.41 mmol, equiv: 0.1) in dichloromethane (28.1 mL) at 0 °C, TBDMS-Cl (2.55 g, 16.9 mmol, equiv: 1.2)



was added, and the mixture was stirred at 0 °C, slowly warming up until 23 °C for 18 hours. Poured into NH₄Cl and extracted with dichloromethane. The organic layers were washed with water and brine, The organic layers were collected and dried over Na₂SO₄. All volatiles were removed under vacuum. The crude material was purified by flash chromatography (silica gel, 12 g, 0% to 50% EtOAc in heptane) to give (1*SR*,5*RS*,7*RS*)-*tert*-butyl 1-(((*tert*-butyldimethylsilyl)oxy)methyl)-7-(2-fluorophenyl)-7-

(hydrazinecarbonyl)-3-azabicyclo[3.2.0]heptane-3-carboxylate (5.27 g, 76% yield) as a colorless oil.

¹H NMR (600 MHz, DMSO) δ ppm 0.00 (t, $J=5.5$ Hz, 6 H) 0.81 (br d, $J=8.0$ Hz, 9 H) 1.12 - 1.34 (m, 10 H) 1.75 - 1.98 (m, 1 H) 2.62 - 2.80 (m, 1 H) 2.95 - 3.23 (m, 3 H) 3.39 - 3.61 (m, 2 H) 3.74 (br dd, $J=17.1, 10.2$ Hz, 1 H) 4.33 (br s, 2 H) 6.95 - 7.39 (m, 4 H) 7.69 - 8.61 (m, 1 H)

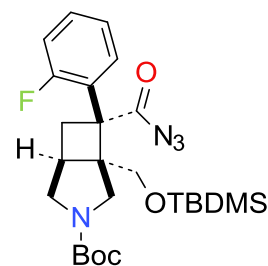
HRMS m/z =494.2831 $[M+H]^+$ calculated from $C_{25}H_{40}FN_3O_4Si$ ($M=493.2753$)

(1SR,5RS,7RS)-*tert*-Butyl 7-(azidocarbonyl)-1-(((*tert*-butyldimethylsilyl)oxy)methyl)-7-(2-fluorophenyl)-3-azabicyclo[3.2.0]heptane-3-carboxylate (101):

A solution of (1SR,5RS,7RS)-*tert*-butyl 1-(((*tert*-butyldimethylsilyl)oxy)methyl)-7-(2-fluorophenyl)-7-

(hydrazinecarbonyl)-3-azabicyclo[3.2.0]heptane-3-carboxylate (4.77 g, 9.66 mmol, equiv: 1.0) in DMF (47.4 mL) is cooled to -5 °C while HCl (9.66 mL, 38.6 mmol, equiv: 4.0) is added with stirring. This is followed by the addition of a precooled mixture

of sodium nitrite (2.32 mL, 11.6 mmol, equiv: 1.2) and DMF (47.4 mL). Five minutes later the excess of HCl is neutralized with triethylamine (2.54 g, 3.5 mL, 25.1 mmol, equiv: 2.6) and the solution is dried briefly over Na_2SO_4 . The organic layer was extracted with ice cold water and EtOAc. The organic layers were collected and dried over Na_2SO_4 . All volatiles were removed under vacuum. The crude material was purified by flash chromatography (silica gel, 12 g, 0% to 70% EtOAc in heptane) to give (1SR,5RS,7RS)-*tert*-butyl 7-(azidocarbonyl)-1-(((*tert*-butyldimethylsilyl)oxy)methyl)-7-(2-fluorophenyl)-3-azabicyclo[3.2.0]heptane-3-carboxylate (3.68 g, 76% yield) as a colorless oil.

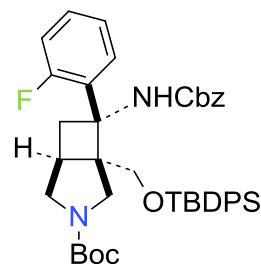


¹H NMR (600 MHz, $CDCl_3$) δ ppm 0.05 - 0.15 (m, 6 H) 0.84 - 0.99 (m, 9 H) 1.26 - 1.46 (m, 8 H) 1.97 - 2.14 (m, 1 H) 2.33 - 4.14 (m, 8 H) 6.77 - 7.43 (m, 5 H)

HRMS m/z =421.1948 $[(M+H)+(-C_4H_8N_2)]$ calculated from $C_{25}H_{37}FN_4O_4Si$ ($M=450.2717$)

(1RS,5RS,7RS)-*tert*-Butyl 7-(((benzyloxy)carbonyl)amino)-1-(((*tert*-butyldimethylsilyl)oxy)methyl)-7-(2-fluorophenyl)-3-azabicyclo[3.2.0]heptane-3-carboxylate (102):

Dissolve (1SR,5RS,7RS)-*tert*-butyl 7-(azidocarbonyl)-1-(((*tert*-butyldimethylsilyl)oxy)methyl)-7-(2-fluorophenyl)-3-azabicyclo[3.2.0]heptane-3-carboxylate (123 mg, 244 μ mol, equiv: 1.0) in toluene (975 μ l) and heat at 120 °C and stir for 2 hours. Add benzyl alcohol (52.7 mg, 50.7 μ l, 487 μ mol, equiv: 2.0) and stir overnight. All volatiles were removed under vacuum. The crude material was purified by flash chromatography (silica gel, 12 g, 0% to 100% EtOAc in heptane). In the ^1H NMR traces of benzyl alcohol was still visible. The major fraction was collected as (1RS,5RS,7RS)-*tert*-butyl 7-(((benzyloxy)carbonyl)amino)-1-(((*tert*-butyldimethylsilyl)oxy)methyl)-7-(2-fluorophenyl)-3-azabicyclo[3.2.0]heptane-3-carboxylate (141 mg, 99% yield) as an orange oil.

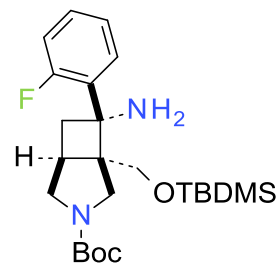


^1H NMR (600 MHz, CDCl_3) δ ppm 0.06 - 0.19 (m, 6 H) 0.91 (br s, 9 H) 1.31 (s, 4 H) 1.41 (s, 5 H) 2.30 - 3.76 (m, 8 H) 4.20 - 4.36 (m, 1 H) 4.70 (s, 2 H) 4.84 (br d, $J=12.3$ Hz, 1 H) 5.02 (br d, $J=12.3$ Hz, 1 H) 6.91 - 7.04 (m, 1 H) 7.06 - 7.18 (m, 1 H) 7.28 - 7.32 (m, 3 H) 7.34 - 7.39 (m, 4 H) 7.40 - 7.51 (m, 1 H) 7.75 - 8.35 (m, 1 H)

LC/MS (ESI) m/z =585.315 $[\text{M}+\text{H}]^+$ calculated from $\text{C}_{32}\text{H}_{45}\text{FN}_2\text{O}_5\text{Si}$ ($M=584.308$)

(1RS,5RS,7RS)-*tert*-Butyl 7-amino-1-(((*tert*-butyldimethylsilyl)oxy)methyl)-7-(2-fluorophenyl)-3-azabicyclo[3.2.0]heptane-3-carboxylate (103):

A solution of (1R,5R,7R)-*tert*-butyl 7-(((benzyloxy)carbonyl)amino)-1-(((*tert*-butyldimethylsilyl)oxy)methyl)-7-(2-fluorophenyl)-3-azabicyclo[3.2.0]heptane-3-carboxylate (3.51 g, 6 mmol, equiv: 1) with palladium on carbon (639 mg, 600 μ mol, equiv: 0.1) in ethanol (600 mL) was hydrogenated at 23 °C for 1 hour in a pressure tube. The catalyst was filtrated and the volatiles were removed under vacuum. To give (1RS,5RS,7RS)-*tert*-butyl 7-amino-1-(((*tert*-



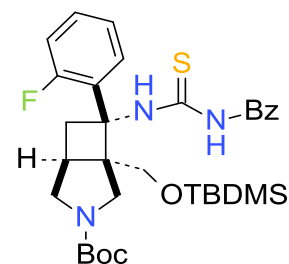
butyldimethylsilyl)oxy)methyl)-7-(2-fluorophenyl)-3-azabicyclo[3.2.0]heptane-3-carboxylate (2.66 g, 98% yield) as a colorless oil.

¹H NMR (600 MHz, CDCl₃) δ ppm 0.07 - 0.15 (m, 6 H) 0.92 (br d, *J*=8.9 Hz, 10 H) 1.27 - 1.45 (m, 9 H) 2.31 (br d, *J*=8.3 Hz, 2 H) 2.71 - 2.93 (m, 1 H) 3.13 - 3.49 (m, 4 H) 3.53 - 4.28 (m, 2 H) 3.65 - 3.65 (m, 1 H) 5.30 (s, 1 H) 6.82 - 7.25 (m, 3 H) 7.31 - 7.52 (m, 1 H)

HRMS *m/z* =451.2791 [M+H]⁺ calculated from C₂₄H₃₉FN₂O₄Si (M=450.2717)

(1RS,5RS,7RS)-*tert*-Butyl 7-(3-benzoylthioureido)-1-(((*tert*-butyldimethylsilyl)oxy)methyl)-7-(2-fluorophenyl)-3-azabicyclo[3.2.0]heptane-3-carboxylate (104):

To a solution of (1RS,5RS,7RS)-*tert*-butyl 7-amino-1-(((*tert*-butyldimethylsilyl)oxy)methyl)-7-(2-fluorophenyl)-3-azabicyclo[3.2.0]heptane-3-carboxylate (2.66 g, 5.9 mmol, equiv: 1) in THF (148 mL) at 0 °C add benzoyl isothiocyanate (1.01 g, 833 μl, 6.2 mmol, equiv: 1.05). Remove the ice bath and let it heat up until 23 °C. Stir at 23 °C during 5 hours



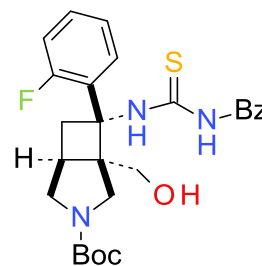
(consumption of starting material verified in TLC). All volatiles were removed under vacuum. The crude material was purified by flash chromatography (silica gel, 100 g, 0% to 30% EtOAc in heptane) to give a clean fraction (3.3g) (1RS,5RS,7RS)-*tert*-butyl 7-(3-benzoylthioureido)-1-(((*tert*-butyldimethylsilyl)oxy)methyl)-7-(2-fluorophenyl)-3-azabicyclo[3.2.0]heptane-3-carboxylate (3.3 g, 91% yield) as a white solid

¹H NMR (600 MHz, DMSO) δ ppm -0.02 - 0.03 (m, 5 H) 0.77 (br s, 9 H) 1.01 - 1.09 (m, 5 H) 1.19 (br s, 3 H) 2.56 (br s, 1 H) 2.73 (br s, 1 H) 2.88 (br s, 1 H) 2.95 (br d, *J*=9.9 Hz, 1 H) 3.04 (br s, 1 H) 3.10 - 3.15 (m, 1 H) 3.27 - 3.34 (m, 1 H) 4.00 (br s, 1 H) 6.96 - 7.03 (m, 1 H) 7.01 (br s, 1 H) 7.13 - 7.22 (m, 1 H) 7.36 - 7.40 (m, 2 H) 7.45 - 7.49 (m, 1 H) 7.50 (br d, *J*=7.3 Hz, 1 H) 7.78 (br d, *J*=7.3 Hz, 2 H) 10.94 (br s, 1 H) 11.84 (br s, 1 H)

HRMS *m/z* =612.273 [M-H]⁻ calculated from C₃₂H₄₄FN₃O₄SSi (M=613.281)

(1RS,5RS,7RS)-*tert*-Butyl 7-(3-benzoylthioureido)-7-(2-fluorophenyl)-1-(hydroxymethyl)-3-azabicyclo[3.2.0]heptane-3-carboxylate (105):

A solution of (1RS,5RS,7RS)-*tert*-butyl 7-(3-benzoylthioureido)-1-(((*tert*-butyldimethylsilyl)oxy)methyl)-7-(2-fluorophenyl)-3-azabicyclo[3.2.0]heptane-3-carboxylate (3.3 g, 5.38 mmol, equiv: 1.0) in THF (24 mL) and TBAF (5.91 mL, 5.91 mmol, equiv: 1.1) was stirred at 0 °C during 2 hours. The reaction was extracted with water and EtOAc, The organic layers were collected and dried over Na₂SO₄. All volatiles were removed under vacuum. The crude material was purified by flash chromatography (silica gel, 40 g, 0% to 50% EtOAc in heptane) to give (1RS,5RS,7RS)-*tert*-butyl 7-(3-benzoylthioureido)-7-(2-fluorophenyl)-1-(hydroxymethyl)-3-azabicyclo[3.2.0]heptane-3-carboxylate (2.47 g, 92% yield) as an light yellow foam.

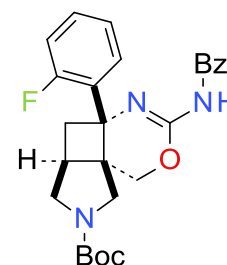


¹H NMR (600 MHz, DMSO) δ ppm 0.97 - 1.58 (m, 10 H) 2.59 - 2.82 (m, 2 H) 2.94 - 3.17 (m, 3 H) 3.45 (br d *J*=11.0 Hz, 1 H) 3.71 - 4.17 (m, 2 H) 5.19 (br s, 1 H) 7.03 - 7.40 (m, 3 H) 7.50 (t, *J*=7.8 Hz, 2 H) 7.54 - 7.61 (m, 1 H) 7.60 - 7.66 (m, 1 H) 7.91 (br d, *J*=7.7 Hz, 2 H) 11.04 (br s, 1 H) 12.00 (br s, 1 H)

HRMS *m/z* =500.1982 [M+H]⁺ calculated from C₂₆H₃₀FN₃O₄S (M=499.1910)

(4aRS,5aRS,8aRS)-*tert*-Butyl 3-benzamido-4a-(2-fluorophenyl)-4a,5,5a,6-tetrahydro-1*H*-pyrrolo[3',4':2,3]cyclobuta[1,2-*d*][1,3]oxazine-7(8*H*)-carboxylate (107):

To a solution of (1RS,5RS,7RS)-*tert*-butyl 7-(3-benzoylthioureido)-7-(2-fluorophenyl)-1-(hydroxymethyl)-3-azabicyclo[3.2.0]heptane-3-carboxylate (100 mg, 200 μmol, equiv: 1.0) in acetonitrile (1 mL), EDC (57.6 mg, 300 μmol, equiv: 1.5) was added. The mixture was stirred at 65 °C during 30 min (TLC showed little conversion) and the temperature was raised until 75 °C during 45 min. The volatiles were removed. The crude material was purified by flash chromatography (silica gel, 12 g, 0% to 50% EtOAc in heptane) to give (4aRS,5aRS,8aRS)-*tert*-butyl 3-benzamido-4a-(2-fluorophenyl)-4a,5,5a,6-tetrahydro-1*H*-pyrrolo[3',4':2,3]cyclobuta[1,2-*d*][1,3]oxazine-7(8*H*)-carboxylate (91 mg, 98% yield) as a colorless oil.

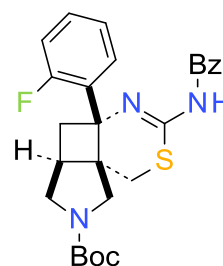


¹H NMR (600 MHz, DMSO) δ ppm 1.02 - 1.51 (m, 16 H) 2.52 - 2.64 (m, 2 H) 2.93 - 3.18 (m, 3 H) 3.43 - 3.63 (m, 1 H) 4.29 - 4.58 (m, 2 H) 7.12 - 7.59 (m, 10 H) 8.03 (br d, $J=7.5$ Hz, 2 H) 11.01 - 11.81 (m, 1 H)

LC/MS (ESI) m/z =466.214 $[M+H]^+$ calculated from C₂₆H₂₈FN₃O₄ (M=465.206)

(4aS,5aR,8aR)-tert-butyl 3-benzamido-4a-(2-fluorophenyl)-4a,5,5a,6-tetrahydro-1H-pyrrolo[3',4':2,3]cyclobuta[1,2-d][1,3]thiazine-7(8H)-carboxylate (106):

To a solution of (1RS,5RS,7RS)-tert-butyl 7-(3-benzoylthioureido)-7-(2-fluorophenyl)-1-(hydroxymethyl)-3-azabicyclo[3.2.0]heptane-3-carboxylate (100 mg, 200 μ mol, equiv: 1.0) in dichloromethane (1 mL) at 0 °C was added 1-chloro-*N,N*,2-trimethylpropenylamine (29.4 mg, 29.1 μ L, 220 μ mol, equiv: 1.1) and the mixture was allowed to reach 23 °C and stirred for 2h. After 2h there was no total conversion so 1-chloro-*N,N*,2-trimethylpropenylamine (29.4 mg, 29.1 μ L, 220 μ mol, equiv: 1.1) was added at 0 °C and let warm up until 23 °C. Added water and the reaction was extracted with EtOAc. The organic layers were collected and dried over Na₂SO₄. All volatiles were removed under vacuum. The crude material was purified by flash chromatography (silica gel, 12 g, 0% to 50% EtOAc in heptane) to give (4aS,5aR,8aR)-tert-butyl 3-benzamido-4a-(2-fluorophenyl)-4a,5,5a,6-tetrahydro-1H-pyrrolo[3',4':2,3]cyclobuta[1,2-d][1,3]thiazine-7(8H)-carboxylate (93 mg, 96.5 % yield) as a colorless oil



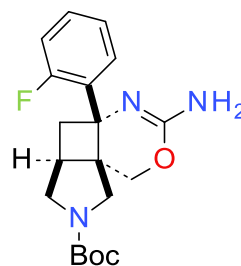
¹H NMR (600 MHz, DMSO) δ ppm 1.03 - 1.20 (m, 8 H) 1.22 - 1.27 (m, 1 H) 1.34 (br s, 5 H) 2.67 - 2.80 (m, 1 H) 2.87 - 3.25 (m, 3 H) 3.43 - 3.59 (m, 1 H) 7.18 - 7.31 (m, 3 H) 7.36 - 7.47 (m, 4 H) 7.49 - 7.57 (m, 2 H) 7.87 - 8.00 (m, 2 H) 10.04 - 11.15 (m, 1 H)

HRMS m/z =482.1933 $[M+H]^+$ calculated from C₂₆H₂₈FN₃O₃S (M=481.1854)

(4aRS,5aRS,8aRS)-tert-Butyl 3-amino-4a-(2-fluorophenyl)-4a,5,5a,6-tetrahydro-1H-pyrrolo[3',4':2,3]cyclobuta[1,2-d][1,3]oxazine-7(8H)-carboxylate (110):

To a solution of (4aRS,5aRS,8aRS)-tert-butyl 3-benzamido-4a-(2-fluorophenyl)-4a,5,5a,6-tetrahydro-1H-pyrrolo[3',4':2,3]cyclobuta[1,2-d][1,3]oxazine-7(8H)-carboxylate (111 mg, 238 μ mol, equiv: 1.0) in MeOH (1.17 mL), K₂CO₃ (98.9

mg, 715 μmol , equiv: 3.0) was added. The mixture was stirred at 50 °C during 4 hours. The reaction was washed with DCM/H₂O. The organic layers were collected and dried over Na₂SO₄. All volatiles were removed under vacuum. The crude material was purified by flash chromatography (silica gel, 12 g, 0% to 100% EtOAc in heptane). The column was washed with DCM/NH₃/MeOH to remove the product (4aRS,5aRS,8aRS)-*tert*-butyl 3-amino-4a-(2-fluorophenyl)-4a,5,5a,6-tetrahydro-1*H*-pyrrolo[3',4':2,3]cyclobuta[1,2-d][1,3]oxazine-7(8*H*)-carboxylate (67 mg, 78% yield) as a light yellow oil.

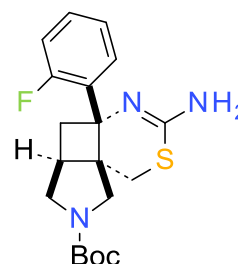


¹H NMR (600 MHz, DMSO) δ ppm 1.10 - 1.44 (m, 10 H) 2.11 - 2.42 (m, 2 H) 2.78 - 2.97 (m, 2 H) 3.10 - 3.24 (m, 2 H) 3.41 (br d, $J=11.2$ Hz, 1 H) 3.47 - 3.61 (m, 1 H) 4.06 - 4.36 (m, 2 H) 5.98 - 6.73 (m, 2 H) 7.02 - 7.58 (m, 4 H)

LC/MS (ESI) m/z =362.187 [M+H]⁺ calculated from C₁₉H₂₄FN₃O₃ (M=361.180)

(4aSR,5aRS,8aRS)-*tert*-butyl 3-amino-4a-(2-fluorophenyl)-4a,5,5a,6-tetrahydro-1*H*-pyrrolo[3',4':2,3]cyclobuta[1,2-d][1,3]thiazine-7(8*H*)-carboxylate (109):

To a solution of (4aSR,5aRS,8aRS)-*tert*-butyl 3-benzamido-4a-(2-fluorophenyl)-4a,5,5a,6-tetrahydro-1*H*-pyrrolo[3',4':2,3]cyclobuta[1,2-d][1,3]thiazine-7(8*H*)-carboxylate (95 mg, 197 μmol , equiv: 1) in MeOH (1 mL), K₂CO₃ (81.8 mg, 592 μmol , equiv: 3) was added. The mixture was stirred at 50 °C during 2 hours. The reaction was washed with DCM/H₂O.



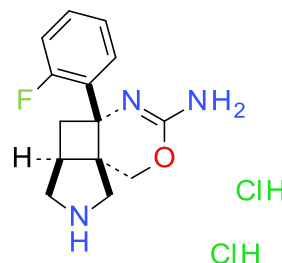
The organic layers were collected and dried over Na₂SO₄. All volatiles were removed under vacuum. The crude material was purified by flash chromatography (silica gel, 12 g, 0% to 100% EtOAc in heptane). After some fractions come off the column with 100% EtOAc, the column was washed with DCM/NH₃/MeOH to remove extra product. After analytics (LC/MS and ¹H NMR) the fraction from the rack and of the washed column were combined to give (4aSR,5aRS,8aRS)-*tert*-butyl 3-amino-4a-(2-fluorophenyl)-4a,5,5a,6-tetrahydro-1*H*-pyrrolo[3',4':2,3]cyclobuta[1,2-d][1,3]thiazine-7(8*H*)-carboxylate (42 mg, 56.4 % yield) as a white solid.

¹H NMR (600 MHz, DMSO) δ ppm 1.11 - 1.34 (m, 9 H) 2.80 - 2.85 (m, 1 H) 2.83 - 2.89 (m, 1 H) 2.86 (br s, 1 H) 3.13 (br s, 1 H) 3.12 - 3.17 (m, 1 H) 3.32 - 3.50 (m, 3 H) 7.00 - 7.19 (m, 1 H) 7.07 - 7.13 (m, 1 H) 7.28 (br s, 2 H)

HRMS m/z =378.1656 $[M+H]^+$ calculated from $C_{19}H_{24}FN_3O_2S$ (M =377.1581)

(4aRS,5aRS,8aRS)-4a-(2-Fluorophenyl)-4a,5,5a,6,7,8-hexahydro-1H-pyrrolo[3',4':2,3]cyclobuta[1,2-d][1,3]oxazin-3-amine dihydrochloride (112):

Suspend (4aR,5aR,8aR)-tert-butyl 3-amino-4a-(2-fluorophenyl)-4a,5,5a,6-tetrahydro-1H-pyrrolo[3',4':2,3]cyclobuta[1,2-d][1,3]oxazine-7(8H)-carboxylate (50 mg, 138 μ mol, equiv: 1.0) in a solution of HCl (in dioxane) (138 μ l, 553 μ mol, equiv: 4.0) and triturate during 2 hours, still starting material in the LC/MS, another equivalent of HCl (in dioxane) (138 μ l, 553 μ mol, equiv: 4) was added. 2 hours later the reaction was filtered and washed with diethyl ether, crystals highly hygroscopic. (4aRS,5aRS,8aRS)-4a-(2-fluorophenyl)-4a,5,5a,6,7,8-hexahydro-1H-pyrrolo[3',4':2,3]cyclobuta[1,2-d][1,3]oxazin-3-amine dihydrochloride (22 mg, 48% yield) as an off-white crystalline material was collected.

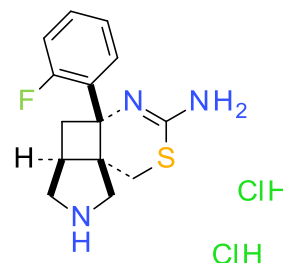


1H NMR (600 MHz, DMSO) δ ppm 2.45 (dd, J =13.1, 8.7 Hz, 1 H) 2.96 (br d, J =9.3 Hz, 1 H) 3.07 (br dd, J =13.2, 8.2 Hz, 1 H) 3.10 - 3.21 (m, 1 H) 3.31 (br dd, J =4.5, 2.3 Hz, 1 H) 3.36 - 3.40 (m, 1 H) 4.48 (br d, J =12.1 Hz, 1 H) 4.75 (dd, J =12.1, 3.7 Hz, 1 H) 7.24 - 7.38 (m, 2 H) 7.47 (br t, J =7.2 Hz, 1 H) 7.50 - 7.58 (m, 1 H) 7.89 - 9.26 (m, 2 H) 9.76 - 10.35 (m, 2 H) 10.58 (s, 1 H)

HRMS m/z =262.1370 $[M+H]^+$ calculated from $C_{14}H_{16}FN_3O$ (M =261.1295)

(4aSR,5aRS,8aRS)-4a-(2-Fluorophenyl)-4a,5,5a,6,7,8-hexahydro-1H-pyrrolo[3',4':2,3]cyclobuta[1,2-d][1,3]thiazin-3-amine dihydrochloride (111)

Suspend (4aSR,5aRS,8aRS)-tert-butyl 3-amino-4a-(2-fluorophenyl)-4a,5,5a,6-tetrahydro-1H-pyrrolo[3',4':2,3]cyclobuta[1,2-d][1,3]thiazine-7(8H)-carboxylate (33 mg, 87.4 μ mol, equiv: 1.0) in a solution of HCl (in dioxane) (87.4 μ l, 350 μ mol, equiv: 4.0) with the help of drops of THF and triturate during 2 h. After 2 h the LC/MS did not showed any conversion (no precipitation was verified) HCl (in dioxane) (87.4 μ l, 350 μ mol, equiv: 4.0) was added and the reaction left to stir over night. Checked by LC/MS no more starting material and the crystals were filtrated and washed with diethyl ether to



give(4aSR,5aRS,8aRS)-4a-(2-fluorophenyl)-4a,5,5a,6,7,8-hexahydro-1H-pyrrolo[3',4':2,3]cyclobuta[1,2-d][1,3]thiazin-3-amine dihydrochloride (17 mg, 56% yield) as an off-white crystalline material.

¹H NMR (600 MHz, DMSO) δ ppm 1.10 - 1.36 (m, 3 H) 2.82 (br dd, $J=13.0$, 6.1 Hz, 1 H) 2.97 - 3.16 (m, 2 H) 3.41 - 3.53 (m, 2 H) 7.28 - 7.38 (m, 2 H) 7.49 (br t, $J=7.5$ Hz, 1 H) 7.52 - 7.59 (m, 1 H) 8.33 (br s, 1 H) 9.22 - 10.22 (m, 2 H) 10.50 - 10.94 (m, 1 H)

HRMS m/z =278.1126 $[M+H]^+$ calculated from C₁₄H₁₆FN₃S (M=277.1053)

BACE1 & BACE2 Enzyme Assay. Enzyme inhibition assays were performed in 384-well microtiter plates (black with clear bottom, non-binding surface from Corning, Cat. No.: 3655) in a final volume of 51 μ l. Test compounds dissolved in DMSO at a concentration of 10mM were serially diluted in DMSO (15 concentrations, 1/3 dilution steps, final concentration range: 200-0.0004 μ M). 1 μ l of diluted compounds were mixed with 40 μ l of enzyme on an H&P Teleshaker for 4 min. After addition of the MR121-labelled substrate, the plates were again strongly shaken for 2 min. The enzymatic reaction was followed by reading the fluorescence emission on a plate: vision reader (Perkin-Elmer) (excitation wavelength: 630 nm; emission: 695 nm) for at least 30 min in a kinetic measurement detecting an increase of MR121 fluorescence following the cutting of the quenched substrate. The slope in the linear range of the kinetic was calculated and the IC₅₀ of the test compounds were determined using a four parameter Hill equation for curve fitting on the calculated %-inhibition values referenced to wells without enzyme and wells with enzyme but no test compound respectively. BACE1 enzyme used in the assay was prepared and purified as described.⁵⁸ The preparation of BACE2 was carried out following exactly the known protocol.⁴⁶ BACE1/2 assay: The final enzyme concentration in the assay was 30 and 125 nM respectively. The assay buffer was 100 mM sodium acetate, 20 mM EDTA, 0.05 % BSA, pH 4.0. The substrate peptide was of sequence WSEVNLDAEFRG-MR121 and used at a final concentration of 300 nM.¹¹

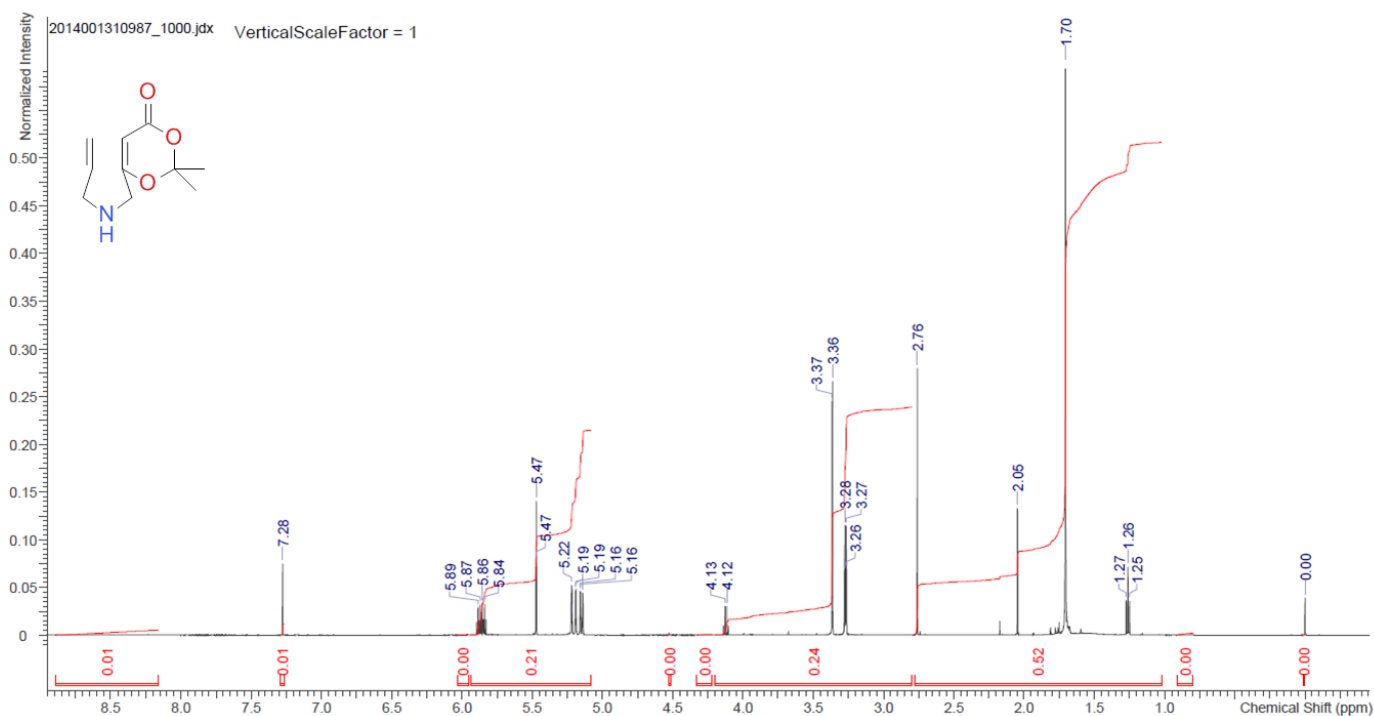
4.5-References

-
- ¹ D. A. Fort, T. J. Woltering, A. M. Alker, T. Bach, *J. Org. Chem.*, **2014**, 79, 7152-7166.
- ² D. Oehlich, H. Prokopcova, H. Gisen, *Bioorg. Med. Chem. Lett.*, **2014**, 24, 2033-2045
- ³ http://www.proteopedia.org/wiki/index.php/Beta_secretase (last consulted 6th of May 2015)
- ⁴ J. Varghese, '*BACE: Lead Target for Orchestrated Therapy of Alzheimer's Disease*', Wiley, **2010**.
- ⁵ European patent: EP 1 942 105 A1, **2008**
- ⁶ P. R. Gerber, K. J. Müller, *J. Comput. Aided Mol. Des.*, **1995**, 9, 251.
- ⁷ T. Woltering, W. Wostl, H. Hilpert, M. Roger-Evans, E. Pinard, A. Mayweg, M. Göbel, D. Banner, J. Benz, M. Travagli, M. Pollastrini, G. Marconi, E. Gabellieri, W. Guba, H. Mauser, M. Andreini, H. Jacobsen, E. Power, R. Narquizian, *Bioorg. Med. Chem. Lett.*, **2013**, 23, 4239-4243
- ⁸ S. Guttman, R. Boissonnas, *Helv. Chim. Acta*, **1958**, 41, 1852
- ⁹ World Patent: WO2010103076, **2010**
- ¹⁰ Europe Patent: EP 2147 914 A1, **2011**
- ¹¹ H. Hilpert, W. Guba, T. Woltering, W. Wostl, E. Pinard, H. Mauser, A. Mayweg, M. Roger-Evans, R. Humm, D. Krummenacher, T. Muser, C. Schnider, H. Jacobsen, L. Ozmen, A. Bergadano, D. Banner, R. Hochstrasser, A. Kuglstat, P. David-Pierson, H. Ficher, A. Polara, R. Narquizian, *J. Med. Chem.*, **2013**, 56, 3980-3995

Supporting Information

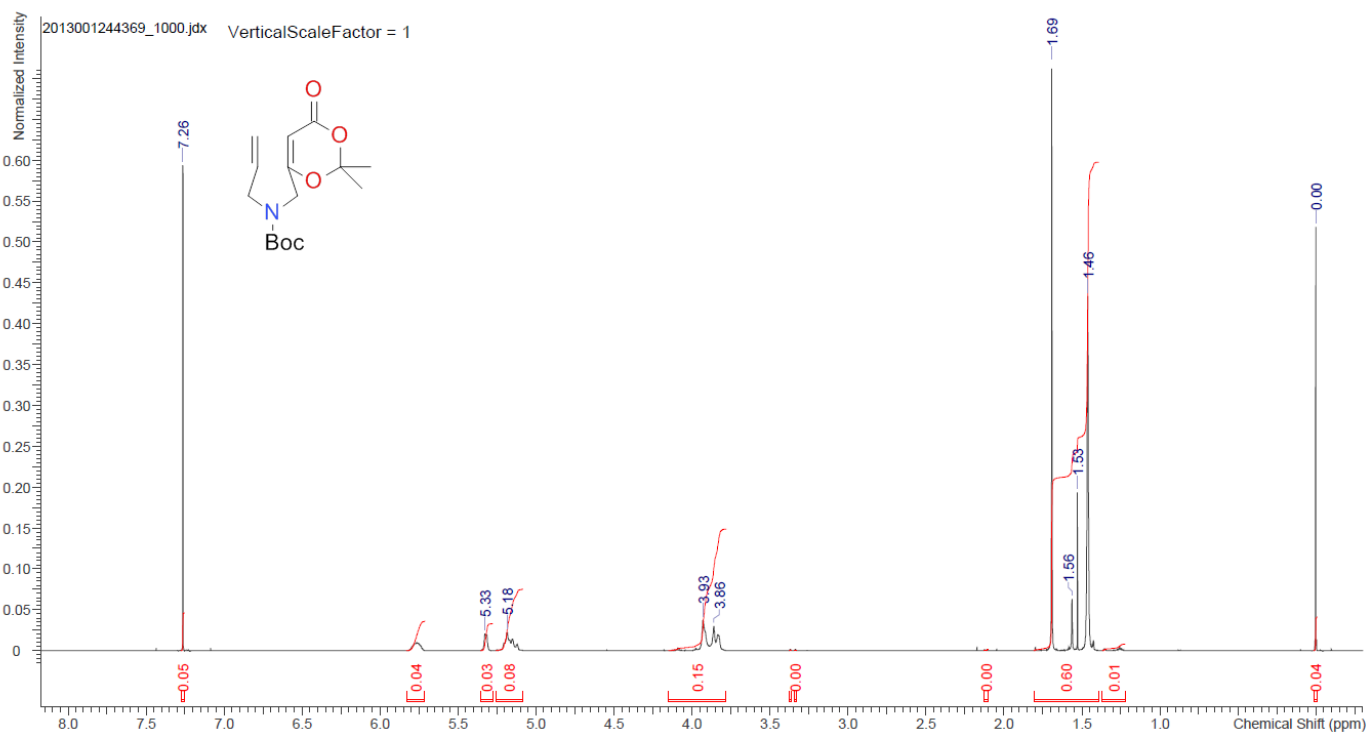
6-((Allylamino)methyl)-2,2-dimethyl-4H-1,3-dioxin-4-one (19):

¹H NMR (600 MHz, CDCl₃, 25 °C)



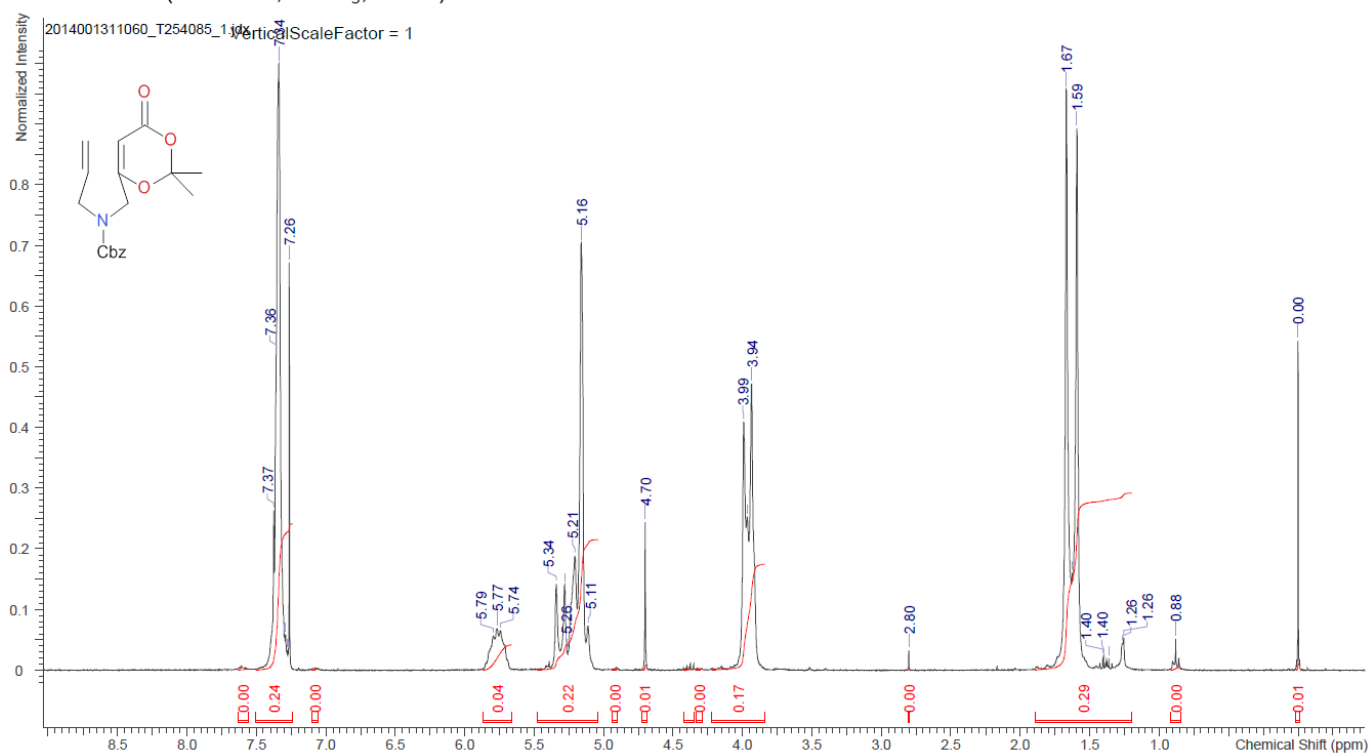
Benzyl allyl((2,2-dimethyl-4-oxo-4H-1,3-dioxin-6-yl)methyl)carbamate (20a):

¹H NMR (600 MHz, CDCl₃, 25 °C)



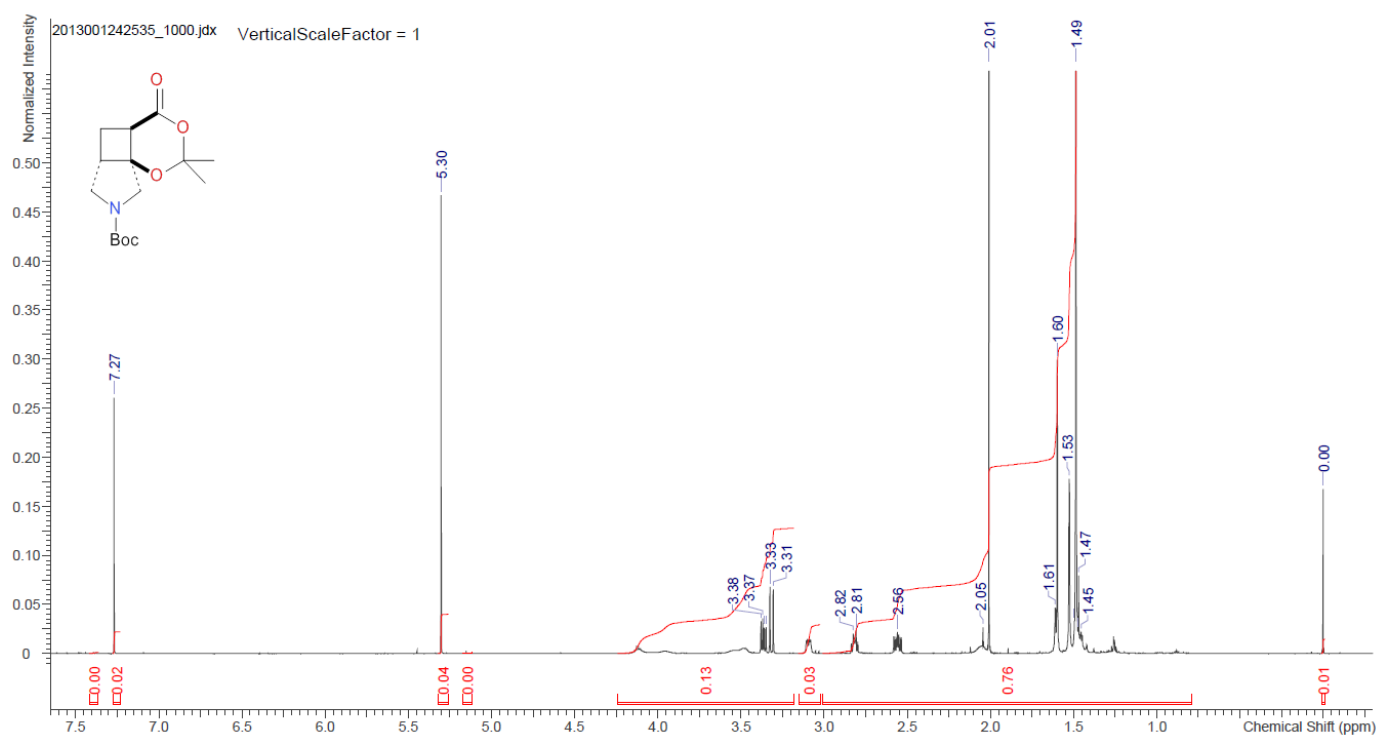
***tert*-Butyl allyl((2,2-dimethyl-4-oxo-4*H*-1,3-dioxin-6-yl)methyl)carbamate (20b):**

¹H NMR (600 MHz, CDCl₃, 25 °C)



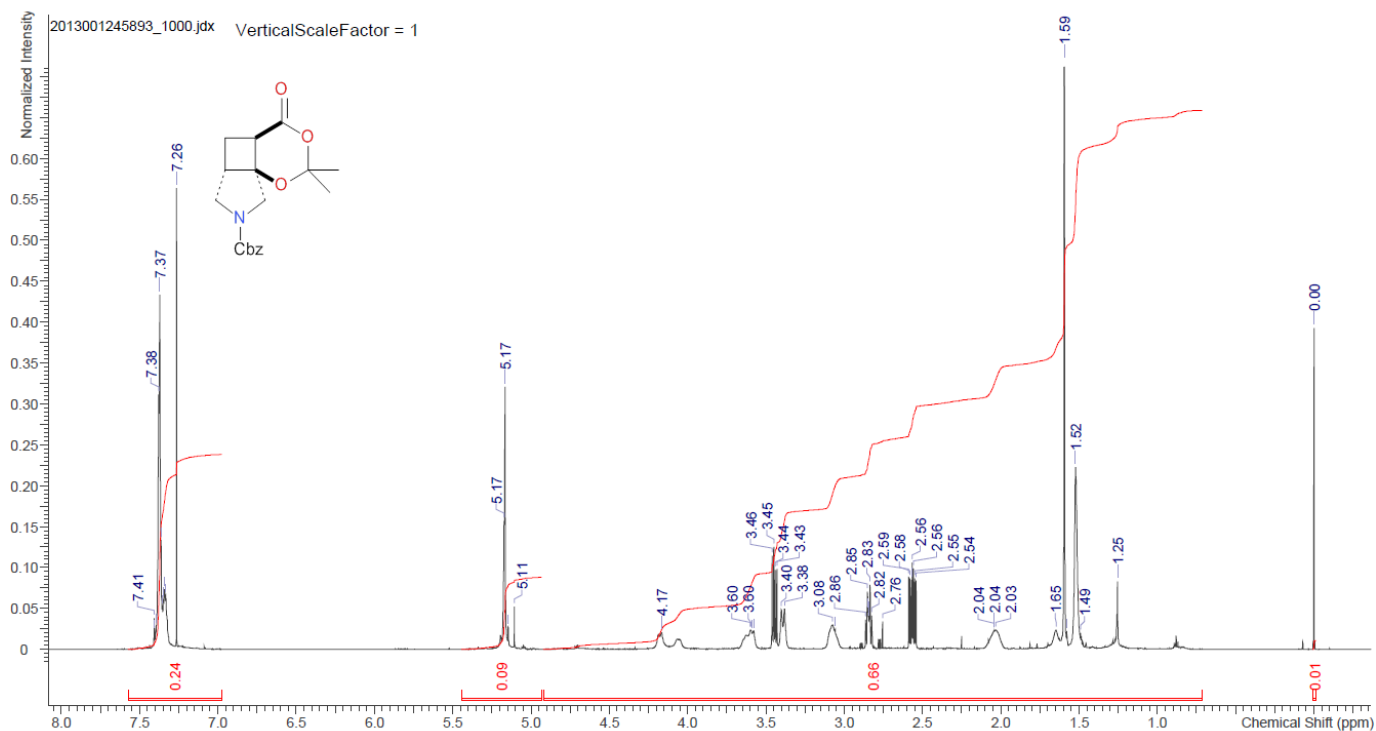
(4*a*RS,5*a*SR,8*a*SR)-*tert*-Butyl 2,2-dimethyl-4-oxotetrahydro-4*H*-[1,3]dioxino[4',5':1,4]cyclobuta[1,2-*c*]pyrrole-7(8*H*)-carboxylate (21a):

¹H NMR (600 MHz, CDCl₃, 25 °C)



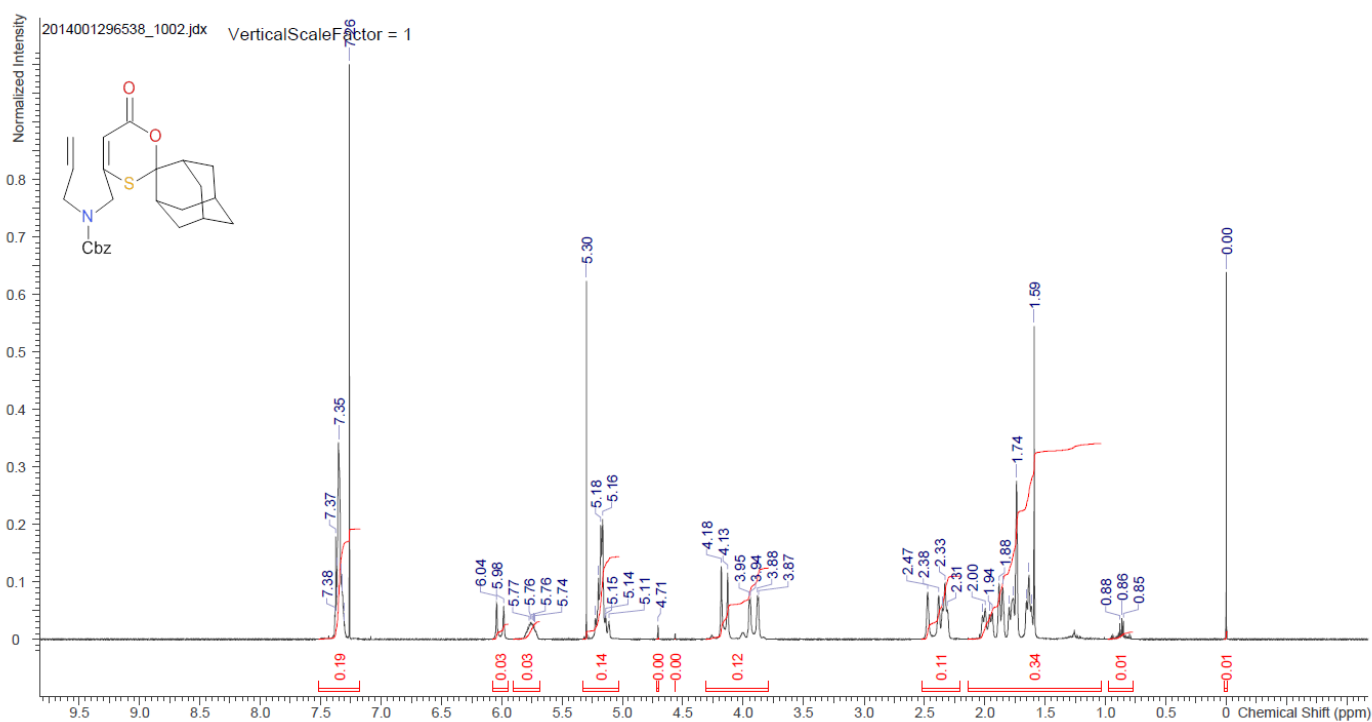
(4aRS,5aSR,8aSR)-Benzyl 2,2-dimethyl-4-oxotetrahydro-4H-[1,3]dioxino[4',5':1,4]cyclobuta[1,2-c]pyrrole-7(8H)-carboxylate (21b):

¹H NMR (600 MHz, CDCl₃, 25 °C)



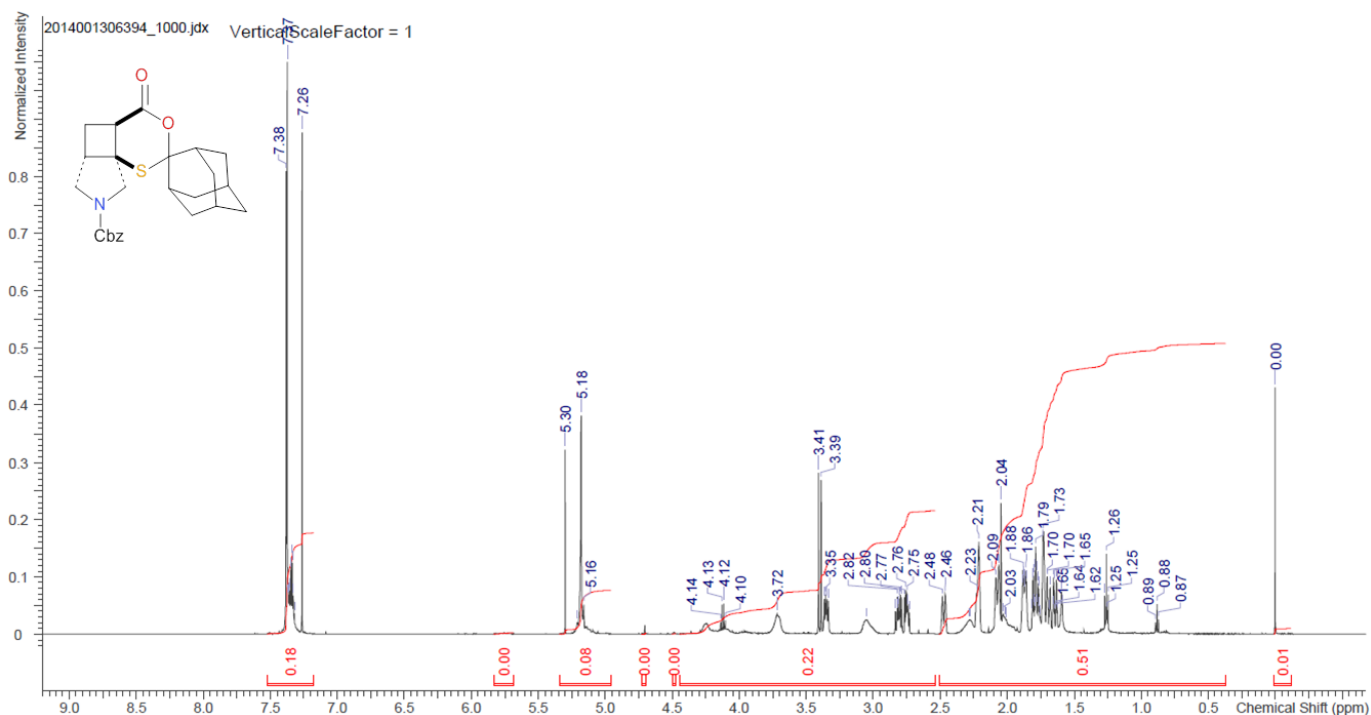
Benzyl allyl(((1R,3R,5R,7R)-6'-oxo-6'-H-spiro[adamantane-2,2'-[1,3]oxathiin]-4'-yl)methyl)carbamate (36):

¹H NMR (600 MHz, CDCl₃, 25 °C)



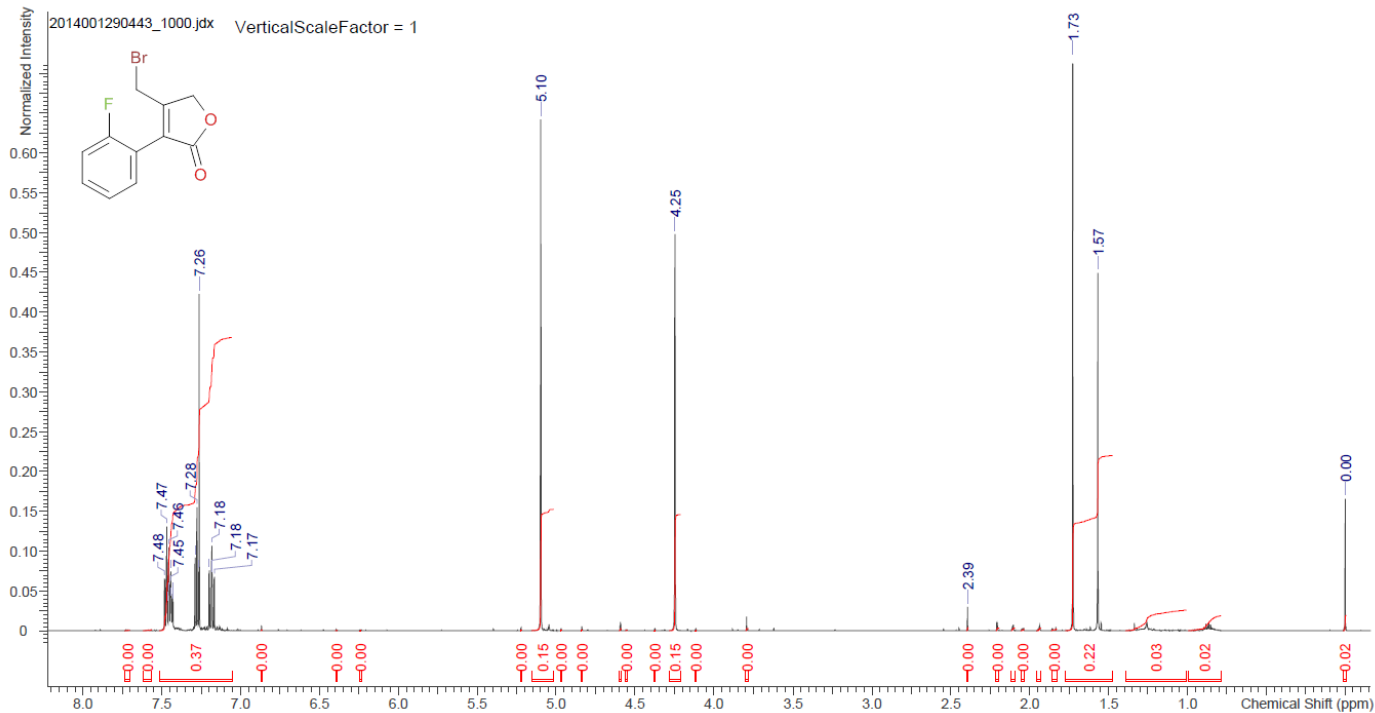
(1'SR,3'SR,4aSR,5aSR,5'SR,7'SR,8aSR)-Benzyl4-oxotetrahydro-4H-spiro[[1,3]oxathiino[4',5':1,4]cyclobuta[1,2-c]pyrrole-2,2'-adamantane]-7(8H)-carboxylate (37):

¹H NMR (600 MHz, CDCl₃, 25 °C)



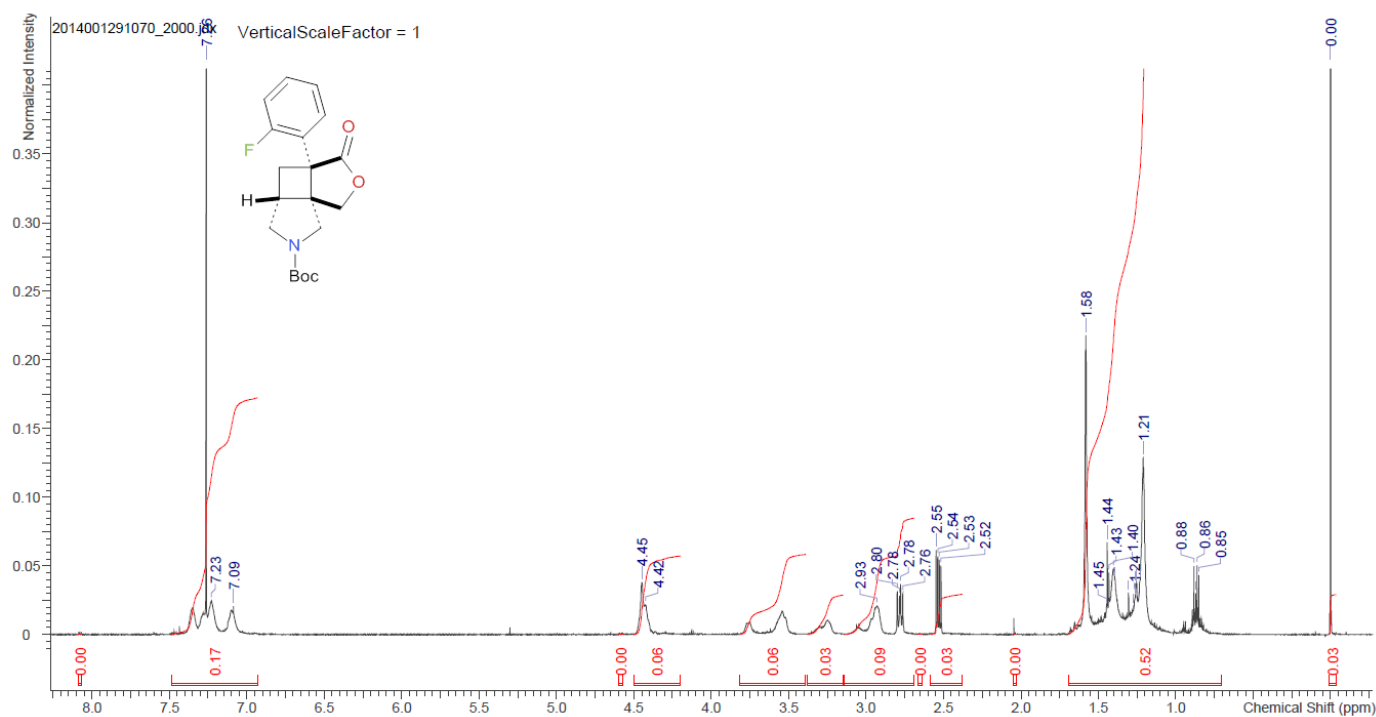
4-(Bromomethyl)-3-(2-fluorophenyl)furan-2(5H)-one (58):

¹H NMR (600 MHz, CDCl₃, 25 °C)



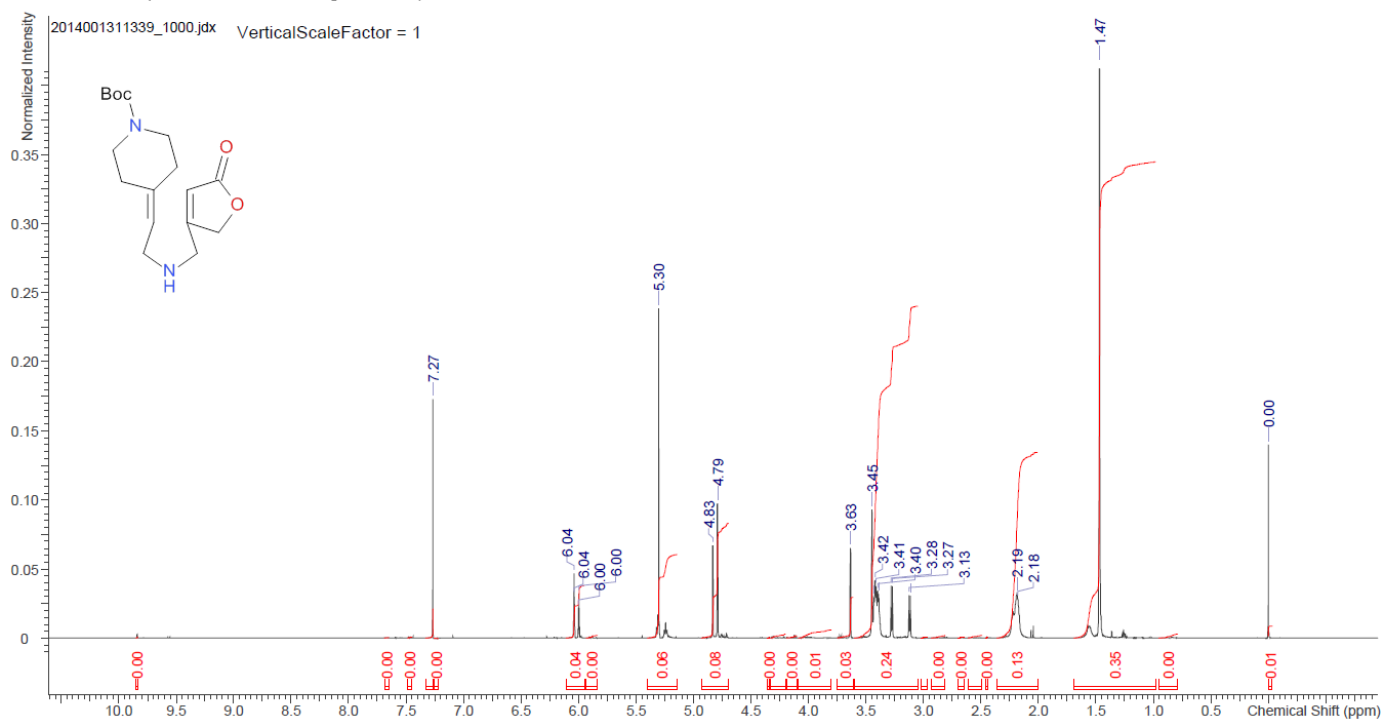
(3aRS,4aRS,7aSR)-*tert*-Butyl 3a-(2-fluorophenyl)-3-oxohexahydrofuro[3',4':1,4]cyclobuta[1,2-c]pyrrole-6(1H)-carboxylate (61):

¹H NMR (600 MHz, CDCl₃, 25 °C)



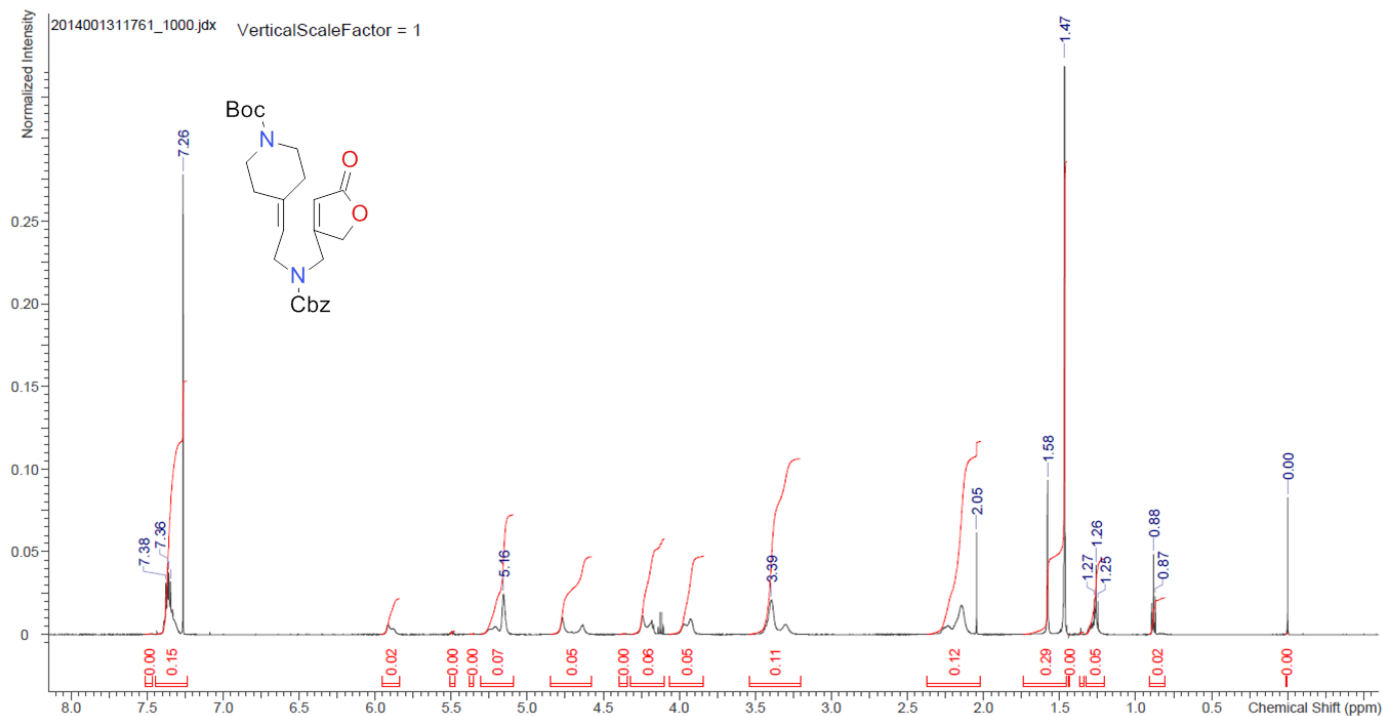
***tert*-Butyl 4-(2-(((5-oxo-2,5-dihydrofuran-3-yl)methyl)amino)ethylidene)piperidine-1-carboxylate (70):**

¹H NMR (600 MHz, CDCl₃, 25 °C)



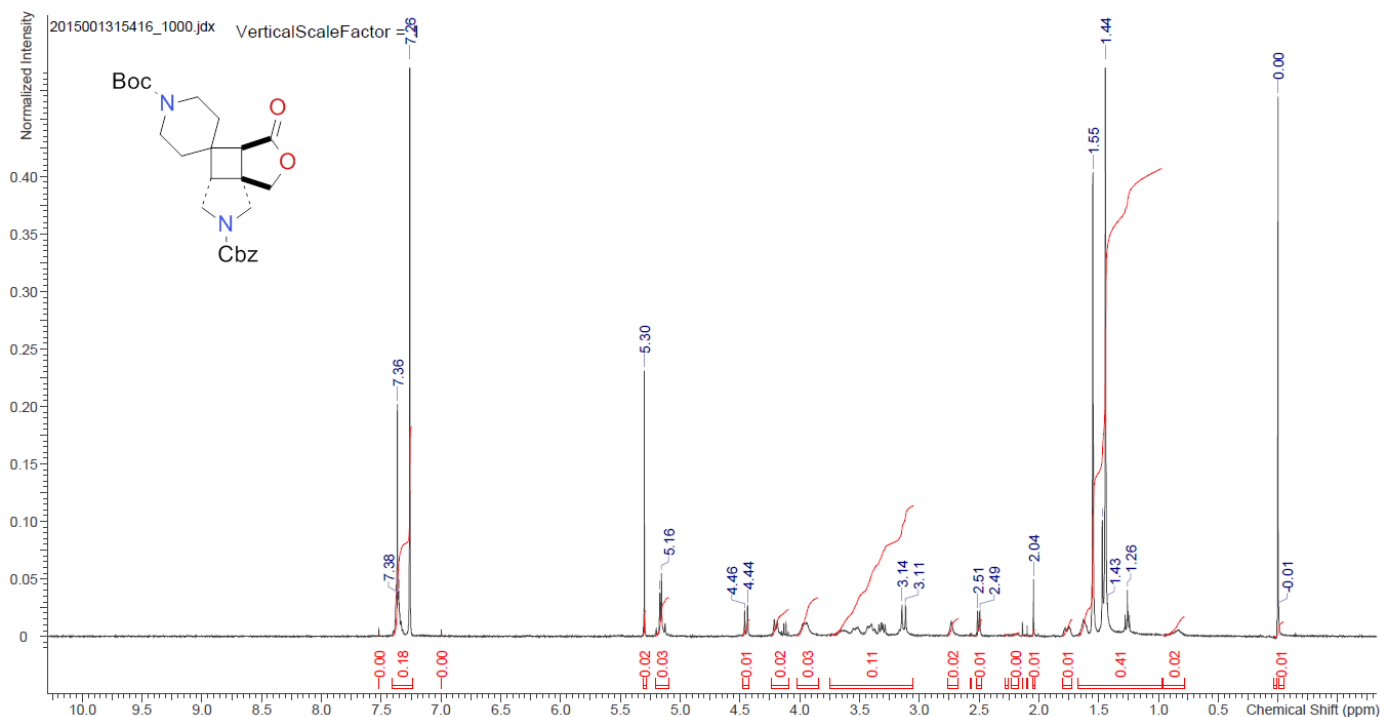
tert-Butyl 4-(2-(((benzyloxy)carbonyl)((5-oxo-2,5-dihydrofuran-3-yl)methyl)amino)ethylidene)piperidine-1-carboxylate (71):

¹H NMR (600 MHz, CDCl₃, 25 °C)



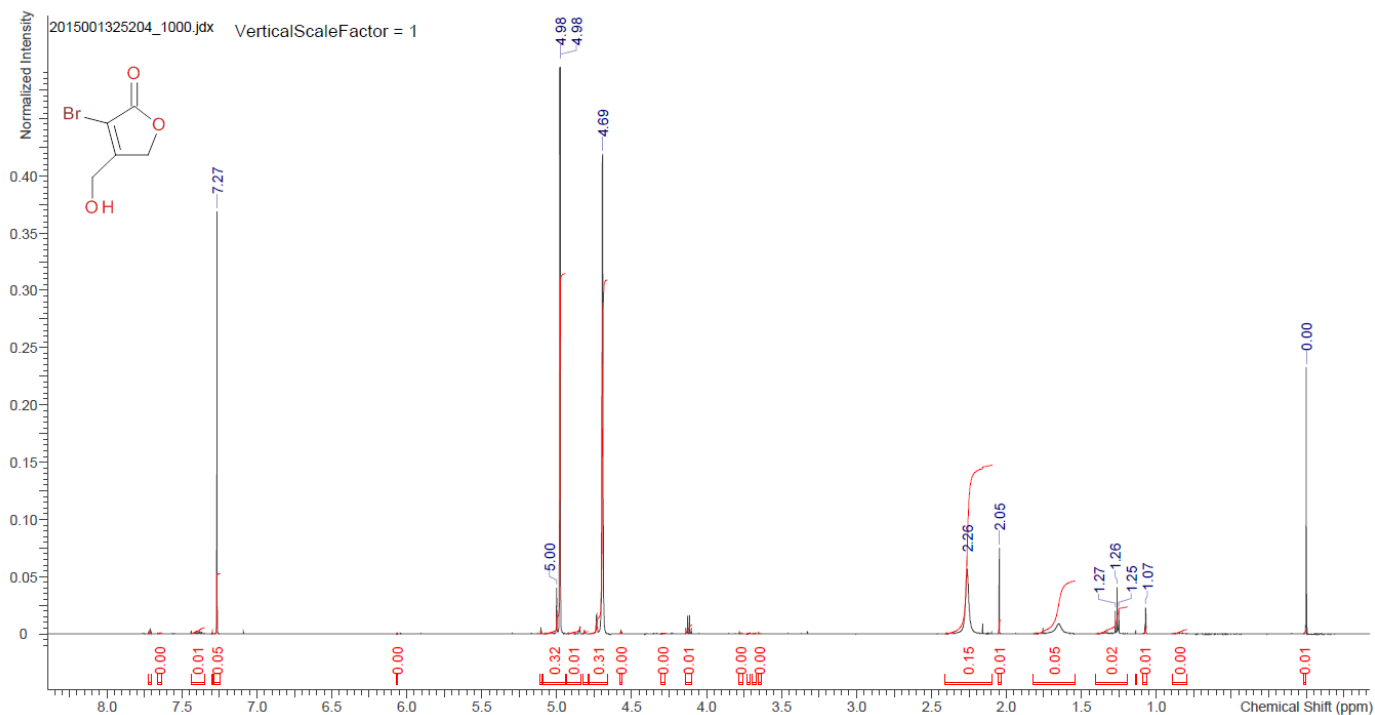
(3aRS,4aRS,7aSR)-6-Benzyl 1'-tert-butyl 3-oxotetrahydro-1H-spiro[furo[3',4':1,4]cyclobuta[1,2-c]pyrrole-4,4'-piperidine]-1',6(7H)-dicarboxylate (72):

¹H NMR (600 MHz, CDCl₃, 25 °C)



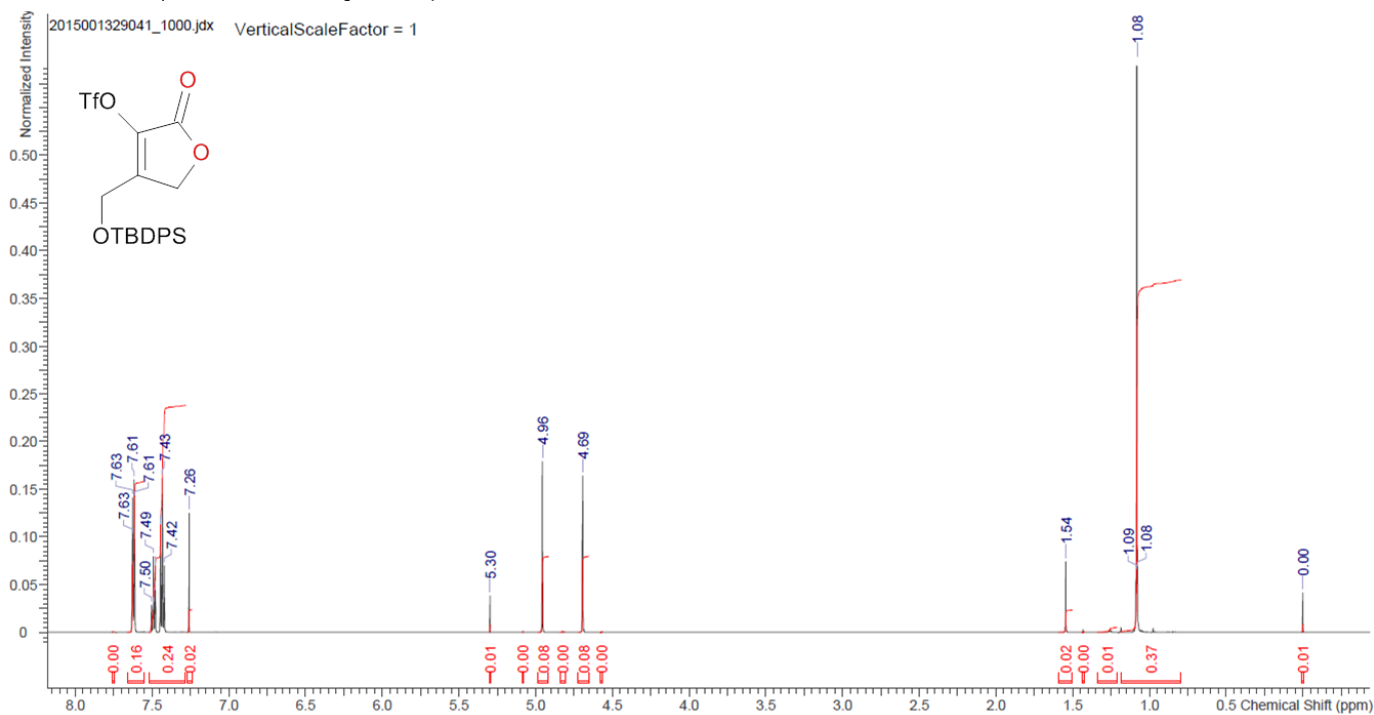
3-bromo-4-(hydroxymethyl)furan-2(5H)-one (73):

¹H NMR (600 MHz, CDCl₃, 25 °C)



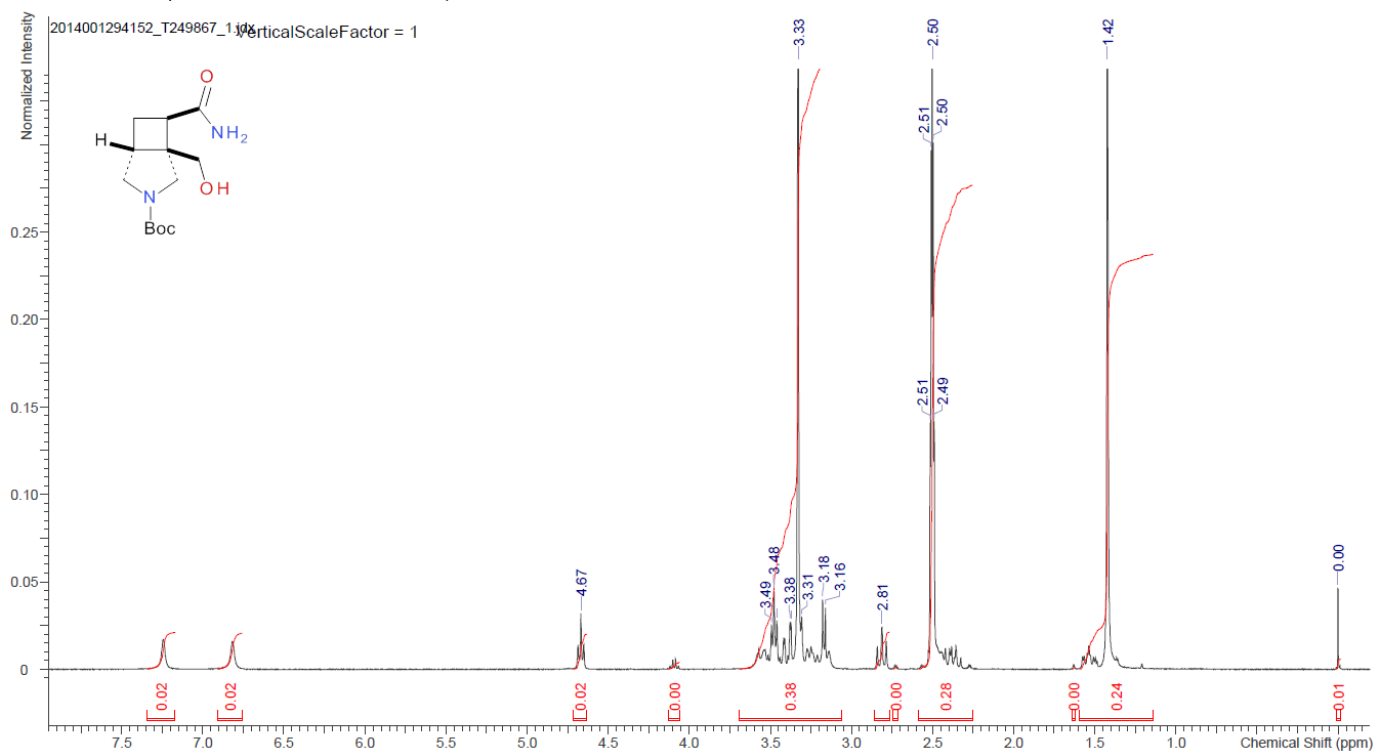
4-(((tert-butyldiphenylsilyl)oxy)methyl)-2-oxo-2,5-dihydrofuran-3-yl trifluoromethanesulfonate (88):

¹H NMR (600 MHz, CDCl₃, 25 °C)



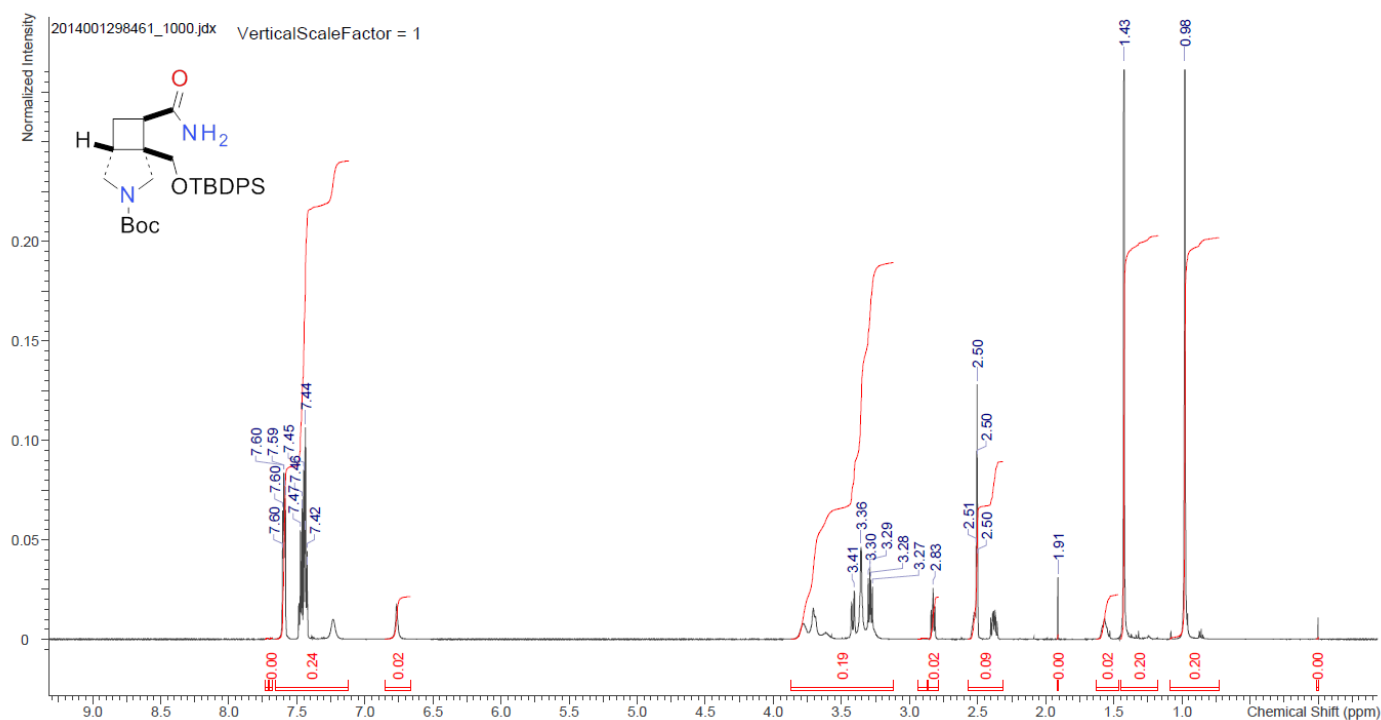
(1S,5RS,7RS)-*tert*-Butyl-7-carbamoyl-1-(hydroxymethyl)-3-azabicyclo[3.2.0]heptane-3-carboxylate (93):

¹H NMR (600 MHz, DMSO, 25 °C)



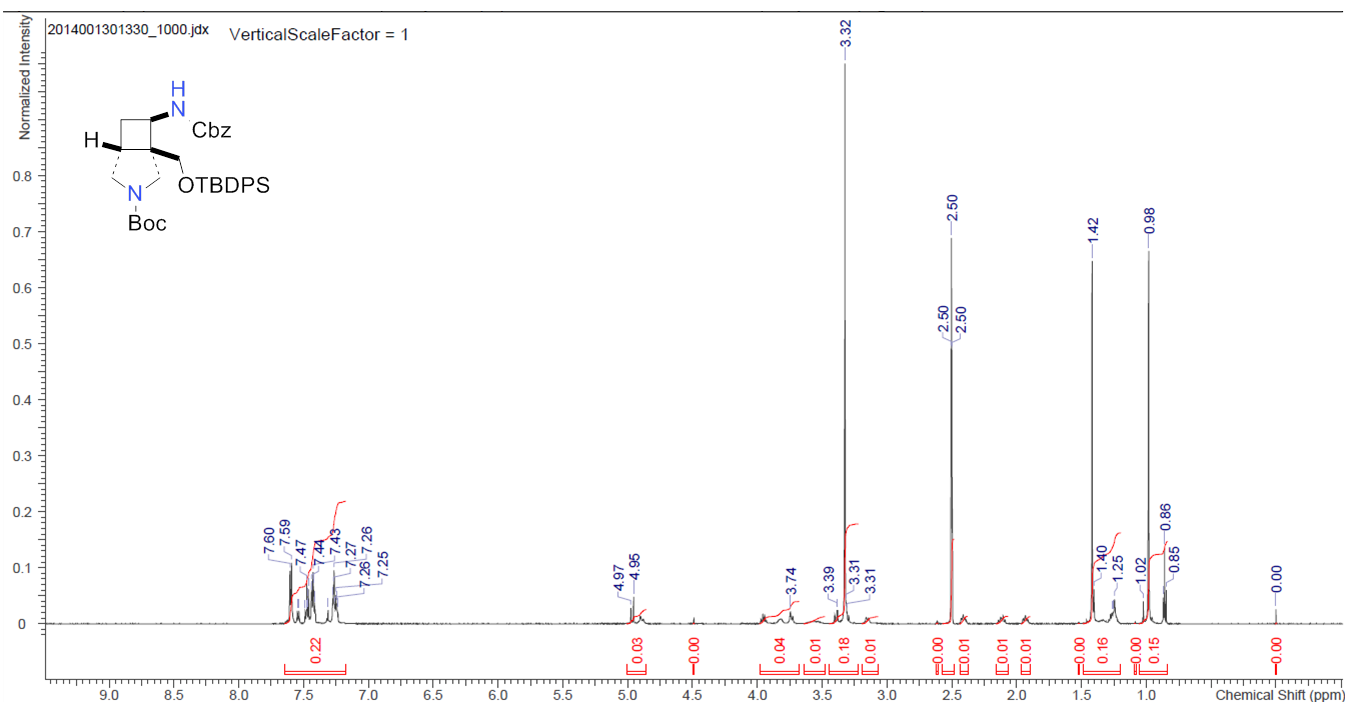
(1S,5RS,7RS)-*tert*-Butyl 1-(((*tert*-butyldiphenylsilyl)oxy)methyl)-7-carbamoyl-3-azabicyclo[3.2.0]heptane-3-carboxylate (94):

¹H NMR (600 MHz, DMSO, 25 °C)



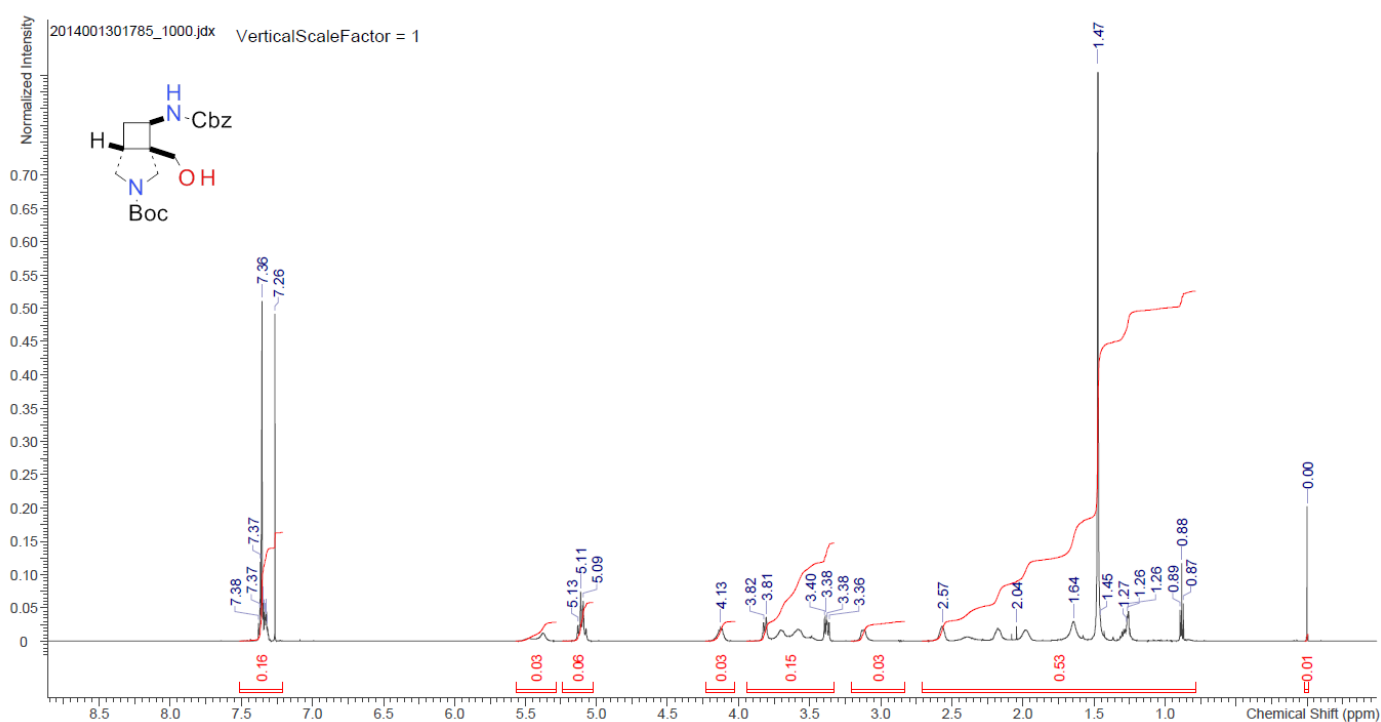
(1*RS*,5*RS*,7*RS*)-*tert*-Butyl 7-(((benzyloxy)carbonyl)amino)-1-(((*tert*-butyldiphenylsilyl)oxy)methyl)-3-azabicyclo[3.2.0]heptane-3-carboxylate (95):

¹H NMR (600 MHz, DMSO, 25 °C)



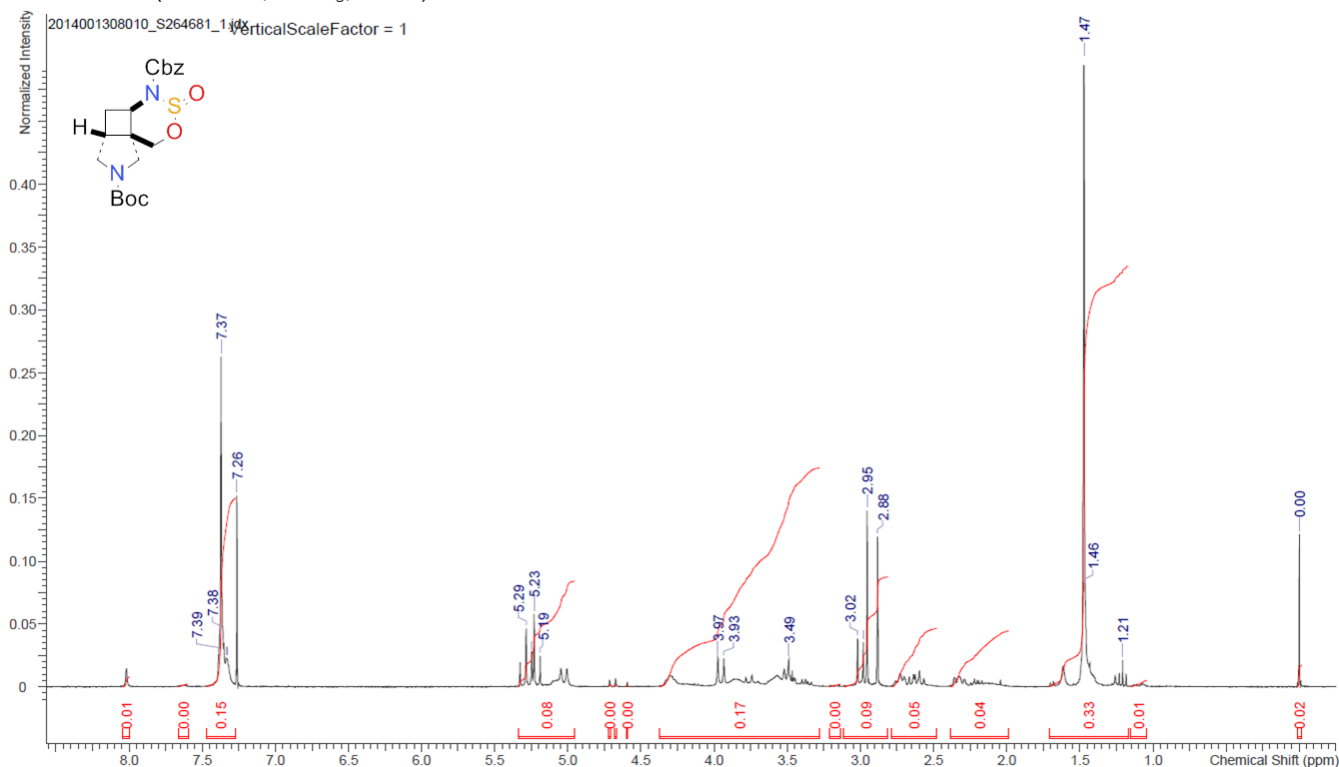
(1*RS*,5*RS*,7*RS*)-*tert*-Butyl 7-(((benzyloxy)carbonyl)amino)-1-(hydroxymethyl)-3-azabicyclo[3.2.0]heptane-3-carboxylate (96):

¹H NMR (600 MHz, CDCl₃, 25 °C)



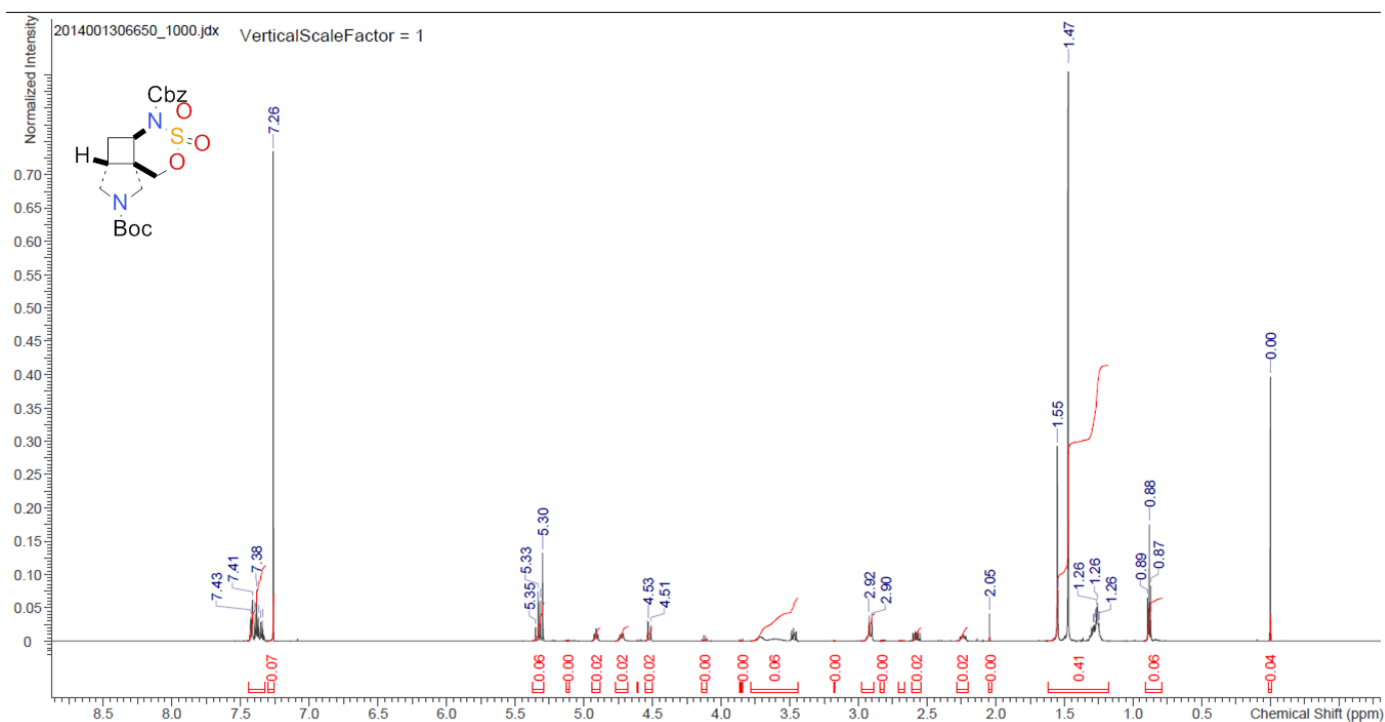
(4aRS,5aRS,8aRS)-4-Benzyl 7-tert-butyl tetrahydropyrrolo[3',4':2,3]cyclobuta[1,2-d][1,2,3]oxathiazine-4,7(1H,8H)-dicarboxylate 3-oxide (97):

¹H NMR (600 MHz, CDCl₃, 25 °C)



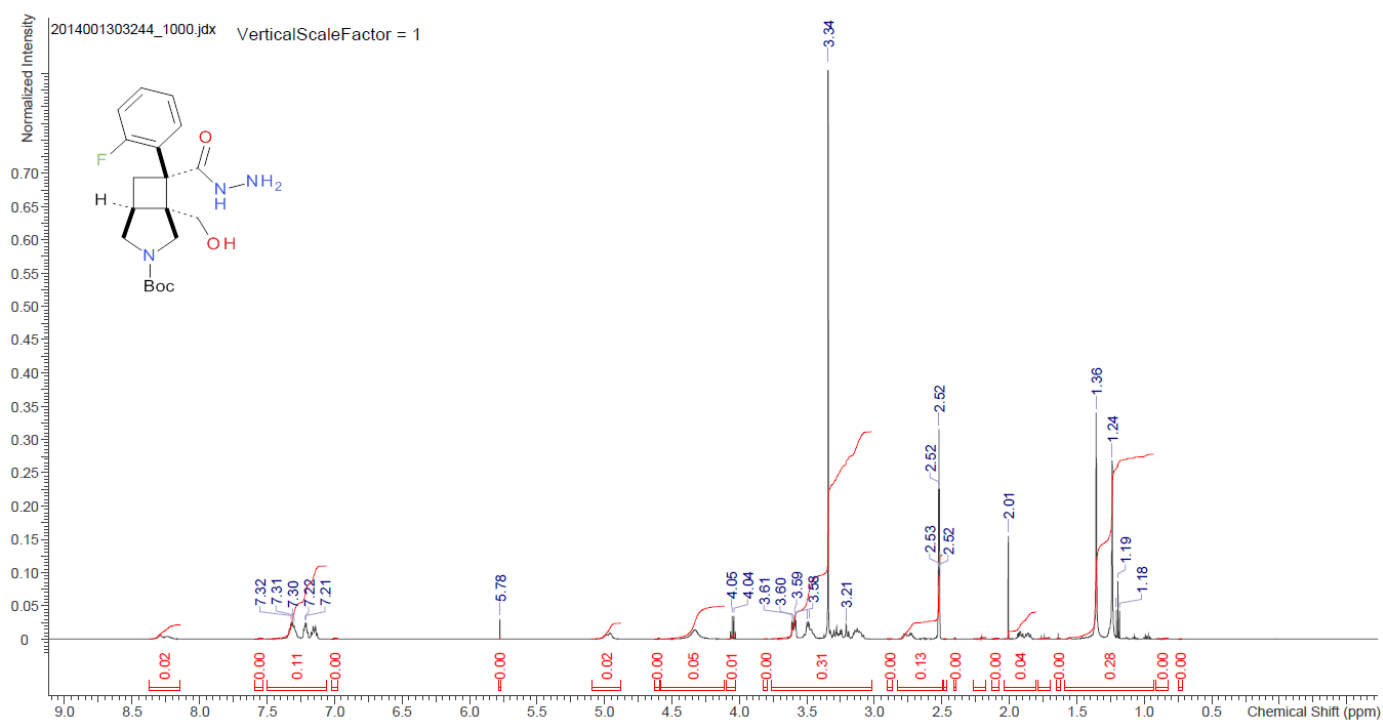
(4aRS,5aRS,8aRS)-4-Benzyl-7-tert-butyl tetrahydropyrrolo[3',4':2,3]cyclobuta[1,2-d][1,2,3]oxathiazine-4,7(1H,8H)-dicarboxylate 3,3-dioxide (98):

¹H NMR (600 MHz, CDCl₃, 25 °C)



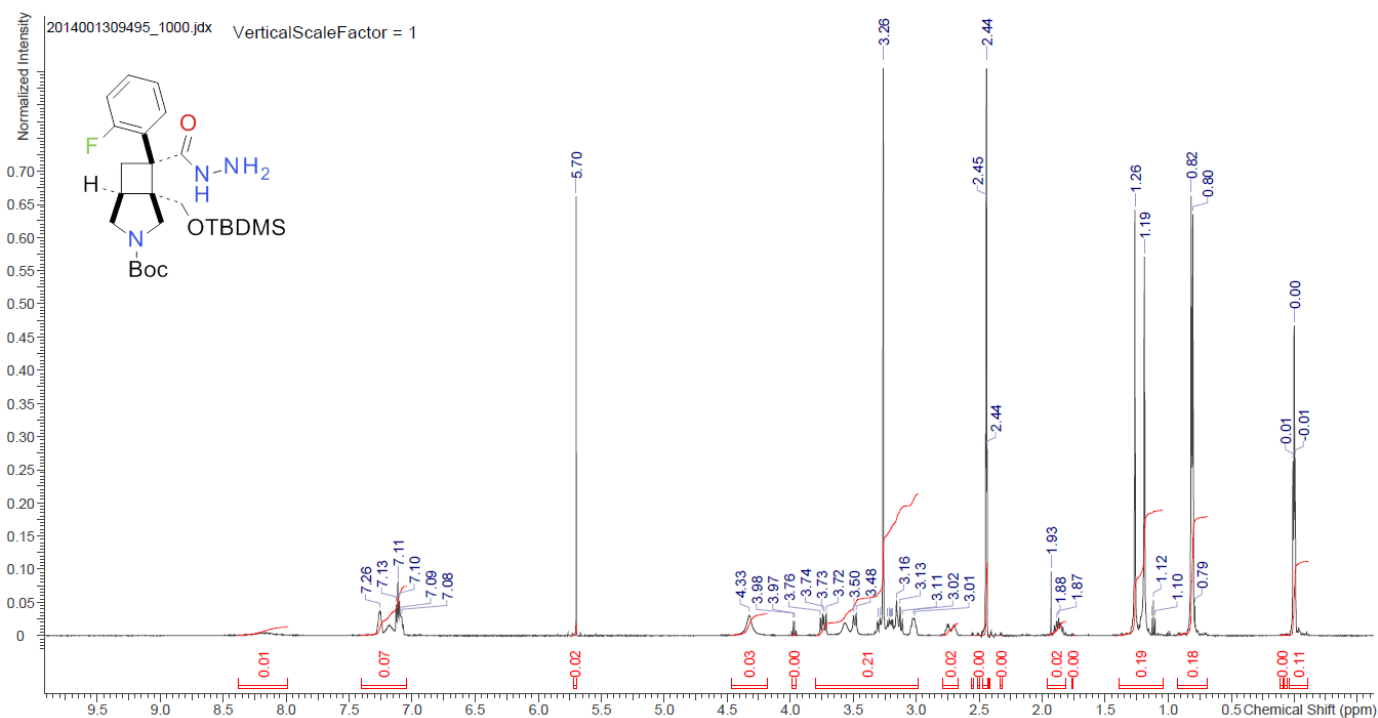
(1S,5R,7R)-*tert*-Butyl 7-(2-fluorophenyl)-7-(hydrazinecarbonyl)-1-(hydroxymethyl)-3-azabicyclo[3.2.0]heptane-3-carboxylate (99):

¹H NMR (600 MHz, DMSO, 25 °C)



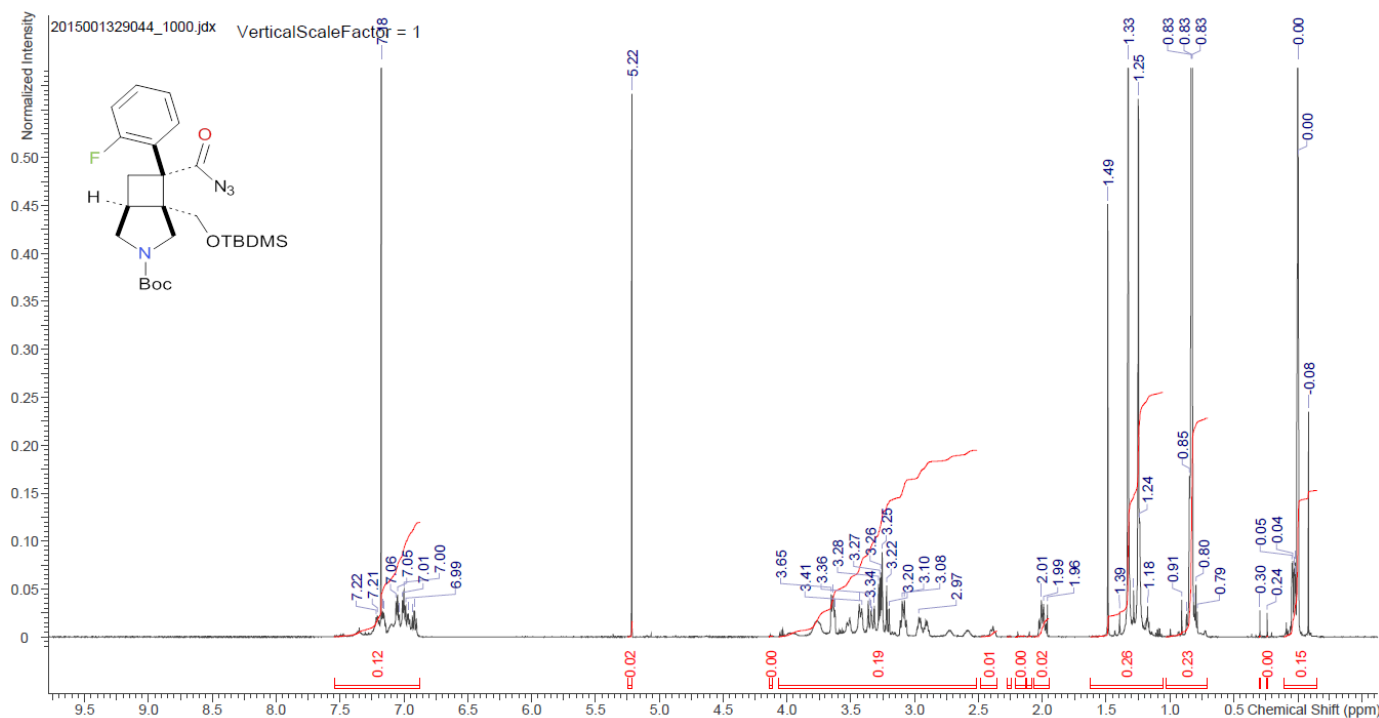
(1S,5R,7R)-*tert*-Butyl 7-(2-fluorophenyl)-7-(hydrazinecarbonyl)-1-(hydroxymethyl)-3-azabicyclo[3.2.0]heptane-3-carboxylate (100):

¹H NMR (600 MHz, DMSO, 25 °C)



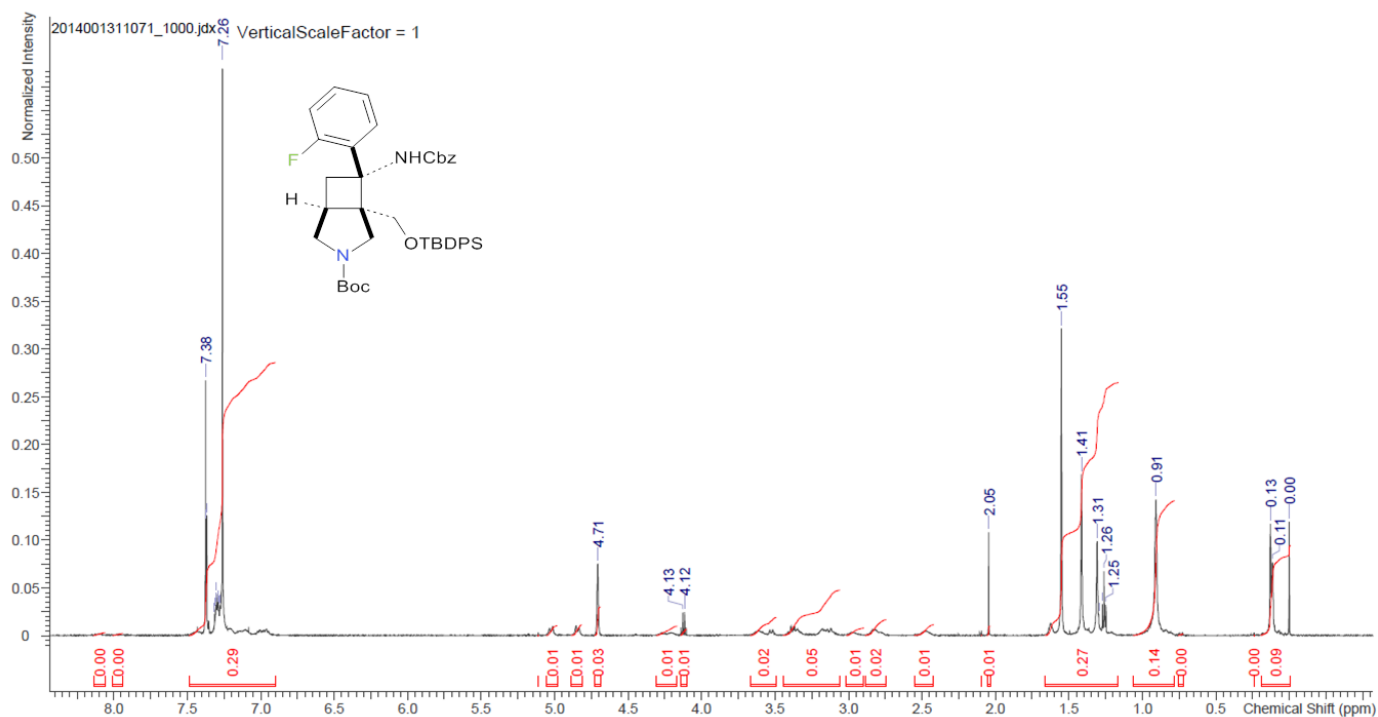
(1*SR*,5*RS*,7*RS*)-*tert*-Butyl 7-(azidocarbonyl)-1-(((*tert*-butyldimethylsilyl)oxy)methyl)-7-(2-fluorophenyl)-3-azabicyclo[3.2.0]heptane-3-carboxylate (101):

¹H NMR (600 MHz, CDCl₃, 25 °C)



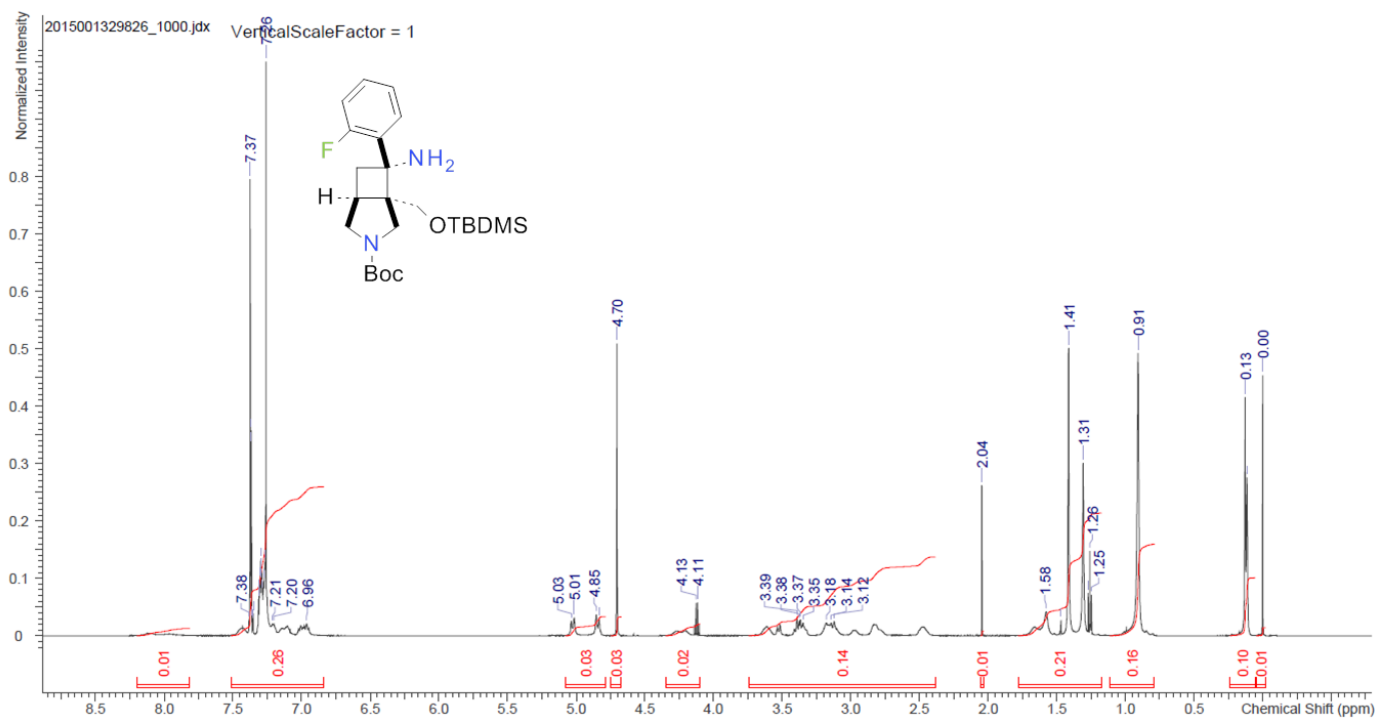
(1*RS*,5*RS*,7*RS*)-*tert*-Butyl 7-(((benzyloxy)carbonyl)amino)-1-(((*tert*-butyldimethylsilyl)oxy)methyl)-7-(2-fluorophenyl)-3-azabicyclo[3.2.0]heptane-3-carboxylate (102):

¹H NMR (600 MHz, CDCl₃, 25 °C)



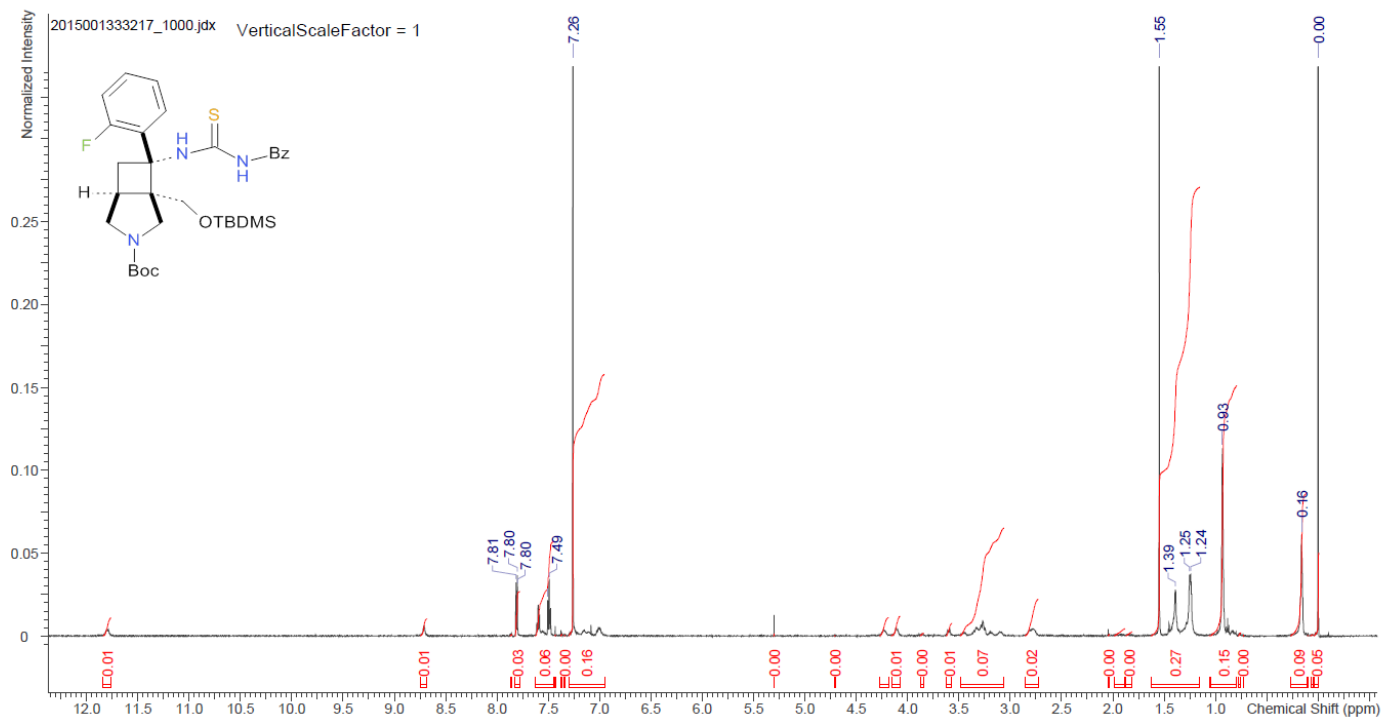
(1*RS*,5*RS*,7*RS*)-*tert*-Butyl 7-amino-1-(((*tert*-butyldimethylsilyl)oxy)methyl)-7-(2-fluorophenyl)-3-azabicyclo[3.2.0]heptane-3-carboxylate (103):

¹H NMR (600 MHz, CDCl₃, 25 °C)



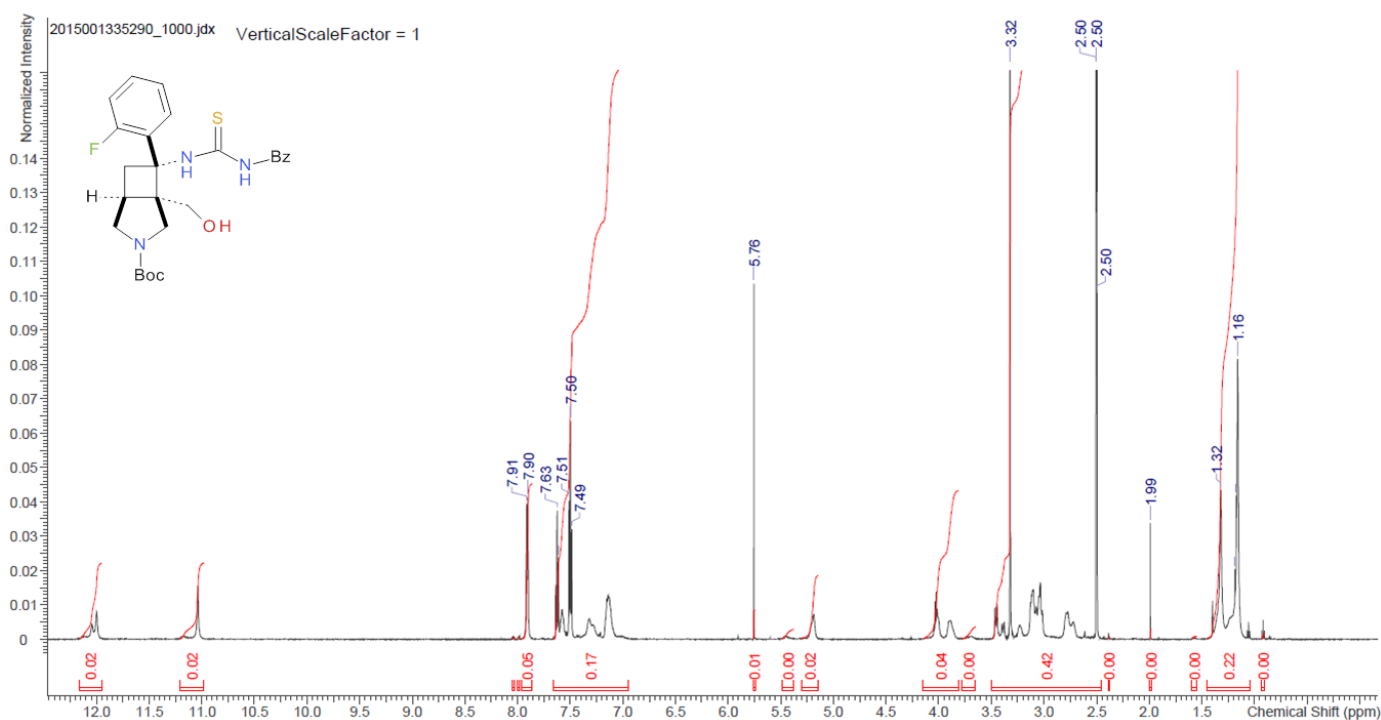
(1*RS*,5*RS*,7*RS*)-*tert*-Butyl 7-(3-benzoylthioureido)-1-(((*tert*-butyldimethylsilyl)oxy)methyl)-7-(2-fluorophenyl)-3-azabicyclo[3.2.0]heptane-3-carboxylate (104):

¹H NMR (600 MHz, CDCl₃, 25 °C)



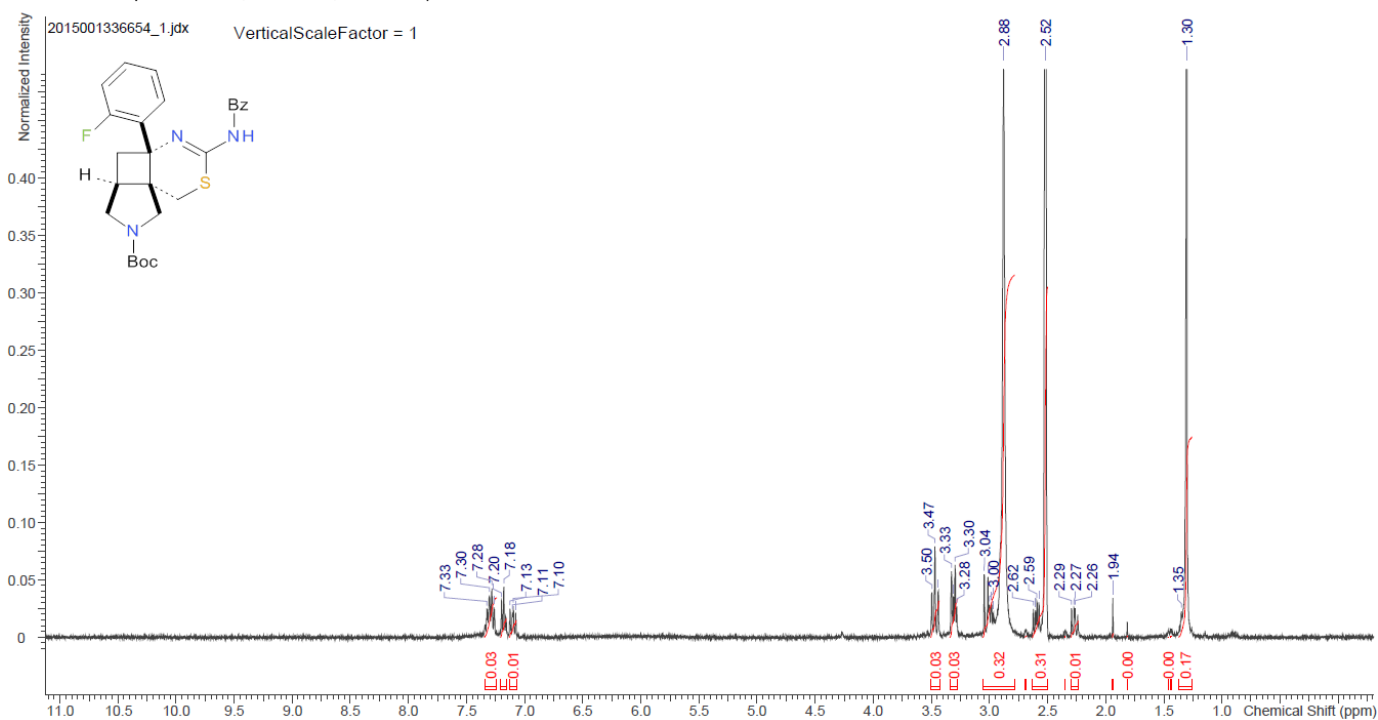
(1*RS*,5*RS*,7*RS*)-*tert*-Butyl 7-(3-benzoylthioureido)-7-(2-fluorophenyl)-1-(hydroxymethyl)-3-azabicyclo[3.2.0]heptane-3-carboxylate (105):

¹H NMR (600 MHz, DMSO, 25 °C)



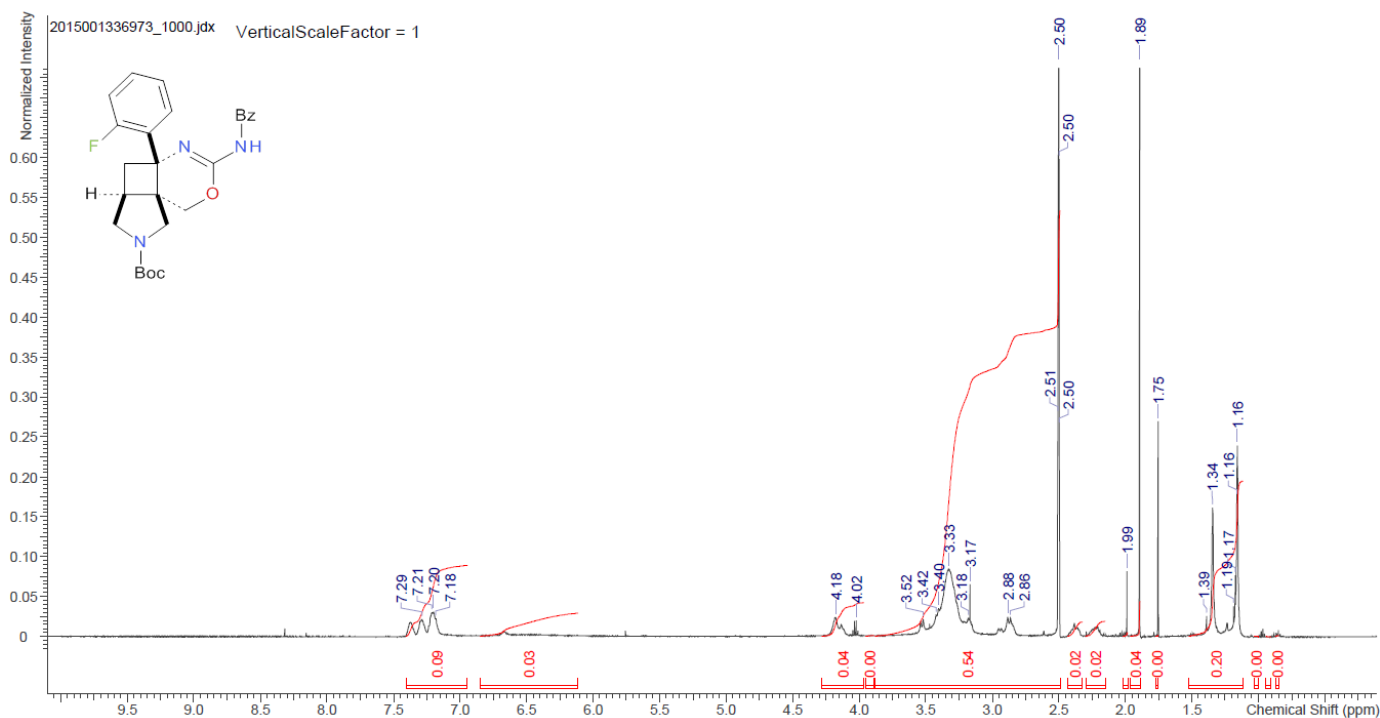
(4*aS*,5*aR*,8*aR*)-*tert*-butyl 3-benzamido-4*a*-(2-fluorophenyl)-4*a*,5,5*a*,6-tetrahydro-1*H*-pyrrolo[3',4':2,3]cyclobuta[1,2-*d*][1,3]thiazine-7(8*H*)-carboxylate (106):

¹H NMR (600 MHz, DMSO, 120 °C)



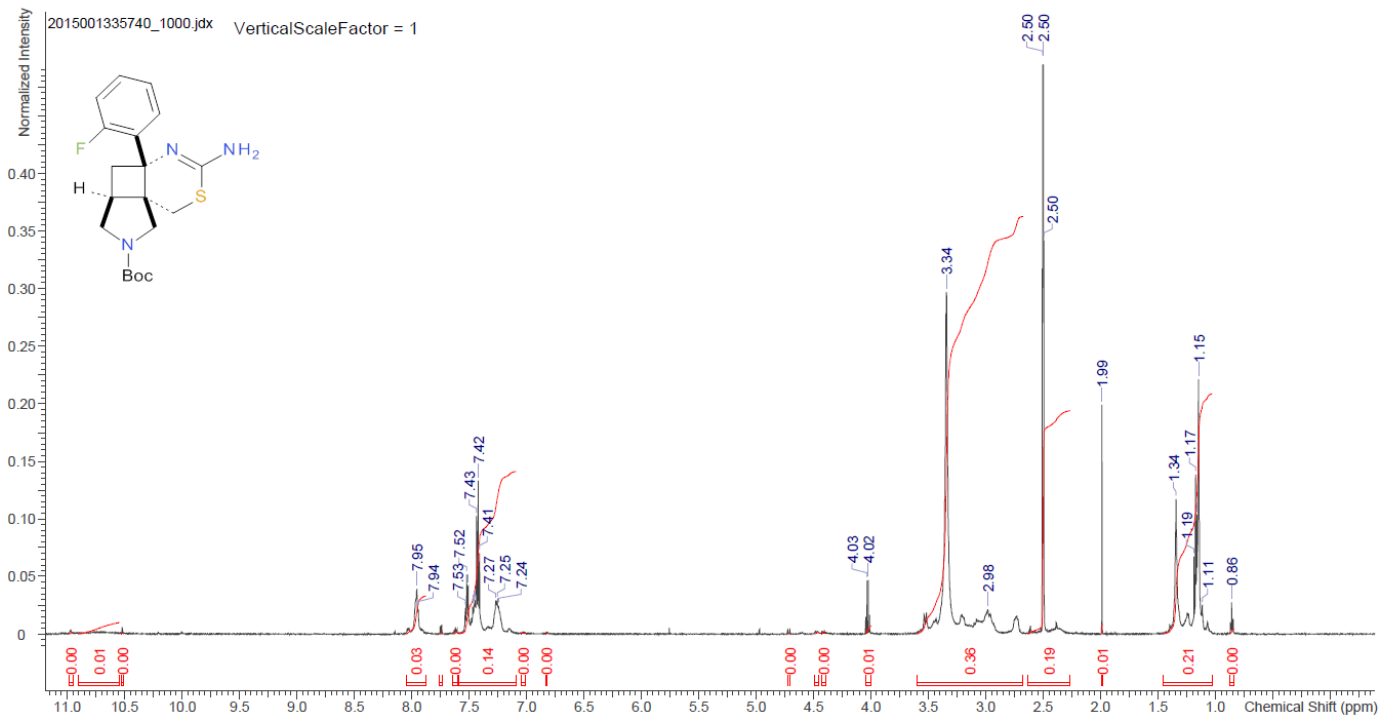
(4aRS,5aRS,8aRS)-tert-Butyl 3-benzamido-4a-(2-fluorophenyl)-4a,5,5a,6-tetrahydro-1H-pyrrolo[3',4':2,3]cyclobuta[1,2-d][1,3]oxazine-7(8H)-carboxylate (107):

¹H NMR (600 MHz, DMSO, 25 °C)



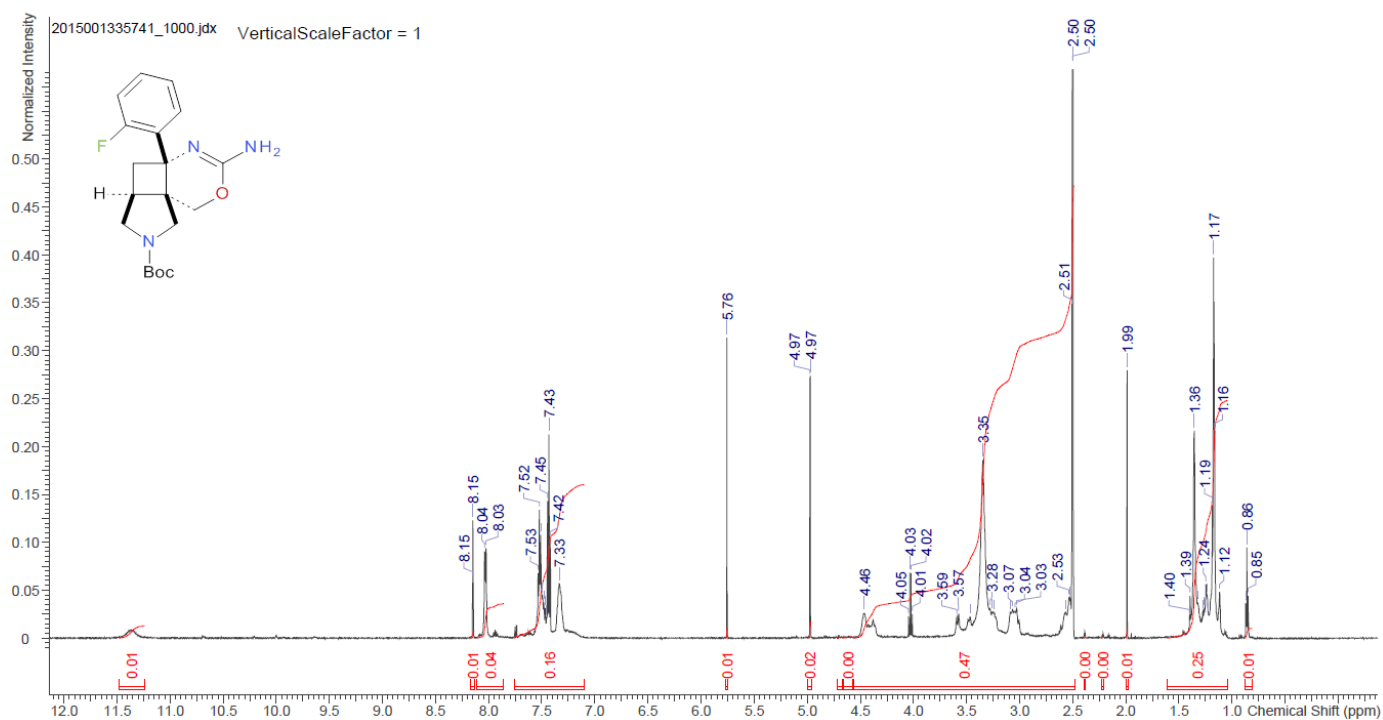
(4aSR,5aRS,8aRS)-tert-butyl 3-amino-4a-(2-fluorophenyl)-4a,5,5a,6-tetrahydro-1H-pyrrolo[3',4':2,3]cyclobuta[1,2-d][1,3]thiazine-7(8H)-carboxylate (109):

¹H NMR (600 MHz, DMSO, 25 °C)



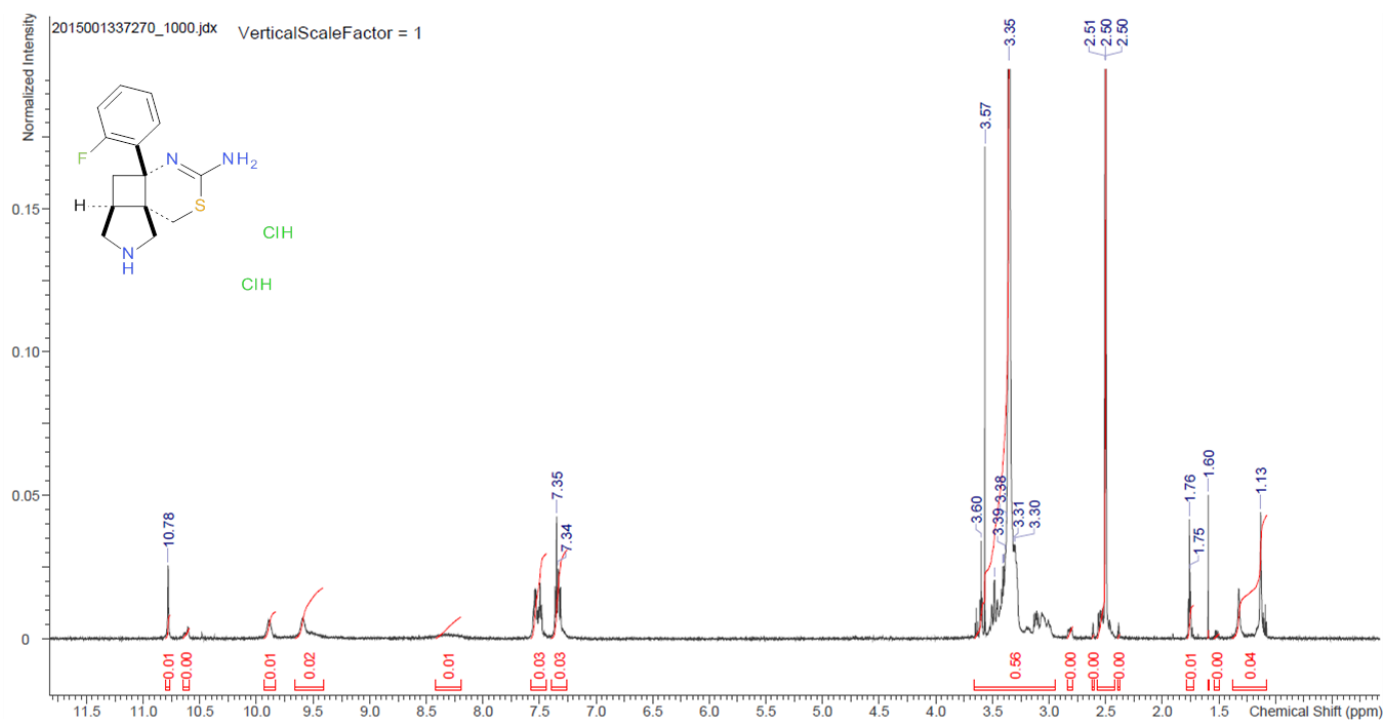
(4aRS,5aRS,8aRS)-*tert*-Butyl 3-amino-4a-(2-fluorophenyl)-4a,5,5a,6-tetrahydro-1H-pyrrolo[3',4':2,3]cyclobuta[1,2-d][1,3]oxazine-7(8H)-carboxylate (110):

¹H NMR (600 MHz, DMSO, 25 °C)



(4aSR,5aRS,8aRS)-4a-(2-Fluorophenyl)-4a,5,5a,6,7,8-hexahydro-1H-pyrrolo[3',4':2,3]cyclobuta[1,2-d][1,3]thiazin-3-amine dihydrochloride (111):

¹H NMR (600 MHz, DMSO, 25 °C)



(4aRS,5aRS,8aRS)-4a-(2-Fluorophenyl)-4a,5,5a,6,7,8-hexahydro-1H-pyrrolo[3',4':2,3]cyclobuta[1,2-d][1,3]oxazin-3-amine dihydrochloride (112):

¹H NMR (600 MHz, DMSO, 25 °C)

